REPORT ON

NASA GRANT 1562

Entitled

"Effects of High Energy Radiation on the Mechanical Properties of Epoxy/ Graphite Fiber Reinforced Composites."

covering the period
January 1, 1986-October 31, 1986

R.E. Fornes
R.D. Gilbert
J.D. Memory
Co-Principal Investigators

North Carolina State University
School of Physical and Mathematical Sciences

Department of Physics

Box 8202, Raleigh, NC 27695-8202

October 31, 1986

Dr. Edward Long
Technical Officer - NASA Grant 1562
MS 399
NASA Langley Research Center
Hampton, VA 23665

Dear Dr. Long:

Enclosed are three copies of the interim report of NASA Grant 1562 entitled "Effects of High Energy Radiation on the Mechanical Properties of Epoxy/Graphite Fiber Reinforced Composites" covering the period January 1, 1986 - October 31, 1986. The report consists of a (1) summary listing of publications, presentations and theses titles that have resulted from our work on radiation effects of composites and related materials, and (2) a copy of the dissertation of Thomas W. Wilson who completed his Ph.D. this year. Two copies of this report have been sent to NASA Scientific and Technical Information Center (NASA-STIC). The final summary report will be sent following the current no-cost extension.

We appreciate the support from NASA for this work and especially appreciate the technical advice that you have given to us.

Sincerely,

R.E. Fornes

R.D. Gilbert
Co-Principal Investigators

REF/RDG/gaw

cc: NASA-STIC (enclosure)
W.K. Walsh, L.B. Sims, J.D. Memory

Publications, Presentations and Theses Completed Which Were Supported, In Part, By NASA Grant 1562.

Publications:

1. R.E. Fornes, J.D. Memory, and N. Naranong, "Effect of 1.33 MeV γ Radiation and 0.5 MeV Electrons on the Mechanical Properties of Graphite Fiber Reinforced Composites," J. Appl. Polym. Sci. 26: 2061-2067 (1981).

2. R.E. Fornes, J.D. Memory, R.D. Gilbert and E.R. Long, Jr., "The Effects of Electron and Gamma Radiation on Epoxy-Based Materials," in Proceedings of Large Space Systems Technology (1981), NASA Conference Publication 2215, Part 3, Nov. 16-19, 1981, pp. 27-36.

3. K. Wolf, R.E. Fornes, J.D. Memory and R.D. Gilbert, "A Review of the Interfacial Phenomena in Graphite Fiber Composites," to be published in Chemistry and Physics of Carbon (Marcel Dekker, New York, Vol. 16 (1982).

4. R.E. Fornes, J.D. Memory, N. Naranong, K. Wolf and W.C. Stuckey, "Radiation Effects on the Mechanical Properties of Graphite Fiber Reinforced Composites," Bull. Amer. Phys. Soc. 24: 285 (1980).

5. N. Naranong, K. Wolf, J.D. Memory, R.D. Gilbert and R.E. Fornes, "Effects of Ionizing Radiation on the Mechanical and Morphological Properties of Graphite Fiber Reinforced Composites," Bull. Amer. Phys. Soc. 26: 399 (1981).

6. K. Schaffer, R.D. Gilbert, J.D. Memory and R.E. Fornes, "Electron Spin Resonance Studies of Epoxy Samples Exposed to 1/2 MeV Electrons," Bull. Amer. Phys. Soc. 26: 432 (1981).

7. M. Kent, K. Schaffer, J.D. Memory, R.D. Gilbert and R.E. Fornes, "Electron Spin Resonance Studies of Epoxy Exposed to γ^{60}Co Radiation," Bull. Amer. Phys. Soc. 27: (3) p. 199 (1982).

8. N. Netravali, R.E. Fornes, R.D. Gilbert and J.D. Memory, "Thermal Analysis of Water Soaked Epoxy Resins," Bull. Amer. Phys. Soc. 27: (3) 358-359 (1982).

9. K. Schaffer, R.E. Fornes, R.D. Gilbert and J.D. Memory, "ESR Study of a Cured Epoxy Resin Exposed to High-Energy Radiation." Polymer, 25: 54-56 (1984).

10. A.N. Netravali, R.E. Fornes, R.D. Gilbert and J.D. Memory, "Investigation of Water and High Energy Radiation Interactions in an Epoxy." J. Appl. Polym. Sci., 29: 311-318 (1984).

11. G.M. Kent, J.D. Memory, R.D. Gilbert and R.E. Fornes, "Variation in Radical Decay Rates in an Epoxy as a Function of Crosslinking Density." J. Appl. Polym. Sci., 28: 3301-3307 (1983).

12. R.E. Fornes, R.D. Gilbert and J.D. Memory, "Investigation of an Epoxy Interaction with H_2O and High Energy Radiation," Journal of Research Communications, Spinal Publication, ARCSL-SP-83030 Proceedings of the 1982 Scientific Conference on Chemical Defense, U.S. Army, Aberdeen, MD 21010 (1983).

13. M. Kent, K. Wolf, J.D. Memory, R.E. Fornes and R.D. Gilbert, "The Effect of 0.5 MeV Electron Radiation on the Crystallinity of Carbon Fibers in Composites," Carbon, 22: 103-104 (1984).

14. K. Wolf, R.E. Fornes, R.D. Gilbert and J.D. Memory, "Effects of 0.5 MeV Electrons in the Interlaminar and Flexural Strength Properties of Graphite Fiber Composites," J. Appl. Physics, 54: 5558-5561 (1983).

15. T. Wilson, R.D. Gilbert, J.D. Memory and R.E. Fornes, "Dynamic Mechanical Analysis of an Epoxy," Bull. Amer. Phys. Soc. 28: 392 (1983).

16. K. Wolf, J.D. Memory, R.D. Gilbert and R.E. Fornes, "Interlaminar Shear Properties of Irradiated Graphite Fiber Composites," Bull. Amer. Phys. Soc. 28: 549 (1983).

17. K.S. Seo, A. Netravali, R.D. Gilbert, J.D. Memory and R.E. Fornes, "Effects of High-Energy Radiation of Surface Energies of TGDDM/DDS Epoxy, Bull. Amer. Phys. Soc. 29: 410 (1984).

18. T. Wilson, J.D. Memory, R.D. Gilbert and R.E. Fornes, "Effects of 0.5 MeV Electron Radiation on Dynamic Mechanical Properties of TGDDM/DDS Epoxy," Bull. Amer. Phys. Soc. 29: 410 (1984).

19. D.R. Coulter, M.V. Smith, F.D. Tsay, A. Gupta and R.E. Fornes, "The Effects of 3 MeV Proton Radiation on Aromatic Polysulfone: J. Appl. Polym. Sci. 30: 1753-1760 (1985).

20. *K.S. Seo, R.D. Gilbert, R.E. Fornes and J.D. Memory, "ESR Studies of Graphite Fiber/Epoxy Composites Irradiated with Ionizing Radiation, Bull. Amer. Phys. Soc. 30: 477 (1985).

21. *J.S. Park, R.D. Gilbert, J.D. Memory and R.E. Fornes, "Effect of Ionizing Radiation on the Interlaminar Shear Strength (ILSS) of Graphite Fiber/Epoxy Composites, Bull. Amer. Phys. Soc. 30: 490 (1985).

22. *T. Wilson, J.D. Memory, R.E. Fornes and R.D. Gilbert, "Effect of 0.5 MeV Electron Radiation on Dynamic Mechanical Properties of TGDDM/DDS Epoxy Resin and T300/5208 and T300 15209 Composites, Bull. Amer. Phys. Soc. 30: 434 (1985).

23. K.S. Seo, R.E. Fornes, R.D. Gilbert and J.D. Memory, The Roles of Cross-linking Density and Oxygen on the Radical Decay Rates of Irradiated Epoxy Bull. Am. Phys. Soc. 31: 457-458 (1986).

24. J.S. Park, R.D. Gilbert, R.E. Fornes and J.D. Memory, "Finite Element Analysis of the Interlaminar Shear Strength of Graphite Fiber/Epoxy Composites Exposed to Ionizing Radiation", Bull. Am. Phys. Soc. 31 460 (1986).

25. Daniel R. Coulter, Amitava Gupta, Mark V. Smith and R.E. Fornes, "The Effects of Energetic Proton Bombardment on Polymeric Materials: Experimental Studies and Degradation Models." JPL Publication 85-101 (June 1, 1986).

26. K.S. Seo, R.E. Fornes, R.D. Gilbert and J.D. Memory, "Effects of Ionizing Radiation on epoxy, Graphite Fiber, and Epoxy/Graphite Fiber Composites Part I Surface Energy Changes" J. Polym. Sci. - Phys. Ed. (Submitted).

27. K.S. Seo, R.E. Fornes, R.D. Gilbert and J.D. Memory, "Effects of Ionizing Radiation on Epoxy, Graphite Fibers and Epoxy/Graphite Fiber Composites Part II Radical Types and Radical Decay Behavior" J. Polym. Sci. - Phys. Ed. (Submitted.).

Theses completed:

1. Naraporn Naranong, M.S. Thesis, "Effect of High Energy Radiation on Mechanical Properties of Graphite Reinforced Composites," (1980).

2. Kevin Schaffer, M.S. Thesis, "Characterization of a Cured Epoxy Resin Exposed to High Energy Radiation with Electron Spin Resonance," (1981).

3. George M. Kent, M.S. Thesis, "X-ray Diffraction and ESR Studies of the Effects of High Energy Radiation on Composite Materials," (1982).

4. Kay W. Wolf, Ph.D. Dissertation, "Effect of Ionizing Radiation on the Mechanical and Structural Properties of Graphite Fiber Reinforced Composites," (1982).

5. Anil Netravali, Dissertation, "The Influence of Water and High Energy Radiation on the Thermal and Spectroscopical Characteristics of an Epoxy, (1984).

6. Kab Sik Seo; Dissertation, "Electron Spin Resonance Investigations and Surface Characterization of TGDDM/DDS Epoxy and T300 Graphite Fiber Exposed to Ionizing Radiation (1985).

7. Thomas Woodrow Wilson, III, Dissertation, "Radiation Effects on the Dynamic Mechanical Properties of Epoxy Resins and Graphite Fiber/Epoxy Composites" (1986).

PRESENTATIONS:

Seminars presented on this work:

Gordon Research Conference on Fiber Science, (July 1981).

Georgia Institute of Technology (May 1981).

The Polymer Group Meeting, Division of the ACS, Raleigh, NC (January 1981).

Jet Propulsion Lab (1983, three seminars).

Lawrence Livermoor Labs (1983, two seminars).

NASA Langley (1981, 1982, 1983 and 1984).

University of Tennessee (1984).

Fiber-Polymer Science Seminar at NCSU (1984, 1986).

Nuclear Engineering Seminar at NCSU (1984).

Honors Seminar at NCSU (1984).

Beijing University (1985).

IBM at San Jose, CA (1985).

Physics Department Seminar (1986).

American Chemical Society (1985, 1986).

Fiber Society (2 papers, 1986).

IUPAC Meeting in the Praque (1986).

Georgia Tech. University (1986).

Gordon Conference on Fiber Science (1986).

(See Bull. Amer. Phys. Soc. citations listed above for presentations at the American Physical Society).

ABSTRACT

WILSON III, THOMAS WOODROW. Radiation Effects on the Dynamic Mechanical Properties of Epoxy Resins and Graphite Fiber/Epoxy Composites. (Under the direction of DR. RAYMOND E. FORNES and DR. RICHARD D. GILBERT.)

The epoxy resin system formed by tetraglycidyl 4,4'-diamino diphenyl methane (TGDDM) and 4,4'-diamino diphenyl sulfone (DDS) was characterized by dynamic mechanical analysis (Rheovibron/Autovibron) and differential scanning calorimetry. Dynamic mechanical properties of graphite/fiber epoxy composite specimens formulated with two different adhesive systems (NARMCO 5208, NARMCO 5209) were determined. The specimens, epoxy and composite, were exposed to varying dose levels of ionizing radiation (0.5 MeV electrons) with a maximum absorbed dose of 10,000 Mrads. Following irradiation, property measurements were made to assess the influence of radiation on the epoxy and composite specimens.

The results established that ionizing radiation has a limited effect on the properties of the epoxy and composite systems. The most notable deleterious property change was a decrease of 30°C to 40°C in the glass transition temperature for the epoxy resins and NARMCO 5208 based composites after an absorbed dose of 10,000 Mrads. The glass transition temperature for the NARMCO 5209 based composites decreased by

20°C. Sorption/desorption studies revealed that plasticization of the network was responsible for a portion of the decrease in glass transition temperature.

A discrepancy between the glass transition temperature for 90° and 0° composites was observed. The 0° composites had glass transition temperatures that were 30°C to 40°C higher than the 90° composites at identical dose levels. An "interfacial" region was proposed to account for the difference in Tg. Models, which incorporated the interfacial region as part of a spring and dashpot system, are proposed for the 90° and 0° composite orientations. The experimental results are in agreement with the model predictions, and suggest that dynamic mechanical analysis is a probe for investigating the interfacial region of composites.

BIOGRAPHY

Thomas Woodrow Wilson III was born March 29, 1956 in Greensboro, North Carolina. He received his elementary and secondary education in Jamestown, North Carolina, graduating from L. C. Ragsdale High School in 1974. He entered North Carolina State University at Raleigh and received a Bachelor of Science in Textile Chemistry in 1978 and a Master of Science in Textile Chemistry in 1981. After completing his Masters degree, he was accepted into the Fiber and Polymer Science program. Upon completion of his degree, he will take a post-doctorate appointment at the University of North Carolina at Chapel Hill in the School of Dentistry.

He is married to the former Miss Rhonda Gayle Beeson.

ACKNOWLEDGEMENTS

The author expresses sincere gratitude and appreciation to Drs. R. E. Fornes and R. D. Gilbert, Co-Chairmen of his Advisory Committee, for their guidance and patience throughout this study. He also thanks the other committee members, Drs. J. D. Memory and W. K. Walsh, for their help. Additionally, the discussions with the late Dr. T. Murayama on dynamic mechanical analysis were most informative.

The help of Mr. G. G. Floyd was invaluable in irradiating the samples. Appreciation is extended to Mr. K. K. Crabtree for his assistance with the electronic equipment. The author expresses his gratitude to Mr. L. Williamson for his assistance in ordering supplies.

The author wishes to thank his family for their continual encouragement and support. Also, he cannot express all the gratitude due his wife Rhonda for her help, encouragement and understanding throughout his degree program.

The author thanks Dr. E. R. Long of NASA for supplying the composite samples. The financial support provided by NASA is gratefully acknowledged.

TABLE OF CONTENTS

TABLE OF CONTENTS (cont'd)

LIST OF TABLES

LIST OF FIGURES

LISTS OF FIGURES (cont'd)

LISTS OF FIGURES (cont'd)

1. INTRODUCTION

Polymeric composite materials are considered as replacements for metal in many structures due to their high strength-to-weight ratio, high modulus and low thermal expansion. One area of interest lies in utilizing these materials for space structures where their low density and excellent mechanical properties make them highly desirable for such applications. However, the durability of polymeric substances in an environment containing constant exposure to ionizing radiation, high vacuum and temperature extremes is questionable. Irradiating polymers causes them to undergo chain scission and crosslinking reactions. The former results in degradation of their mechanical properties, while the later creates a stiffer network, eventually leading to embrittlement.

Polymers with a high concentration of aromatic groups display an increased resistance to radiation induced degradative processes when compared to predominantly aliphatic polymers (1). The epoxy resin system TGDDM (tetraglycidyl 4,4'-diamino diphenyl methane) cured with DDS (4,4'-diamino diphenyl sulfone) is currently used as a matrix material for graphite fiber reinforced composites. This resin system contains a high concentration of aromatic groups, and therefore, it should possess good radiation

stability. However, when considering the large doses of radiation (10,000 Mrads) that an object may encounter during an extended period in space, an understanding of radiation induced property changes (chain scission and crosslinking) is important (2-4).

Durability can be evaluated through the application of various tests. Dynamic mechanical testing offers the advantage of maintaining sample integrity while exposing the sample to cyclic deformation, thereby providing valuable information about its in-use response (5).

The objective of this research was to study the effect of ionizing radiation on the dynamic mechanical properties of TGDDM/DDS epoxy resin systems and graphite fiber/epoxy composites. Dynamic mechanical analysis and differential scanning calorimetry were used to examine the effect of radiation on the mechanical and thermal properties of the systems described above.

2. REVIEW OF LITERATURE

Analysis of the dynamic mechanical response of a system can yield useful data for the characterization of an engineering material. Elastic (E') and loss moduli (E") along with the damping ratio (E"/E') produce a measure of the system stress-strain response as a function of time or temperature. The glass transition temperature (Tg), which is generally assumed to occur in the region of maximum damping, is related to and may provide information on molecular weight, extent of crystallinity and/or crosslink density depending upon the morphology of the system. Other transitions, β or γ, yield information such as the temperature associated with the onset of small rotational motions. In systems such as epoxies, reactions may occur during the measurements, sometimes manifesting themselves as changes in damping peaks. A wealth of information about system properties and property changes can be obtained as a result of a careful and extensive dynamic mechanical study (5-10).

Epoxy resin systems are ideally suited to dynamic mechanical characterization. They can generally be cast as uniform, thin films which is a necessary requirement for Rheovibron/Autovibron studies. Epoxy resins are usually highly crosslinked amorphous polymers, and they yield fairly well-defined glass transitions. In contrast, glass

transitions are often difficult to measure in highly crystalline polymer systems (5,10).

In the following review a discussion is presented of epoxy curing mechanisms. Dynamic and static testing techniques are discussed. Previous studies of the characterization of TGDDM/DDS epoxy using different mechanical tests are reviewed. Finally, radiation effects on epoxy resins, graphite fiber/epoxy composites and elastomers are discussed.

Currently, the TGDDM/DDS epoxy system is widely used as a matrix for structural composites in the aerospace industry. The system is quite attractive for such applications due to its high glass transition temperature, elastic modulus and radiation resistance. Since TGDDM/DDS based composites are used extensively in critical structures, the discussion will focus primarily on the curing and testing of TGDDM/DDS epoxy systems. The details related specifically to TGDDM/DDS epoxy are generally applicable to other thermosetting epoxy resin systems (4,5,11).

2.1 Epoxy Curing Mechanisms

Epoxy resins may be cured with a curing agent having chemically reactive groups such as amines, phenols, carboxylic acids and acid anhydrides, or by epoxy homopolymerization under the proper conditions (8,12). The epoxide or oxirane functional group is illustrated below (I):

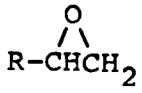

(I)

The curing reaction proceeds by a ring-opening process with the resultant structure (II):

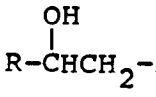

(II)

R' may be any species containing a functional group capable of opening the oxirane ring. Since TGDDM/DDS is an epoxy-amine system, the reactions pertinent to it will be discussed.

The initial step in the curing reaction of an epoxy-amine system is assumed to be nucleophilic attack of the oxirane ring by the primary amine (III):

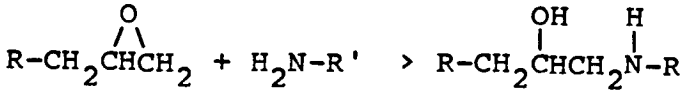

(III)

A subsequent reaction is that of the secondary amine formed in the preceding step with the epoxide (IV):

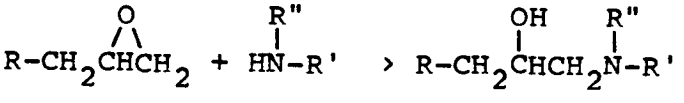

(IV)

The oxirane ring can also react with hydroxyl groups formed in previous reactions (V):

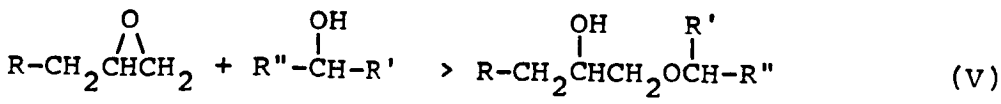

(V)

The above reaction yields ether linkages and regenerates an hydroxyl group. Furthermore, there is the possibility of homopolymerization of the epoxide rings (8,12).

When the structure of the reactants and the resultant polymer is considered, it is possible that steric hindrance may reduce reaction by the secondary amine. Indeed Gupta et al. (13) as well as others (11,14-17) present evidence that sterically hindered secondary amine groups effectively render the tetrafunctional DDS to be a difunctional moiety. According to Gupta et al. (13), cure proceeds by epoxide-primary amine reaction (chain extension) until the primary amine is consumed or the reaction terminates due to system vitrification. The extent of cure is dependent upon the cure temperature. Next, the epoxide-hydroxyl reaction proceeds, <u>even in the vitrified state</u>, to further crosslink the system. Fourier transform IR studies provided evidence that cure proceeds in the vitrified state by showing changes in amine and hydroxyl bands during cure. Other less sterically hindered systems tend to crosslink by way of the epoxide-secondary amine reaction, but this reaction is considered improbable for the TGDDM/DDS system (13). On the contrary, Danieley and Long (18) contend that the secondary amine reacts completely before the epoxide-hydroxyl reaction occurs. Reports in the literature by other workers, however,

do not support this contention (11,13-17).

Studies of thermosetting epoxy resin systems by Gillham and co-workers (19-28) reveal two important temperatures, Tgg and Tg_∞. Tgg is the glass transition temperature of the reactive system at its gel point. Tg_∞ is the ultimate glass transition temperature of the fully cured resin system ($Tgg<Tg_\infty$). With these two "critical temperatures", an isothermal cure gives rise to three possible curing situations:

1. $Tcure<Tgg$
2. $Tgg<Tcure<Tg_\infty$
3. $Tg_\infty<Tcure$.

If $Tcure<Tgg$, then the resin system may form a brittle glass (vitrify) prior to reaching a gel state. The system remains capable of flow upon reheating, since it has not attained a three-dimensional macrostructure. This cure condition is the basis for "B-stage" technology, since storage at a temperature at which uncured resins are glassy limits their reactivity, thus giving them an extended shelf-life (19,21,23-25).

In the second situation, $Tgg<Tcure<Tg_\infty$, the reaction proceeds through a viscous liquid state and forms a gel. The reaction continues until the glass transition temperature of the reactive system is equal to or slightly greater than Tcure. At this point, vitrification occurs, quenching most reactions in the system. Heating the resin to a temperature

greater than Tcure will cause devitrification, but it is a three-dimensional crosslinked macrogel and cannot flow. Also, heating will cause additional curing (19,21,23-25).

The last situation, Tg_∞<Tcure, leads to gelation but not vitrification (at the cure temperature). No post-cure is required in this situation provided that there is sufficient time to complete the cure. From the previous discussion it is obvious that the curing history introduces important factors in the dynamic mechanical response of epoxy-amine polymers (19,21,23-25).

Attaining the optimal cured state of the polymer is a major concern when utilizing epoxy-amine thermosetting resins. As mentioned previously, the epoxy-secondary amine reaction in TGDDM/DDS epoxy is inhibited due to steric hindrance. When the system cures, the glass transition temperature of the resin approaches that of the cure temperature (provided the cure temperature is less than the ultimate glass transition temperature, Tg_∞), and vitrification terminates most reactions (13,18-24,29,30). A post-cure above Tg_∞ becomes essential in stabilizing the final network structure and optimizing the mechanical properties of the polymer (18,21,22,31).

2.2 Mechanical Testing

Mechanical testing can be divided into two areas: dynamic and static testing. Dynamic testing considers the

effects of continuous cyclic loading and the resultant material response. Static (or quasi-static) testing generally involves response under constant load or response under increasing load to deformation and/or failure. Loadings in dynamic tests are small and rarely cause permanent sample distortion or failure. Therefore, dynamic testing maintains sample integrity except when temperature cycling alters material response. Since dynamic testing has the advantage of maintaining sample integrity while subjecting it to cyclic loading, it is thought to represent reasonably well what a sample would often experience during actual use (5,10,32).

Dynamic mechanical testing of any substance, polymeric or otherwise, can be divided into four different classifications:

1. Free vibration
2. Resonance vibration
3. Wave propagation
4. Sinusoidal excitation and response.

The Rheovibron and the Autovibron, which are the instruments used in the present study of the TGDDM/DDS system, are classified in the fourth group (5).

2.2.1 Principle of the Rheovibron

The Rheovibron DDV-II is a direct reading dynamic viscoelastometer designed to measure the dynamic mechanical properties (complex modulus, elastic modulus, loss modulus,

loss tangent and related compliances) of a sample over a wide range of temperatures, -150 C to +300 C, at selected frequencies of 0.01 to 1.0, 3.5, 11, 35 and 110 Hz. The Rheovibron was developed by Takayanagi (33) in the early 1960's. Since the instrument is relatively easy to operate and gives readings of the loss tangent ($\tan\delta = E''/E'$) directly without the need of involved calculations, it has been used extensively for rapid polymer characterization (5,34).

The Rheovibron operates by imposing a sinusoidal tensile strain of amplitude ε_o to a sample and then measuring the sinusoidal tensile stress response of amplitude σ_o with a stress transducer placed at one end. The tangent of the phase angle is directly displayed. The phase angle δ by which the stress leads the strain is bounded by $0 \leq \delta \leq \pi/2$, with $\delta = 0$ for a perfectly elastic solid and $\delta = \pi/2$ for a perfectly viscous fluid. With a sample of length L between the clamps and of cross sectional area A, the magnitude of the complex modulus $/E^*/$ can be expressed as:

$$/E^*/ = \frac{\sigma_o}{\varepsilon_o} \frac{L}{A} \qquad (2.1)$$

The instrument provides a potentiometer reading D, termed dynamic force, which is inversely proportional to the stress response σ_o. Stress and strain amplitudes can be expressed in terms of instrument calibration constants as:

$$\sigma_o = 1.0 \times 10^{7}\ N/D \quad \text{(dynes)} \qquad (2.2)$$

$$\varepsilon_o = 5.0 \times 10^{-3}\ (AF)N \quad \text{(cm)} \qquad (2.3)$$

The terms AF and N are dimensionless machine constants which are dependent upon the position of the amplitude factor and tanδ range, respectively. A combination of equations 2.1, 2.2 and 2.3 yields the standard operational equation 2.4 of the Rheovibron:

$$/E^*/ = \frac{2 \times 10^9}{D(AF)} \frac{L}{A} \qquad (2.4)$$

with the complex compliance /S*/ expressed as:

$$/S^*/ = \frac{1}{/E^*/} \qquad (2.5)$$

From the vector diagram in Figure 2.1, the relationships between complex modulus-/E*/, elastic modulus-E', loss modulus-E" and loss tangent-tanδ are evident (equations 2.6-2.9) (5).

$$/E^*/^2 = E'^2 + E"^2 \qquad (2.6)$$

$$E' = /E^*/ \cos\delta \qquad (2.7)$$

$$E" = /E^*/ \sin\delta \qquad (2.8)$$

$$\tan\delta = E"/E' \text{ (read directly from Rheovibron)} \qquad (2.9)$$

The previous equations appear quite adequate for analyzing samples using the Rheovibron; however, there is an inherent error in the measurements arising from instrument compliance. The error can substantially alter the data for high modulus materials. From equation 2.4, it is apparent that a plot of D(AF) versus L/A should be linear with an

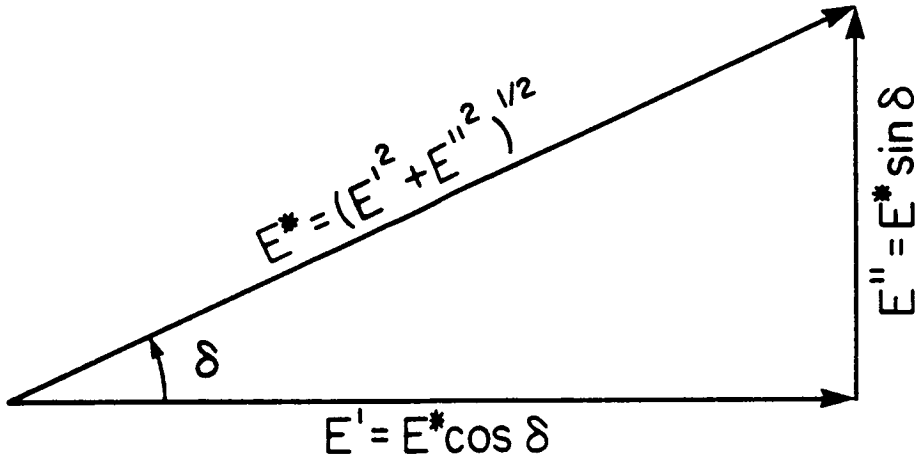

Figure 2.1 Modulus vector diagram

intercept at D(AF)=0 for an extrapolated sample length of zero. When the extrapolation is conducted, it is linear, but there is some positive value of D(AF) at L/A=0. The intercept represents a combination of two errors. One error value is the machine error which is a constant for all samples. The machine error arises from the compliance of the components of the drive train. The other error value arises from compliance of the sample in the grips. As yet, no relationship between sample composition and sample error has been derived. The combined errors (machine and sample), labelled Do, are easily accounted for in a modified Rheovibron equation:

$$/E^*/ = \frac{2 \times 10^9}{(AF)(D-Do)} \frac{L}{A} \qquad (2.10)$$

with E',E" and tan retaining their previous forms (8,35,36).

A more rigorous modelling of the Rheovibron was undertaken by Massa (36) in the interest of providing results on an "instrument-free" basis and of making the data more reproducible among different researchers. He considered additional effects such as "the deformation of components along the drive train, finite amplitudes in the force-monitoring Tl strain gauge, sample yielding in the holder grips, and system inertia." A significant result of the treatment by Massa involved the realization that the measured loss tangent differs from the "instrument-free" loss tangent. Consequently, Massa denoted the measured loss

tangent as "tanα" and the corrected loss tangent as "tanδ". From his analysis the following equations arise:

$$/E^*/ = \frac{2 \times 10^9 \ (1-M\omega^2/S_m^o)}{(AF)(D(1+(Doc/D)^2-2(Doc/D)\cos\alpha)^{1/2}-Dov)} \frac{L}{A} \quad (2.11)$$

$$E'' = \frac{/E^*/ \sin\alpha}{(1+(Doc/D)^2-2(Doc/D)\cos\alpha)^{1/2}} \quad (2.12)$$

$$E' = \frac{/E^*/(1-Doc/D\cos\alpha) \cos\alpha}{(1+(Doc/D)^2-2(Doc/D)\cos\alpha)^{1/2}} \quad (2.13)$$

$$\tan\delta = \frac{\tan\alpha}{(1-Doc/D\cos\alpha)} \quad (2.14)$$

The variables not previously mentioned are M-the mass of the drive train, ω-the frequency of the forced oscillations, S_m^o-the machine compliance, Doc-the machine error due to compliance of the drive train, Dov-the sample error due to compliance of the sample in the grips, and Do is the sum Dov+Doc. The term $M\omega^2/S_m^o$ is a correction for inertia effects and can be neglected for all usable frequencies except 110 Hz. Even at 110 Hz the correction is small ($3.8\pm1.7\%$). The frequency of ·35 Hz is considered unusable since it is the natural frequency of the machine for lateral vibrations. The precise modelling applied by Massa provides the experimenter with a more accurate measure of the dynamic mechanical properties of a system and an improved method of determining small changes in sample properties as treatment conditions are varied (8,35-37).

Recent modifications and improvements of the Rheovibron

have further reduced data variability and expanded the scope of measurements available (5,8,34,35,38-40). The most significant development is an automated Rheovibron, also known as the Autovibron (5,34,39,40). The automation system consists of a Hewlett-Packard Multiprogrammer, a Princeton Applied Research Model 5204 Lock-in Amplifier and a Slo-Syn synchronous stepping motor. The standard Rheovibron DDV-II-C testing base and electronics are retained. Some advantages of the Autovibron are:

1. constant sample tensioning which facilitates reproducibility,
2. low stress and strain requirements preventing permanent sample distortion,
3. accurate temperature control,
4. measurements available on an "almost" continuous basis ($\Delta T < 1.5^{o}C$ between readings),
5. data logging and reduction performed with a microcomputer,
6. more clearly defined secondary transitions,
7. accurate measurements of very small phase shifts,
8. measurements of very large phase shifts up to a $\tan\delta=3$ ($\tan\delta=1.2$-1.7 on manual Rheovibron), and
9. no requirements for constant operator attention.

The Autovibron thus facilitates measurement of material properties more accurately and in a shorter time frame than the Rheovibron (5,39,40).

2.2.2 Other Dynamic Test Methods

Among the other methods of dynamic mechanical analysis, the torsional braid analyzer (TBA) has been used most widely in the study of epoxy resin systems. The TBA is a free vibration instrument with a torsional pendulum. It was developed by Gillham and is described in several of his publications (20,23,24-26). The TBA is especially suited for the study of epoxy resins since one can follow the dynamic mechanical response through changes in the physical states from a viscous liquid to a rubbery solid and ultimately to a glass. Furthermore, relaxations of the cured resin system can be identified with the same instrument (19,25-27,41).

Another useful dynamic test method is the vibrating reed or cantilever. This device measures the amplitude of vibration as a function of frequency at fixed temperatures. A small strip is clamped on one end in a variable frequency electromagnetic oscillator. The free end traverses an amplitude maximum when the natural resonance of the sample is reached (5,32,34). The above is a simple arrangement, and it has been used to measure changes in dynamic mechanical properties of rubber samples *in situ* during irradiation (9).

2.3 Previous Results on Epoxies

2.3.1 Dynamic Mechanical Testing

2.3.1.1 TGDDM/DDS Epoxy

Utilizing a Rheovibron, research on the dynamic mechanical properties of TGDDM/DDS epoxy has been conducted previously by Keenan (8), Keenan et al. (42) and Bucknall and Partridge (43,44). Gillham has performed TBA investigations of the curing and transitions of TGDDM/DDS (45). Von Kuzenko et al. (46) conducted dynamic mechanical tests in a torsion mode and measured shear moduli and loss tangent of TGDDM/DDS. The work by Keenan, Keenan et al. and Von Kuzenko et al. addressed the additional effect of sorbed/desorbed moisture on the dynamic response of TGDDM/DDS epoxy.

Keenan (8) and Keenan et al. (42) conducted a study of TGDDM/DDS epoxy using a Rheovibron. The study utilized five different ratios of TGDDM to DDS with each sample containing a small percentage (7.7-8.5 wt%) of DGEBA, diglycidylether of bisphenol-A. The samples were cured at 120-177^{o}C for 30 minutes and at 177^{o}C for two hours. Testing on the Rheovibron was performed at a frequency of 11 Hz and equation 2.10 was utilized in data analysis. Another aspect of their work involved measurement of the dynamic mechanical properties of T300/5208 unidirectional composite tapes (Thornel 300 graphite fibers/NARMCO 5208 epoxy resin) (section 2.3.1.2).

Keenan (8) and Keenan et al. (42) found three transitions (α, β and ω) for TGDDM/DDS epoxy in the temperature range of -160°C to 320°C. A low temperature β-transition which occurred around -50°C was "attributed to a crankshaft rotational motion of the glycidyl portion of the epoxide group in TGDDM after reaction with DDS" (42). This finding was in agreement with other studies (7,31). The β-peak magnitude increased with increasing concentration of DDS, implying that more epoxide groups reacted with the DDS. The temperature of the peak did not vary with DDS concentration. It should be noted that other authors refer to this transition as a γ-transition (5,10).

The ω-transition, ca. 100°C, was a broad, low intensity transition arising from regions of dissimilar crosslinking and/or unreacted chain segments. The magnitude of the ω-transition depended more upon moisture content than DDS concentration. Significant peak broadening was observed as the moisture content of the sample increased. With water acting like a plasticizer of limited solubility, peak broadening would occur when a large distribution of molecular weights are participating in the transition.

The α-transition, or glass transition temperature of the system, displayed vastly different behavior dependent upon DDS concentration. At relatively minimal amounts of DDS (<18 wt%), the α-peak transition split into two peaks (above this composition only one α-transition was observed). The two

α-peaks were due to an additional cure, ie. $T_{gg} < T_{cure} < T_{g_\infty}$. A retesting of the sample revealed only one α-peak at the ultimate glass transition temperature of samples with a greater amount of DDS (>22 wt%). Therefore, after a post-cure above the ultimate glass transition temperature of the system, varing amounts of DDS had a limited effect upon the final glass transition temperature, implying similar network structures (8,42).

An additional effect that Keenan (8) mentioned briefly was the appearance of a shoulder on the main transition when the concentration of DDS was higher than 24 wt%. The shoulder was not ubiquitous to the system, since it did not appear at every TGDDM/DDS composition. The temperature at which the shoulder occurred was approximately the same as that of the first α-peak which disappeared upon subsequent testing of samples with lower DDS concentration (<18 wt%); although, Keenan failed to note this occurrence. Apparently the shoulder and the curing peak could arise from the same phenomena which will be addressed later.

Bucknall and Partridge (43,44) conducted a dynamic mechanical analysis on TGDDM/DDS epoxy which contained a relatively low molecular weight polyether sulfone (PES) modifier. A rather extreme time-temperature cure cycle was utilized with a maximum cure temperature of 200^{o}C for four hours. The Rheovibron was operated at a frequency of 110 Hz, and it was inferred that suitable corrections were made in

accord with Wedgewood and Seferis (35) who had extended the work of Massa (36).

Bucknall and Partridge (43,44) reported a Tg of 242°C for TGDDM/DDS epoxy while using the temperature at which tanδ first reaches a value of 0.15 to define the Tg. Tanδ peaks of 0.4 and higher have been found by others (8,42), and if Tg were defined as the temperature at which tanδ is a maximum, then the Tg peak may be 15 - 20°C higher than the values reported by Bucknall and Partridge. Dynamic mechanical analysis revealed a shoulder to the main transition in a mixed epoxy system (trifunctional epoxy (triglycidyl p-aminophenol) + TGDDM + DDS + PES). They attributed the shoulder to phase separation of the PES additive. Evidence of nodules of PES supposedly crosslinked with epoxy were observed by scanning electron microscopy and energy dispersive X-ray microanalysis. However, not every sample with an α-peak shoulder was reported to contain nodules. Since nodules were not always observed, they made the assumption that the separated phase in those samples was too small to be resolved by SEM. They found no evidence of phase separation in pure TGDDM/DDS epoxy.

The PES additive was hydroxy-terminated and could react with the epoxide groups. However, reaction with the epoxy would increase its solubility and hinder phase separation. Therefore, a crosslinked, PES rich nodule would be difficult to imagine.

Dynamic mechanical data from Bucknall and Partridge (43,44) reveal two important points. First, a separated phase containing an additive can cause a low temperature shoulder to the main transition. Second, pure TGDDM/DDS (77/23 wt/wt ratio) epoxy displayed no shoulder. However, a low temperature shoulder at the α-transition in samples containing >24 wt% DDS was reported by Keenan (8), suggesting an anomaly. A quite plausible explanation may be due to the curing conditions. Bucknall and Partridge mixed their samples at a higher temperature than did Keenan and used a longer, higher temperature cure cycle. The differences in mixing and curing probably resulted in a more rapid gelation of the samples tested by Bucknall and Partridge than those of Keenan. Phase separation is hindered or totally quenched in a gel (43,44); therefore the absence of a shoulder to the main transition appears plausible.

Gillham (45) made two important observations about TGDDM/DDS epoxy. First, the ultimate glass transition temperature occurs around 250°C, and second, temperatures above 220°C causes polymer degradation. The above implies that reaching Tg_∞ will cause some polymer degradation.

Research by Von Kuzenko et al. (46) revealed a glass transition temperature for TGDDM/DDS epoxy of 250°C at a frequency of 15.85 Hz in a torsional mode. Their research involved base resins of differing viscosity, which revealed that as the viscosity of base resins increases the loss

tangent α-peak becomes more disperse and the elastic shear modulus becomes lower at the onset of rubbery behavior. Tanδ peak broadening arose due to the high viscosity resins having a higher molecular weight between crosslinks (Mc) than the low viscosity resins. Consequently, the crosslink density was greater for the low viscosity base resin samples. The above explanation is supported by their shear moduli data. Their samples were cured for nine hours at 177^{o}C, ie. one hour cure and eight hours post-cure, and there was no mention of additional cure while testing. The incremental heating program for testing could have been slow enough that additional cure at each new temperature was complete when the sample was tested. Furthermore, there was a faint shoulder to the main transition at lower test frequencies, 15.90 mHz and 158.5 mHz, but no mention of it appeared in their discussion.

The appearance of a shoulder on the α-peak was reported in three separate studies in which two different techniques were used. Keenan (8) mentioned the observation but offered no explanation. Bucknall and Partridge (43,44) attributed it to an additive, and Von Kuzenko et al. (46) failed to address it. Attributing the shoulder to an additive seems plausible for the systems under consideration, but the polymers tested by Keenan and Von Kuzenko et al. supposedly contained no additives. In the case of Keenan, the shoulder was observed in close proximity to the temperature of the α-peak that

disappeared upon retesting the same specimen. However, the split α-peak was apparent only in samples of DDS concentration below 18 wt%, and the shoulder only at DDS concentration >24 wt%. Apparently an unusual transition occurred in the system which was somehow related to the cure conditions and the curing agent concentration. The obvious explanation for the shoulder is that it was a separated phase of somewhat lower than average crosslink density or that inhomogeneous mixing occurred. From the work of Bucknall and Partridge, it is apparent that a relatively lower crosslink density, separated phase containing an additive can create a shoulder, and from the work of Keenan it appears that a portion of gel-like material underwent additional cure during testing of the sample. The gel-like portion would be of lower crosslink density than the surrounding matrix; hence, the shoulder could arise from a relatively low crosslink density portion.

2.3.1.2 Graphite Fiber/Epoxy (TGDDM/DDS) Composites

Dynamic tests on unidirectional composite specimens have provided limited information due to the high modulus graphite fibers dominating the composite response. The β and ω-transitions were not evident due to the influence of the graphite fibers, thus substantiating the contention that those transitions were due to small chain molecular motions. Although the α-peak appeared, it was diminished in intensity due to the influence of the graphite fibers, and it was

shifted to higher temperature. The presence of the α-peak revealed that it did involve large segmental motions that occur in the glass transition temperature region (8).

Keenan (8) found excellent agreement between experimental results and theoretical predictions for the composite modulus using a "rule of mixtures" calculation. The experimental result is subject to operator error suggesting that the agreement found by Keenan may have been fortuitous.

The following calculation will illustrate the magnitude of this error. The Rheovibron (Section 2.2.1) provides a measure of material response in terms of a compliance (termed dynamic force) which is inversely proportional to the complex modulus. Keenan used equation 2.10 for data manipulation and determined that Do, the error constant, was 19. The composite specimens were 0.01 cm thick (other dimensions were not stated). If one takes typical sample dimensions (as suggested in the Rheovibron Product Bulletin (47)) of 5.0 cm X 0.4 cm and the complex modulus given by Keenan (8) for the composite ($E^* = 6.7 \times 10^{11}$ dynes/cm^2), then D in equation 2.10 can be determined. The calculation yields a D=3.7 (ie. the experimentally measured dynamic force is D+Do or 22.7). This is a very low value, especially since the scale for D ranges from 0 to 1000. Furthermore, Do is more than 5 times greater than the sample response. (It should also be noted, for those not familiar with the Rheovibron, that fractional

values of D are difficult to determine.) Hence, the fortuitous agreement in the "rule of mixtures" calculation is probably not accurate.

2.3.1.3 Epoxies Other than TGDDM/DDS

Several investigations have been made concerning the dynamic mechanical properties of epoxy resin systems other than TGDDM/DDS (5,6,19,22,48). Using torsional braid analysis, Gillham (23,24) has provided a general understanding of the extent of cure as it relates to the cure temperature (Section 2.1). May and Weir (49) found a low temperature (-60°C) γ-transition for an epoxy (diglycidyl ether of bisphenol-A reacted with m-phenylenediamine). This type of transition is generally common to epoxy systems, and it is presumed to arise from a crankshaft motion of the glycidyl portion of the molecule. Furthermore, relationships between dynamic mechanical properties and crosslink density have provided a better understanding of epoxy network structure (6,49).

The relationship between crosslink density and dynamic mechanical properties of epoxies were investigated by Bell (48) and Murayama and Bell (6). Rheovibron and solvent swelling studies were used to characterize epoxy films. The films were made by reacting various ratios (-6 to +102% stoichiometric amount of amine) of the diglycidyl ether of bisphenol-A with methylene dianiline. Estimates were made of crosslink density from stoichiometry and swelling studies

(48). By using the modulus of the polymer in the rubbery plateau region, estimates of crosslink density were derived from the theory of rubber elasticity. There was favorable agreement on the crosslink density as determined by these methods.

Specific changes in the dynamic mechanical properties were apparent as the crosslink density increased. The elastic modulus at room temperature and above the glass transition increased with increasing crosslink density. Also, the sharp decline in modulus, which is associated with main chain molecular motion, was shifted to higher temperature. The α-dispersion (loss tangent) decreased in magnitude and shifted to higher temperature with increased crosslink density. Changes in the α-dispersion revealed a less mobile network structure. In general, highly crosslinked epoxy systems should exhibit the type of behavior found by these investigations (5,10,19,22).

2.3.2 Static Testing of TGDDM/DDS Epoxy

Static (or quasi-static) testing on TGDDM/DDS epoxy has dealt primarily with mechanical characterization of the system, the effects of differing cure schedules and of sorbed/desorbed moisture on the properties of the resin. Some of the more important aspects of each will be discussed.

Morgan and O'Neal (14) conducted an extensive analysis and review of TGDDM/DDS epoxy. A number of pertinent

observations can be cited from their efforts. Through static tensile tests, they found that TGDDM/DDS epoxy of varying composition (10 to 35 wt% DDS) exhibited a broad glass transition region between 200°C and 250°C. The broad glass transition was evidenced by the "gradual decrease in tensile strength and modulus and the increase in ultimate elongation" as a function of increasing temperature (14). Also, the large ultimate extensions (>15%) encountered at the glass transition implied that crosslinking was low.

The amount of DDS in the cured epoxy directly affected the measured glass transition temperature. Increasing the weight percent of DDS up to 30% caused the Tg to increase, reaching a maximum of 250°C. Steric and diffusional limitations hindered reaction above 25 wt% DDS. Consequently, DDS concentrations higher than 30 wt% resulted in poor dispersion of the DDS, thereby causing plasticization of the cured resin at elevated temperature with a concomitant lowering of Tg. However, when considering the stoichiometry, a 37 wt% DDS weight fraction is required to react one-half of the epoxide groups. Therefore, the incomplete solubility of DDS in TGDDM can severely inhibit the extent of reaction with primary amines.

The SEM studies of Morgan and O'Neal (14) and Morgan et al. (15) on films strained directly in the electron microscope revealed a homogeneous crosslink density for epoxies with 15 to 35 wt% DDS. At lower DDS concentration

(10 to 15 wt%) a heterogeneous network was present. Upon failure, the heterogeneous material fractured into 2.5 nm diameter particles which are approximately the size of the TGDDM molecule. The homogeneity of the matrix is subject to question since the heterogeneity (with this analytical technique) may not have been resolved, even though its existence can be confirmed by a different method (8,43,44).

The failure mode of the resin was initiated by a crazing process with some evidence of limited shear banding. Right angle steps in the fracture topography were observed, confirming the shear banding failure mode. Since failure by crazing would yield small extensions, the shear banding was presumed to facilitate the unusually large extensions that occurred near the glass transition region (14,15).

Danieley and Long (18) studied the effects of time and temperature of cure on the glass transition temperature and moisture absorption of TGDDM/DDS epoxy. They discovered a direct dependence of the glass transition temperature, measured by an indentation method, on temperature and time of cure. The glass transition temperature approached an asymptotic limit of 240^{o}C with the effect of increased cure temperature being more pronounced than that of increased time of cure. It should be noted that the highest cure temperature was 504^{o}K (231^{o}C). Therefore it is possible that the ultimate glass transition temperature may not have been attained, since vitrification may have arrested further

reaction. They found that moisture absorption increased with an increase in the extent of cure. They concluded that moisture absorption occurs primarily at hydroxyl groups. Also, they suggested that moisture uptake is a more sensitive measure of the extent of cure than is the glass transition temperature.

Recent work by Yang (50) confirms increased moisture absorption with an increase in the extent of reaction. However, moisture uptake was shown to be approximately inversely proportional to room temperature polymer density in TGDDM/DDS epoxy. As the extent of reaction increases, there are increases in the room temperature free volume of the polymer and room temperature density decreases. Yang suggested that water absorption occurs through the electrostatic attraction between functional groups and water, "and the degree of H_2O uptake is determined by unoccupied volume of the epoxy resin."

McKague et al. (51) measured the effects of humid environments on the glass transition temperature of NARMCO 5208 resin. A depression of the dry glass transition temperature was found after moisture exposure. The glass transition temperature for dry NARMCO 5208 resin, measured by a loaded-column expansion test, was 246°C. Decomposition of the material occurred at 316°C.

Measurements of property losses in TGDDM/DDS epoxy which was exposed to high temperatures and humidities were

conducted by Browning (52). The maximum cure was 177°C for 30 minutes. The glass transition temperature, measured by a deflection method, was 177°C. The short cure time that Browning employed led to the glass transition temperature being substantially lower than other reported values for this system cured at 177°C.

From the previous studies, it is apparent that the glass transition temperature of TGDDM/DDS epoxies is variable (Table 2.1). It is highly dependent upon the TGDDM/DDS ratio, additives in the epoxy, cure conditions, method of measurement, ie. static or dynamic, and the definition used for Tg. Considering the significance placed upon the glass transition temperature, especially of materials used in extreme service conditions, it is important to establish an accurate determination of its value by a precisely defined technique.

2.4 Effect of Radiation

The effects of ionizing radiation on the mechanical properties and molecular structure of polymers vary widely. Some polymers such as polypropylene lose approximately 50% of their original tensile strength after a dose of 10 Mrads. Others, such as polystyrene, retain almost 100% of their original tensile strength when irradiated to a dose of 10,000 Mrads. Polystyrene is "protected" from degradative radiation effects by the aromatic ring on each repeat unit (1). Since

Table 2.1 Glass transition temperatures of TGDDM/DDS epoxy[1]

Tg(°C)	TGDDM/DDS content	Cure °C/hrs	Method of Measurement
177	na[2]	177/0.5	Indentation (52)
246	NARMCO 5208	204/4	Loaded-column (51)
88	12 wt% DDS	177/5	Tensile test: E'rt/2[3] (14)
185	17 wt% DDS	177/5	" " "
230	23 wt% DDS	177/5	" " "
250	30 wt% DDS	177/5	" " "
235	35 wt% DDS	177/5	" " "
70	na	149/1	Indentation (18)
150	na	149/9	"
130	na	175/1	"
200	na	175/9	"
200	na	203/1	"
225	na	203/9	"
230	na	231/1	"
240	na	231/9	"
208	11phr DGEBA/19phr DDS[4]	177/2	Rheovibron: 11 Hz[5] (8)
205	11phr DGEBA/22phr DDS	177/2	"
270	11phr DGEBA/25phr DDS	177/2	"
290	11phr DGEBA/28phr DDS	177/2	"
292	11phr DGEBA/32phr DDS	177/2	"
250	na	na	TBA: 1 Hz (45)
230	na	177/9	Torsion: 15.90 mHz[6] (46)
242	30phr DDS	200/4	Rheovibron: 110 Hz (43)

[1] many values estimated from graphs.
[2] not available.
[3] Tg is presumed to occur when the elastic modulus reaches 1/2 its room temperature value.
[4] phr - parts/hundred parts TGDDM; DGEBA - diglycidyl ether of bisphenol-A.
[5] Tg is peak value of loss tangent.
[6] Tg is where value of loss tangent = 0.15.

the TGDDM/DDS molecules each have two aromatic rings, they should be resistant to radiation induced degradation.

According to Parkinson and Sisman (1), aromatic compounds "can absorb energy in going to an excited state and can dissipate this excitation energy through a process which does not disrupt the molecule." Up to a dose of 10^9 rads (1,000 Mrads), they found almost no apparent loss in flexural strength for an aromatic amine-cured (diamino diphenyl methane) epoxy which was exposed to reactor radiation. It was further demonstrated that aromatic compounds, when used as additives in non-aromatic substances, yield a greater resistance to radiation than the individual components would have provided if irradiated separately.

Radiation induced polymer degradation results from chain scission. Quaternary carbon atoms in the main chain are the focal point of chain scission reactions (however, polypropylene undergoes chain scission and has no quaternary carbon atoms) (1). The curing reactions proposed for TGDDM/DDS epoxy do not yield any quaternary carbon atoms. As will be shown by the following investigations, the aromatic nature of the TGDDM/DDS system, combined with the lack of main chain quaternary carbon atoms, should provide a high resistance to radiation induced degradative processes.

Netravali (53) measured the thermal response of TGDDM/DDS epoxy samples on a DSC using a scanning rate of $20^{\circ}C$/min. Samples were evaluated prior to and after

irradiation with 0.5 MeV electrons and ^{60}Co gamma radiation. Epoxy samples which were cured below the ultimate glass transition temperature (ie., Tg_{∞}) will undergo additional cure during the DSC scan, resulting in an exothermic reaction. Both types of radiation produced a decrease in the curing energy. The curing peak temperature decreased slightly compared to a control sample. These results indicate that either type of radiation, electrons or gamma, continues the cure in the sample. The doses were relatively low (700 Mrads for electrons, 160 Mrads for gamma radiation) when considering the exposure to radiation during the lifetime of structures in some space applications.

Naranong (54) studied unidirectional T300/5208 and several other unidirectional composites after exposure to 0.5 MeV electrons. Flexural modulus and flexural stress were measured in a three point bending test on an Instron. The flexural stress and flexural modulus increased slightly after a 5,000 Mrad dose of electron radiation. These tests suggest that composites are highly radiation resistant.

Wolf (2) examined the mechanical properties of T300/5208 composite tapes with different fiber orientations. The composite specimens had been irradiated with 0.5 MeV electrons to dosages up to 10,000 Mrads. Flexural stress of the samples increased for each orientation as measured by a three point bending test on an Instron. Interlaminar shear stress (ILSS), measured on notched samples in a tensile mode

with an Instron, increased in samples irradiated up to a dose of 1,000 Mrads. Above 1000 Mrads,the interlaminar shear stress declined. The initial increase in ILSS was assumed to arise from a release of internal stresses by chain scission of the more highly strained bonds. Subsequently degradation at the interface occurred, yielding a decline in ILSS.

Wolf also reported the tensile properties of transversely oriented fiber composites. Samples were tested in three point bending. This test provides a measure of interfacial bond strength. The flexural stress and flexural modulus both increased with radiation up to dosages of 10,000 Mrads.

Park et al. (55) measured interlaminar shear stress (ILSS) of T300/5208 unidirectional four-ply composites in compression and tension modes and with a support fixture to prevent peel. Samples were irradiated up to a dose of either 9,000 or 10,000 Mrads with 0.5 MeV electrons. The irradiated samples had a higher ILSS compared to the control. Park proposed two qualitative explanations for the increase in ILSS. His first explanation was based on the results from ESCA analysis conducted by Wolf (2) and Seo (56). They found an increase in the oxygen content after irradiation. As a result of this finding, Park suggested that the additional oxygen could increase the interfacial interaction energy, thus increasing the ILSS. His second explanation was that radiation could cause matrix shrinkage. Matrix shrinkage

creates a radial compressive stress normal to the fiber surface which could increase the bond strength between matrix and fiber. A possibility that the author did not suggest is that the crosslink density at the interface may also be affected by radiation.

The study by Sykes et al. (4) on T300/Fiberite 934 (TGDDM/DDS/ester epoxy/BF3 catalyst) composites which were tested prior to and after irradiation revealed several interesting phenomena. The damping, measured with a Dupont 981 DMA, displayed a fairly narrow peak ca. 200°C for the control. After a dose of 10,000 Mrads, the peak broadened considerably, increased in magnitude and shifted down to 150°C. Radiation caused a lowering of the softening temperature and an increase in sample expansion when compared to a control. These changes were consistent with radiation induced matrix degradation. However, the modulus below 100°C increased for the irradiated samples over a control. Sykes et al. suggested that matrix embrittlement led to the higher modulus. Evidence from other tests (TMA and vacuum weight loss) suggested that volatile degradation products were generated during irradiation. They proposed that the free volume increased (lower Tg), and degradation products filled the free volume to "freeze out" and embrittle the matrix below 100°C. Above 100°C these degradation products plasticized the matrix, yielding a lower Tg and a lower modulus. Even though some samples show degradation with

radiation, on balance, both the TGDDM/DDS matrix and graphite fiber/(TGDDM/DDS) epoxy composites retain excellent mechanical properties after large doses of radiation.

By employing different dynamic mechanical techniques, several authors (9,32,57,58) have studied the change in modulus of elastomers during exposure to ionizing radiation. Since elastomers are analogous to thermosets with a low crosslink density, then mention of these studies is noteworthy. Jenkins (9) studied the dynamic properties of three elastomers using a miniaturized vibrating reed technique in situ during gamma irradiation. The modulus first decreased and then increased with dose. The initial reduction in modulus could occur due to chain scission being the dominant process. Subsequently, crosslinking would dominate, yielding an increase in modulus. It should be noted that a combination of crosslinking and chain scission occur in the region of increasing slope in the modulus/dose curve.

Traeger (32) and Traeger and Castonguay (57,58) investigated the dynamic mechanical response of several silicone rubbers and styrene-butadiene rubbers prior to and after exposure to gamma radiation. The dynamic mechanical measurement technique employed a twin transducer that permitted frequency scans as well as temperature scans. They included measurements of sample hardness (Shore A) and solvent swelling on control and irradiated specimens. Their

dynamic mechanical results were in agreement with Jenkins (9) in that the modulus first decreased and subsequently increased. They concluded that chain scission occurred initially, causing a decrease in modulus. As the radiation dose was increased, crosslinking predominated yielding an increase in modulus. However, the loss tangent peak in the styrene-butadiene rubbers broadened and shifted to lower frequencies (temperatures) with increasing radiation dosages. These loss tangent peak changes occurred even though the crosslink density (measured by solvent swelling) increased with dose. The investigation by Jenkins revealed similar changes in the loss tangent spectrum. The loss tangent peak should shift to higher frequency with an increase in crosslink density. This behavior is contrary to what would be expected, but no explanation was presented. If the polymers were plasticized by degradation products, then the loss tangent could shift to lower frequency. However, the sol content (soluble fraction extracted by solvent swelling) decreased with dose; therefore, plasticization resulting from degradation products is unlikely.

Characterization of the mechanical properties of TGDDM/DDS epoxy has been attempted by various means. The results vary widely. From these studies it appears that the result one obtains will be strongly dependent upon cure time, cure temperature and measurement technique. TGDDM/DDS epoxy as a composite matrix material appears to be highly resistant

to ionizing radiation. Its high concentration of aromatic rings and lack of main chain quaternary carbon atoms probably explain this fact. Radiation induced degradation may cause a reduction in the dynamic elastic modulus of the epoxy alone, but apparently composites are not adversely affected.

3. EXPERIMENTAL PROCEDURE

3.1 Materials

3.1.1 TGDDM/DDS Epoxy

The epoxy resin system used in this study was predominantly TGDDM (tetraglycidyl 4,4'-diamino diphenyl methane) cured with DDS (4,4'-diamino diphenyl sulfone). Ciba-Geigy manufactures TGDDM under the name MY-720 Araldite Epoxy and DDS under the name HT-976 Hardener. The chemical structures are illustrated below.

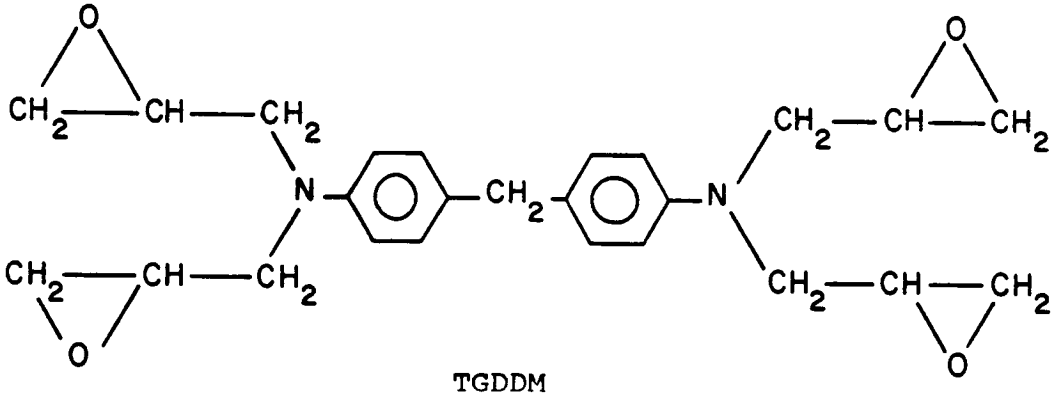

TGDDM

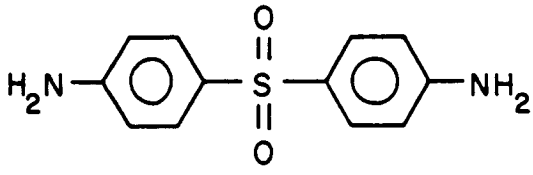

DDS

The resin and hardener were used without further purification (59,60).

3.1.2 Composites

The graphite fiber reinforced composites investigated consisted of Thornel 300 (T300) graphite fibers (Union Carbide) and either NARMCO 5208 or NARMCO 5209 epoxy resins (Celanese). They are referred to as T300/5208 and T300/5209, respectively. T300 filaments have a mean diameter of 7 microns and are supplied as a 3,000 filament tow. NARMCO 5208 is a TGDDM/DDS based epoxy system (61). NARMCO 5209 is a TGDDM/DGEBA/DDS epoxy system. DGEBA is the diglycidylether of bisphenol-A (its chemical structure is illustrated below).

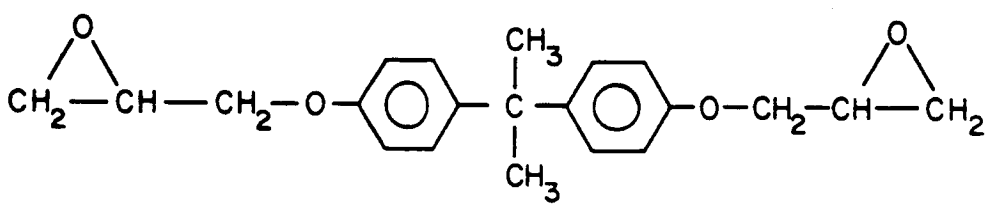

DGEBA

T300/5208 and T300/5209 composite specimens were all fabricated and cured at NASA Langley Research Center, Hampton, Virginia. The maximum cure temperatures were 177°C and 121°C for the T300/5208 and T300/5209 composite specimens, respectively. Three different fiber lay-ups were available: one-ply longitudinal (0° fiber orientation), one-ply transverse (90° fiber orientation) and four-ply transverse (orientation is relative to the long dimension of the specimen). Longitudinal and transverse one-ply samples, as received, had approximate dimensions of 7.62cm x 1.27cm x 0.03cm. Transverse four-ply samples had approximate

dimensions of 7.62cm x 1.27cm x 0.06cm. One-ply specimens with fibers oriented 45° were obtained from unidirectional composite sheets approximately 30cm x 30cm x 0.03cm.

3.2 Equipment

3.2.1 Radiation Source

The radiation source was an electron accelerator which was manufactured by High Voltage Engineering Corporation. It was operated at 500,000 volts from an insulated core transformer with a beam current of 8.3 milliamperes. The beam was distributed (raster scanned) over an area with dimensions 6" wide x 48" high. Samples were vertically suspended on a conveyor system. During one revolution through the accelerator enclosure, samples were struck by the beam alternately on each side. The conveyor speed was 10 ft/min. A 5 Mrad dose was imparted during each pass through the beam (10 Mrads per revolution).

3.2.2 Dynamic Mechanical Characterization Equipment

A Rheovibron DDV-II and an Autovibron DDV-II-C, both of which were manufactured by Toyo Baldwin Company of Japan and distributed in the United States by Imass, were used to evaluate the dynamic mechanical properties of the materials investigated in this study. Both instruments provide a measure of complex modulus, elastic modulus, loss modulus and loss tangent of thin film specimens in a tensile mode as a function of temperature at constant frequency.

3.2.3 Thermal Characterization Equipment

Thermal characterization of epoxy specimens was measured by differential scanning calorimetry (DSC). A Dupont 990 Thermal Analysis System (located at the University of North Carolina at Chapel Hill) fitted with a DSC cell was used for the investigation of calorimetric properties. Measurements were made in a nitrogen atmosphere. Specimens were sealed in aluminum sample pans for this study.

3.3 Procedures

3.3.1 Epoxy Sample Preparation

TGDDM/DDS epoxy resins were prepared in the following weight/weight ratios of TGDDM/DDS - 85/15, 80/20, 73/27 and 63/37. The procedure consisted of weighing approximately 150-200g of TGDDM (MY-720) into a tared beaker. The TGDDM was heated to 105-110^{o}C while stirring, then the calculated amount of DDS (HT-976) (for the desired ratio) was added slowly. Since DDS dissolves slowly in TGDDM, the mixture was maintained at 105-110^{o}C and stirred for 30 minutes after all the DDS was apparently dissolved. The mixture was poured into aluminum weighing dishes which were placed in a heated (110^{o}C) vacuum desiccator and deaerated for 30 minutes. Samples were cooled in the desiccator, removed and stored in nitrogen filled Ziploc^{R} bags in a freezer at 5^{o}C. The above procedure provided the B-stage prepolymer used in thin film preparation.

Rheovibron/Autovibron studies require thin, bubble-free films with a uniform thickness. The following procedure was used to fabricate the epoxy film specimens. Teflon sheets (7.5cm X 10cm) were placed in a heated vacuum desiccator (150^{o}C). Next, several pieces of B-stage epoxy (approximately 1.5g) were placed on the teflon sheets. After melting for 5 to 10 minutes under slight vacuum, the teflon sheets with melted epoxy were removed, a Mylar^{R} spacer (0.02cm thick) was placed between the two sheets, and the sheets were pressed together. Two aluminum sheets (7.5cm X 10cm) were placed on the teflon sheets for support (using spring clips to hold them in place), and the sample was returned to the desiccator (Figure 3.1). Samples were cured under slight vacuum in a nitrogen atmosphere.

When using the Rheovibron/Autovibron, specimen size is important. Generally, the width is >0.5cm, the length is >8.0cm and the appropriate thickness is determined by the sample modulus. Epoxy and composite specimens were cut to a width of approximately 0.4cm with a miniature table-top saw. After cutting, the epoxy samples were sanded with 600wt sandpaper in order to obtain a more uniform thickness. After sanding, the epoxy samples were judged suitable for testing. To prevent moisture absorption, specimens were stored in a vacuum desiccator at ambient temperature prior to and after irradiation.

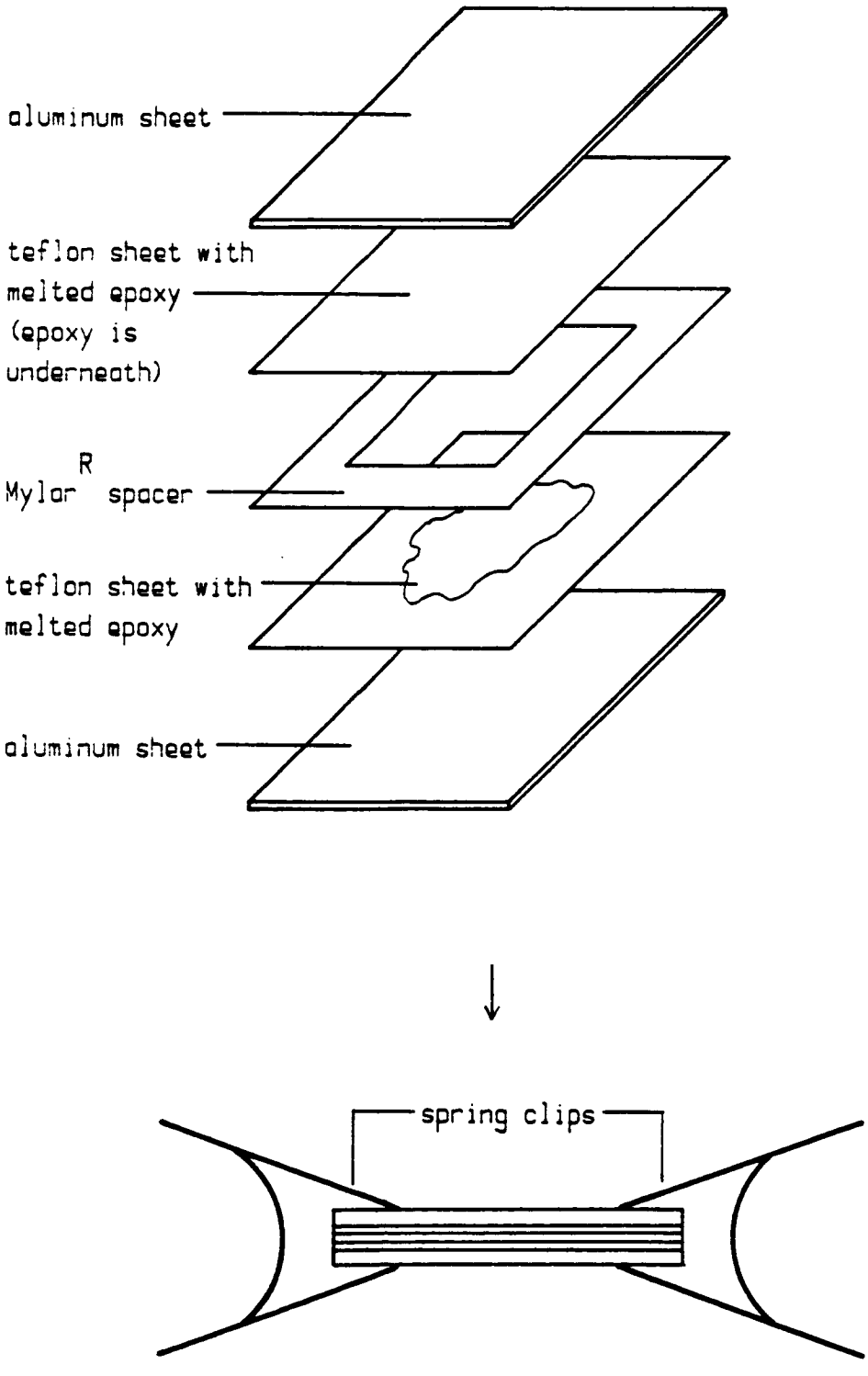

Figure 3.1 Diagram of specimen holder for film preparation

3.3.2 Irradiation Procedure

Prior to radiation exposure, the samples were placed in a vacuum desiccator at ambient temperature for at least one week in order to remove oxygen and other gases. Samples were then removed from the desiccator, placed flat on a sheet of aluminum foil and held in place with tape. The foil was folded, and the top and edges were sealed with a fast curing epoxy glue. As the top was sealed, a piece of glass tubing was positioned to permit direct vacuuming of the aluminum foil bag. The aluminum foil bag was placed in a vacuum desiccator and evacuated overnight. The aluminum foil bag was removed from the desiccator, a vacuum line was attached to the glass tube, and the tube was heat sealed. Sealed aluminum foil bags were placed in nitrogen filled Ziploc^{R} bags and suspended from the conveyor on the accelerator during irradiation exposure.

3.3.3 Dynamic Test Procedure

Rheovibron and Autovibron testing was conducted according to the instruction manuals supplied with the equipment. All tests were conducted at a frequency of 11 Hz. The temperature ranges over which measurements were made and the specimen dose levels are listed in Table 3.1 for each type of specimen. Measurements of complex modulus (E*), elastic modulus (E'), loss modulus (E") and loss tangent (tanδ) are reported. The glass transition temperature was

Table 3.1 Summary of specimen types, irradiation doses and temperature ranges investigated by dynamic mechanical analysis

Sample	Temperature range (°C)	Dose Levels[1]
T300/5209/90/1[2]	30 - 200	c,1,2,3,4,5,10
T300/5209/90/4	30 - 200	c,1,2,3,4,5,10
T300/5209/45/1	30 - 200	c,1,2,3,4,5,10
T300/5209/0/1	30 - 230	c,1,2,3,4,5,10
T300/5208/90/1	30 - 320	c,1,2,3,4,5,10
T300/5208/90/4	30 - 320	c,1,2,3,4,5,10
T300/5208/45/1	30 - 320	c,1,2,3,4,5,10
T300/5208/0/1	30 - 330	c,1,2,3,4,5,10
80/20 TGDDM/DDS	-120 - 320	c,1,2,3,4,5,10
73/27 TGDDM/DDS	-120 - 320	c,1,2,3,4,5,10
63/37 TGDDM/DDS	-120 - 320	c
85/15 TGDDM/DDS	30 - 320	c

[1] c = control, 1 = 1000 Mrads, 2 = 2000 Mrads, 3 = 3000 Mrads, 4 = 4000 Mrads, 5 = 5000 Mrads, 10 = 10,000 Mrads.

[2] Composite specimens will be designated in this manner: fiber/resin/fiber orientation (to long direction)/number of plys.

assumed to occur at the peak maximum of the loss tangent spectrum (α-transition). The loss tangent magnitude reported in the tables was the maximum tanδ attained (62).

3.3.4 DSC Measurements

The specimens which were used in the DSC study were obtained from the epoxy films by fracturing the films into suitably sized pieces. The samples were scanned from $0^{\circ}C$ to $300^{\circ}C$ at $20^{\circ}C$ per minute scanning rate. The area of the exothermic peak was determined manually. Using the peak area, the exothermic curing energy in cal/gm was determined.

3.3.5 Sorption/Desorption Procedure

A limited number of samples were exposed to a sorption/desorption cycle in order to remove low molecular weight products. Sample weights were measured on a Sartorius balance which was accurate to 0.01 milligrams. Samples that had been vacuum desiccated to constant weight were placed in acetonitrile (Aldrich) at $37^{\circ}C$. Solvent uptake was followed to equilibrium. Samples were desorbed in a vacuum oven ($100^{\circ}C$) to constant weight. The weight loss was determined by taking the difference between sample weight prior to sorption and after desorption. Following desorption, samples were tested on the Autovibron to detect any differences in dynamic mechanical properties.

4. RESULTS AND DISCUSSION

The initial phase of this investigation involved characterizing the dynamic mechanical properties of the TGDDM/DDS epoxy resin system on a Rheovibron. Various weight/weight ratios of TGDDM to DDS were evaluated. Based on their dynamic mechanical response, two of the four ratios were chosen for radiation exposure, namely 73/27 and 80/20 TGDDM/DDS. Composite specimens, fabricated at NASA Langley were also evaluated (section 3.1.2). Since the epoxy and composite specimens are high modulus materials, an error correction was applied in accordance with the procedure outlined by Massa (36).

Subsequently, an Autovibron (automated Rheovibron) became available for sample characterization. The epoxy and composite samples were exposed to different dose levels (1000, 2000, 3000, 4000, 5000 and 10,000 Mrads) of ionizing radiation (0.5 MeV electrons). The initial results on the Autovibron indicated that certain portions of the dynamic mechanical spectrum were erroneous; ie. there was no significant decrease in elastic modulus above Tg, and the intensity of the loss tangent was suppressed. An analysis of the Autovibron by Imass revealed that the machine was not functioning properly, and that results on calibrated samples could not be reproduced. After this correction was made, it was necessary to repeat the measurements. However, it was

observed that, although the loss tangent was suppressed, the glass transition temperature was the same before and after the modification was made. Therefore, only two of each composite type have been evaluated at each dose level, and three epoxy samples have been evaluated at each dose level after the correction was made (total number of composite and epoxy specimens is 154). Since there were only two or three replicates, extensive statistical analysis was not done. The measured properties are reported in the tables as mean values, and they are consistent. In the figures, the dynamic mechanical spectra are for a single sample.

As noted above, the glass transition temperatures from the original investigation were in agreement with the glass transition temperatures in the second investigation. (The initial problems with the Autovibron did not affect the determination of Tg.) Therefore, the glass transition temperatures from the two investigations have been combined and a 95% confidence interval has been developed through statistical methods.

The error correction procedure reported by Massa (36) for the Rheovibron had to be modified for the Autovibron. In the interest of accurately assessing variations in elastic moduli, an error correction procedure was developed for the Autovibron. The changes in elastic moduli reported in the tables have been corrected using the procedure outlined in the Appendix, although the DMA scans have not been corrected.

4.1 Dynamic Mechanical Characterization

A dynamic mechanical analysis can provide several types of information per test (32). The Autovibron provides the typical dynamic mechanical properties (E*, E', E" and tan delta) at constant frequency as a function of temperature. It can also measure two other parameters which are useful in understanding material properties. One measurement is the change in length as a function of temperature. The other measurement is the specimen contraction following a thermal cycle. The change in length is analogous to an expansion coefficient. When an increase in slope is exhibited in the expansion curve, the sample has gone through a glass transition (Tg), or there is sample yielding. The sample contraction after a thermal cycle may indicate a release of internal stresses and/or a loss of volatile material from the sample.

4.1.1 Preliminary Investigations of TGDDM/DDS Epoxy

Epoxy resin film specimens were fabricated in four different weight/weight ratios of TGDDM/DDS (63/37, 73/27, 80/20, 85/15). Shown in Figures 4.1 - 4.4 are typical dynamic mechanical spectra (Autovibron) for 63/37, 73/27, 80/20 and 85/15 TGDDM/DDS specimens, respectively. The curves are quite reproducible (Figures 8.3 and 8.4 in the Appendix).

A response that is characteristic of a crosslinked epoxy

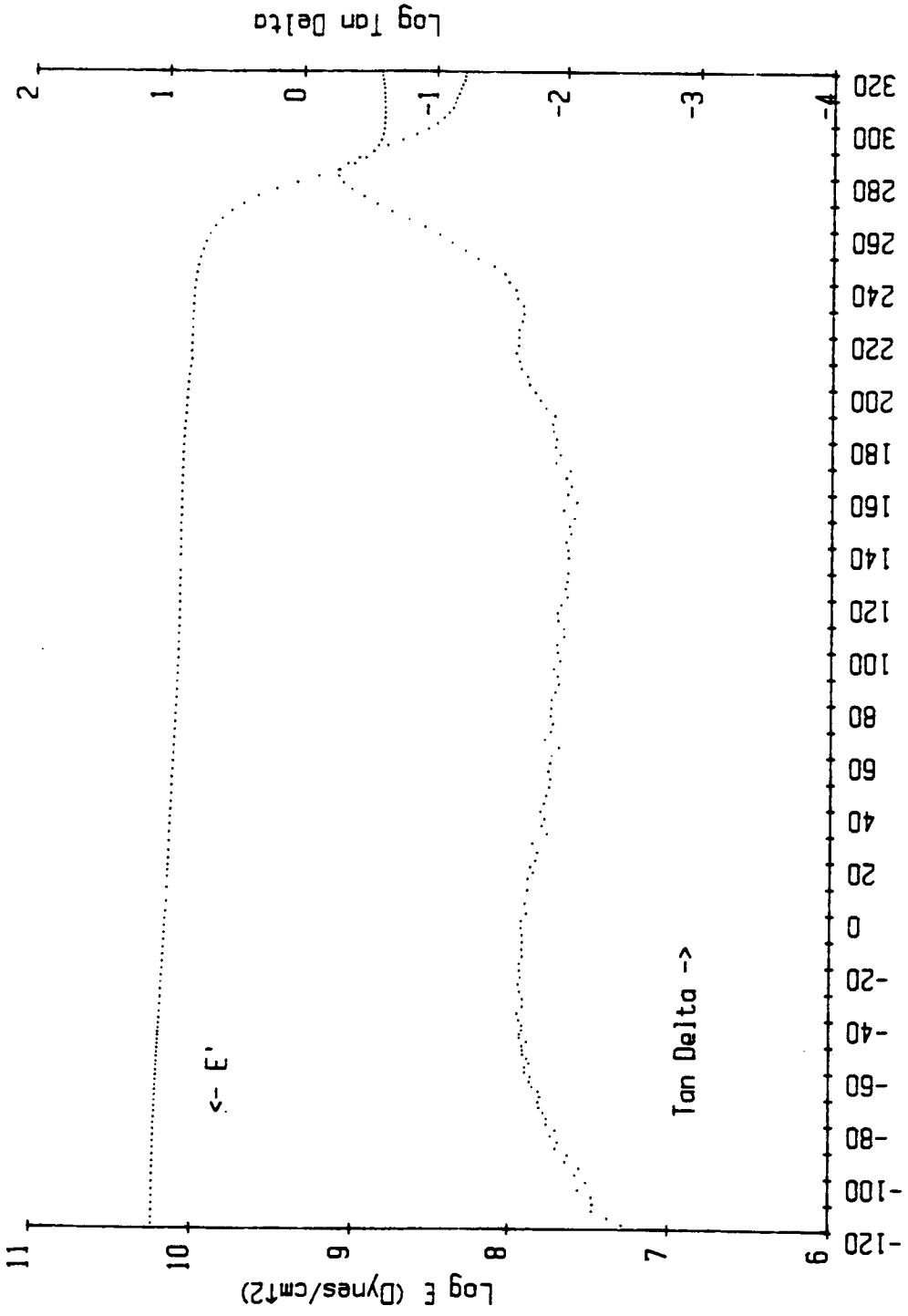

Figure 4.1 Dynamic mechanical spectrum of cured 63/37 TGDDM/DDS epoxy

network is shown by the elastic modulus (E') and loss tangent (tanδ) spectra for a 63/37 ratio of TGDDM/DDS. A slight, monotonic decrease is displayed by the elastic modulus in the temperature range of -120°C to +230°C. Above 230°C, there is more than an order of magnitude decline in E' which is confined to a very small temperature range (250°C to 290°C). The onset of main chain molecular motion is indicated by the decrease in E' and is associated with the glass transition region. Above 290°C, E' levels off, and this flat region is known as the "rubbery plateau region." In this temperature region, typical rubbery behavior is displayed by the resin.

The loss tangent spectrum provides information on molecular motions and internal friction (damping). In Figure 4.1, there are three distinct damping peaks. The peak at lowest temperature is usually referred to as the γ-transition. This transition is a very broad, low intensity transition ca. -45°C. The γ-transition, in epoxy systems, is generally thought to arise from a crankshaft rotational motion of the glycidyl portion of the molecule after it has been reacted (8,42). As suggested by another study (63), up to five different relaxation phenomena constitute the γ-transition in crosslinked epoxies. However, only one relaxation in this region was resolved in Autovibron analysis.

The γ-transition appears to be a common feature in crosslinked epoxies. It does occur in other polymers, such

as, bisphenol-A polycarbonate. The presence of the γ-transition has been associated with high impact strength. This type of transition would be beneficial in an adhesive for high performance structural composites.

The next damping peak occurs at 215°C and is due to additional curing reactions in the sample, ie. $Tgg < Tcure < Tg_\infty$ (section 2.1). This type of behavior is well documented (5,6,8,10,42) and provides a qualitative measure of the extent of cure in a sample. In other words, the lower the degree of cure, the more intense the curing transition and the lower the onset of the transition. If the specimen is subsequently cooled after it is tested at temperatures exceeding Tg_∞ and tested again, then the curing peak is no longer present (8,42,47). The exothermic curing energy associated with this transition will be discussed in section 4.2.

The ultimate glass transition temperature is ca. 280°C. Traversing the α-transition region indicates that the sample has changed from a brittle, glassy solid to a viscous, rubbery solid. The temperature of the α-transition "can be considered the most important material characteristic of a polymer as far as mechanical properties are concerned" (10). A primary focus of the present investigation will be concerned with variations in the α-peak as a function of dose. It should be noted, however, that the samples have been modified by the additional curing reaction noted above

when the α-transition is reached.

In Figure 4.2, the elastic modulus and loss tangent for a 73/27 TGDDM/DDS epoxy are displayed. The elastic modulus, E', decreases in a slight monotonic fashion up to 155°C. As the temperature is scanned from 155°C to 240°C, E' first decreases and then increases. These changes in E' are consistent with additional curing reactions. The 73/27 TGDDM/DDS has a greater epoxy excess than the 63/37 TGDDM/DDS, and the original extent of cure in 73/27 TGDDM/DDS is less than in 63/37 TGDDM/DDS. Again the situation $T_{gg} < T_{cure} < T_{g_\infty}$ is demonstrated. The cure reaction is more pronounced in the 73/27 TGDDM/DDS system than in the 63/37 TGDDM/DDS system due to the greater excess of epoxide groups in the former case. In other words, during the original cure the primary amines are consumed rapidly (chain extension), followed by crosslinking through epoxide-hydroxyl reactions. However, the Tg of the system becomes greater than Tcure and vitrification occurs. Gupta et al. (13) have found that the epoxide-hydroxyl reaction continues in the vitrified state, but the total (available) cure is not completed. The increase in modulus between 200°C and 240°C arises due to the system revitrifying at a higher temperature as the crosslinking reactions proceed. Above 240°C, all functional groups have apparently reacted, and the modulus of the 73/27 TGDDM/DDS exhibits similar behavior to the 63/37 TGDDM/DDS.

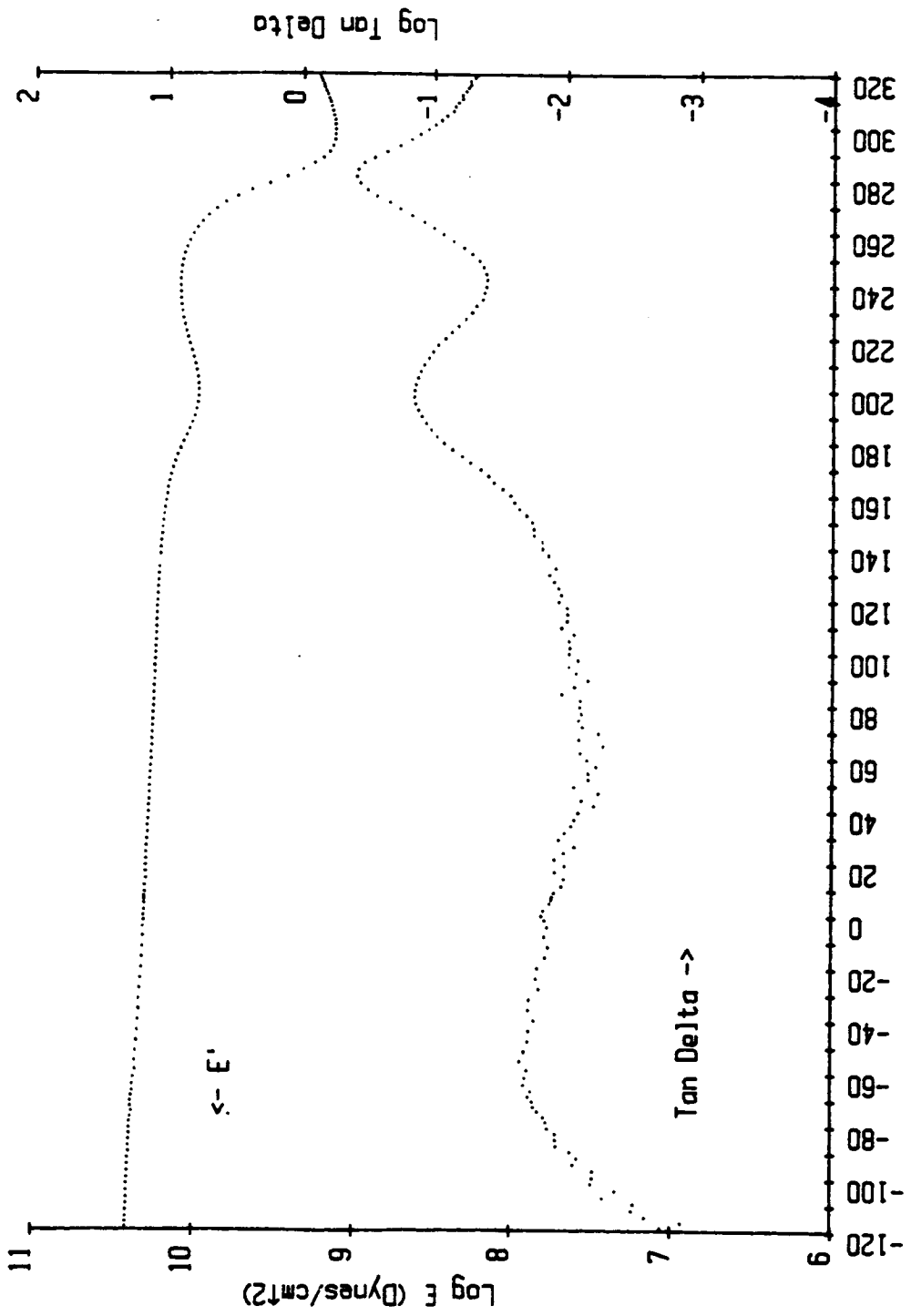

Figure 4.2 Dynamic mechanical spectrum of cured 73/27 TGDDM/DDS epoxy

The loss tangent spectrum for the 73/27 TGDDM/DDS has three distinct transitions, which are similar to the transitions displayed by the 63/37 TGDDM/DDS specimen. The transitions arise due to analogous molecular motions. The major difference, as would be expected from the response of the elastic modulus, is a more intense curing peak. The α-transition occurs at 280^{o}C, suggesting that the (final) network structure for each ratio is similar after Tg_{∞} has been exceeded (8).

The dynamic mechanical spectrum for the 80/20 TGDDM/DDS epoxy is illustrated in Figure 4.3. Based on sample stoichiometry, the additional curing reactions in an 80/20 TGDDM/DDS specimen during the analysis should be more evident than in the 73/27 and 63/37 TGDDM/DDS specimens. Indeed, the curing reactions are more pronounced. The decrease in E' as the temperature is increased from 150^{o}C to 210^{o}C is greater in the 80/20 ratio than in the two previous ratios.

The loss tangent spectrum in the 80/20 system shows a curing peak of greater magnitude and breadth than has been observed for the other specimens. The curing peak overlaps the α-transition, implying that the sample remains somewhat rubbery throughout this temperature region (150^{o}C to 320^{o}C).

The 85/15 TGDDM/DDS dynamic mechanical spectrum is shown in Figure 4.4. In this sample, the molar ratio of epoxide groups to amine groups is so high that the extent of cure is decreased. Furthermore, the cure schedule employed with this

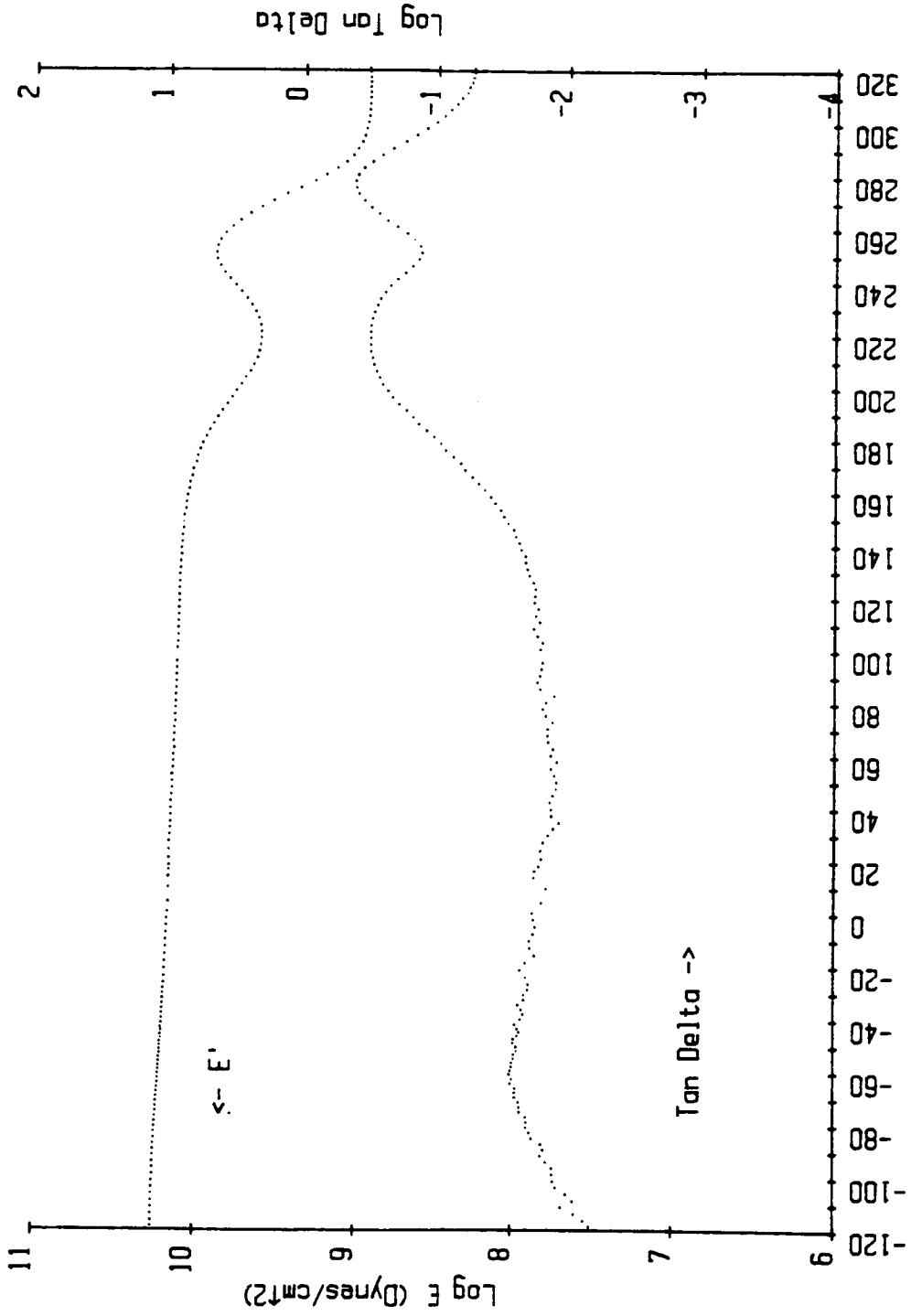

Figure 4.3 Dynamic mechanical spectrum of cured 80/20 TGDDM/DDS epoxy

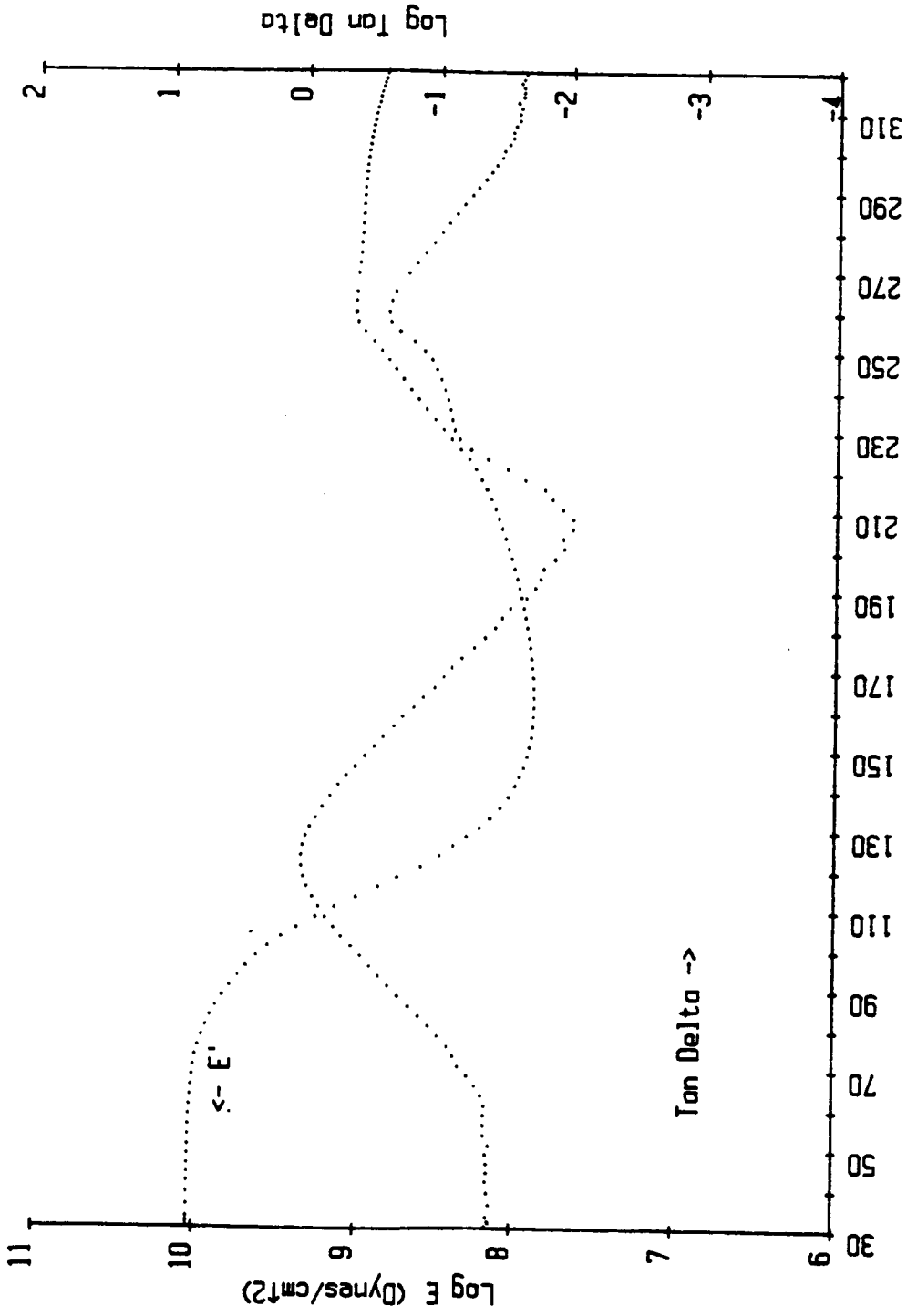

Figure 4.4 Dynamic mechanical spectrum of cured 85/15 TGDDM/DDS epoxy

sample had a maximum cure temperature of 160°C (the maximum cure temperature of the other ratios was 177°C). It should be noted that the temperature scale (30°C to 320°C) in Figure 4.4 is different from that of the other epoxy specimens. The 85/15 TGDDM/DDS had originally been tested on a Rheovibron in the earlier phases of this investigation, and its properties were considered unacceptable for further study. A sample was tested on the Autovibron for comparison with the other ratios. The elastic modulus of the 85/15 TGDDM/DDS begins its decline at 80°C and drops over two orders of magnitude by the time the temperature has reached 160°C. Additional curing reactions begin at a temperature which is not readily apparent from the spectra. Although the loss tangent is difficult to interpret, it indicates a loose network structure. That is, the specimen, as fabricated, is not highly crosslinked (14,15).

In the early phases of this investigation, repeated thermal cycling of the 73/27 TGDDM/DDS epoxy was conducted on the Rheovibron. The results (Figure 4.5) are consistent with a small degree of thermal degradation. There is a lowering of the Tg with each cycle and a broadening of the loss tangent peak. However, with five thermal cycles to 300°C or above, the sample integrity did not appear to suffer. The systems are quite stable and should be able to withstand extreme conditions without experiencing catastrophic failure.

As noted above, two other sample characteristics that

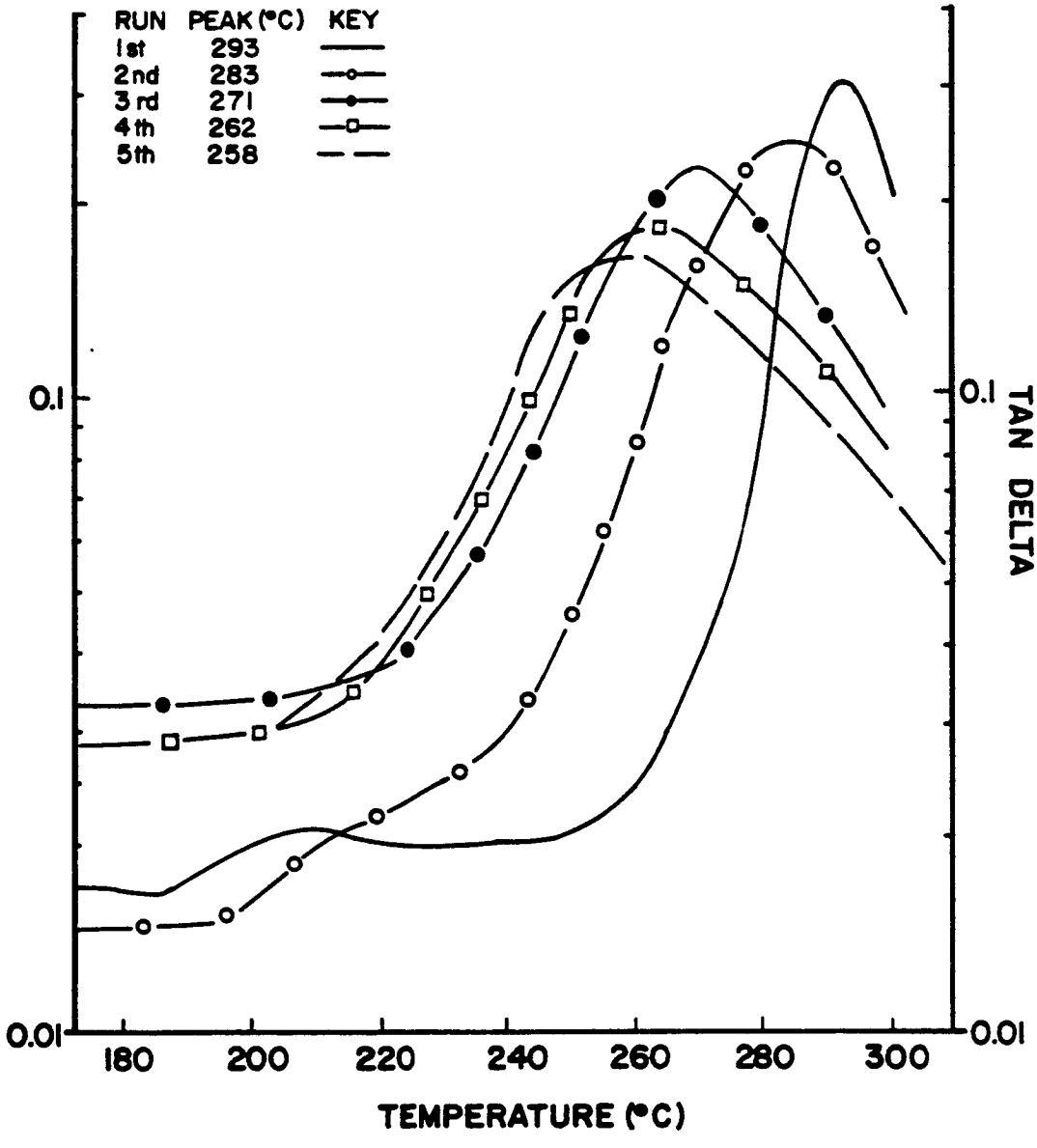

Figure 4.5 Effect of thermal cycling on the loss tangent spectrum of 73/27 TGDDM/DDS epoxy

can be determined from Autovibron dynamic mechanical testing are change in length and sample contraction following a thermal cycle. The epoxy resin specimens do not display any contraction following a thermal cycle. The absence of any contraction (which does occur in the composite specimens) is due to specimen yielding. The yielding occurs in the rubbery plateau region (ca. 290^{o}C) after the network has attained sufficient mobility as shown in Figure 4.6. Large extensions above Tg during tensile tests have been observed for TGDDM/DDS epoxies (14,15). As shown in Figure 4.6, there are two regions (170^{o}C and 270 ^{o}C) where the slope changes abruptly. These regions correspond approximately to the Tg of the as fabricated sample (Tgg) and the Tg of the ultimately cured sample (Tg_{∞}). The slope change provides another measure of Tg. This measure fits closely with the classical definition of Tg which is derived from dilatometry, ie. a change in slope in the volume/temperature curve.

Based on the four preliminary investigations, it was decided that the 80/20 and 73/27 TGDDM/DDS ratios would be used to study the effect of ionizing radiation on the epoxy resins. The 85/15 ratio appears useless (it is extremely brittle at room temperature), and any changes that occurred in it due to ionizing radiation would be difficult to interpret due to the extensive additional cure that occurs during the DMA measurements. Therefore, the 85/15 ratio was not considered for further investigation. The 63/37

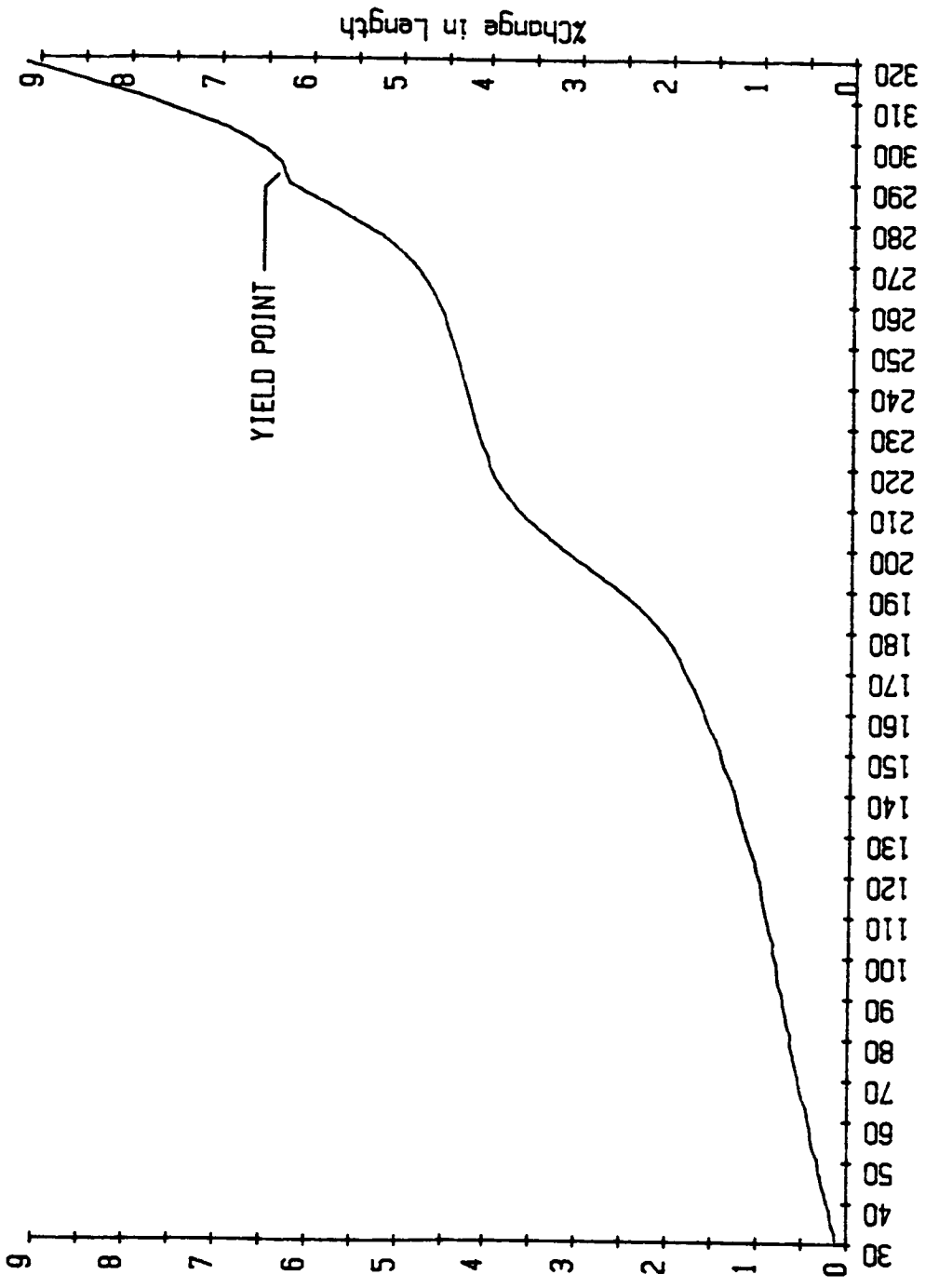

Figure 4.6 Percent change in length as a function of temperature for cured 73/27 TGDDM/DDS

TGDDM/DDS had a propensity to gel. Gelation occurred either during mixing before the DDS completely dissolved, or before the prepolymer could be thoroughly melted on the teflon sheets. Gelation of the samples made fabrication extremely difficult. Therefore, the 63/37 ratio was not considered for further investigations.

4.1.2 Effect of Ionizing Radiation on 73/27 and 80/20 TGDDM/DDS Epoxies

It would be expected that the dynamic mechanical spectrum of irradiated epoxies and composites would display changes as a function of radiation dose in several regions. The elastic modulus at room temperature (E'rt) will change slightly with variations in crosslink density. The elastic modulus can be further influenced by both the release of internal stresses and the presence of degradation products. The elastic modulus in the rubbery plateau region is associated with the molecular weight between crosslinks (Mc), and E' is typically measured at an arbitrary temperature above the α-transition maximum. Murayama (5) chose 40°C above Tg (E'_{Tg+40}) as the temperature at which to measure the elastic modulus in the rubbery region. The same temperature will be employed in the current investigation. The temperature location and the magnitude of the α-transition in the loss tangent spectrum will be influenced by various changes in the network structure. These variations will be

discussed later.

The effects of increasing the radiation dose on E' and tan delta for 73/27 TGDDM/DDS epoxy are illustrated in Figure 4.7 (150^{o}C to 320^{o}C). At an absorbed dose of 1000 Mrads, the curing reactions appear almost complete as there is a reduced tanδ peak in the loss tangent ca. 210^{o}C, indicating a small amount of additional curing. At 2000 Mrads and above, there is no evidence of additional curing reactions during the dynamic mechanical analysis. This observation is consistent with the earlier results of Netravali et al. (64) which showed that radiation induces additional cure. An analogous response is displayed by the 80/20 TGDDM/DDS specimens (Figure 4.8). The additional cure, which is evident in the spectra generated on the Autovibron, will be compared to DSC results on exothermic curing energy in section 4.2.

In Figure 4.9, the length change as a function of temperature for the 73/27 TGDDM/DDS specimens are shown (control, 2000 Mrads and 10,000 Mrads). The change in slope at 170^{o}C, which indicates additional curing reactions in the control specimens, is not evident in the irradiated specimens. The change in slope indicative of Tg_{∞} is very broad, and there is no clear indication of its location.

The obvious effect of increasing the radiation dose is that of shifting the onset of rubbery behavior to lower temperature. The transition region broadens as the dosages are increased. The variation in the glass transition

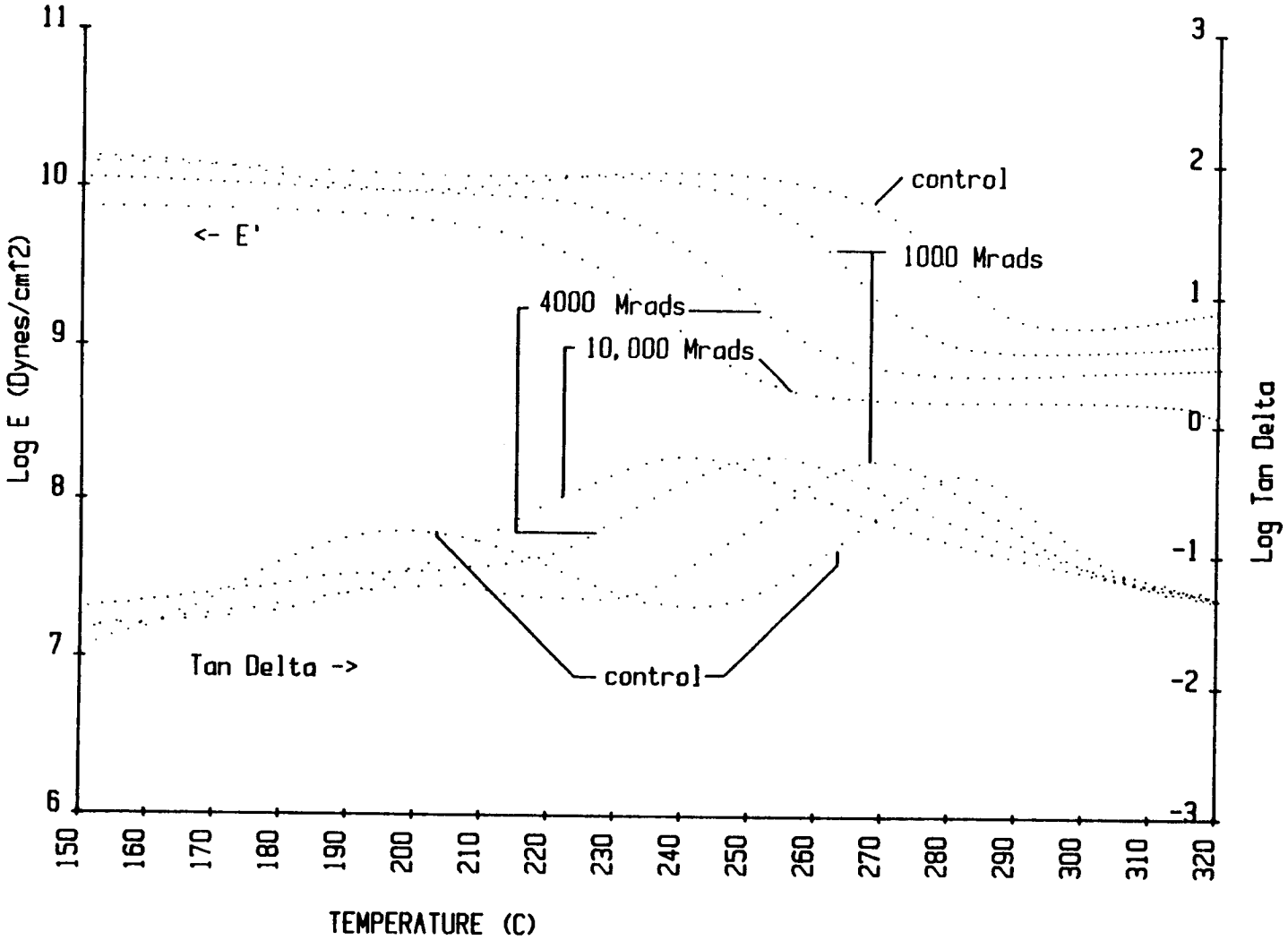

Figure 4.7 Elastic modulus and loss tangent of cured 73/27 TGDDM/DDS epoxy as a function of temperature (control, 1000 Mrads, 4000 Mrads and 10,000 Mrads)

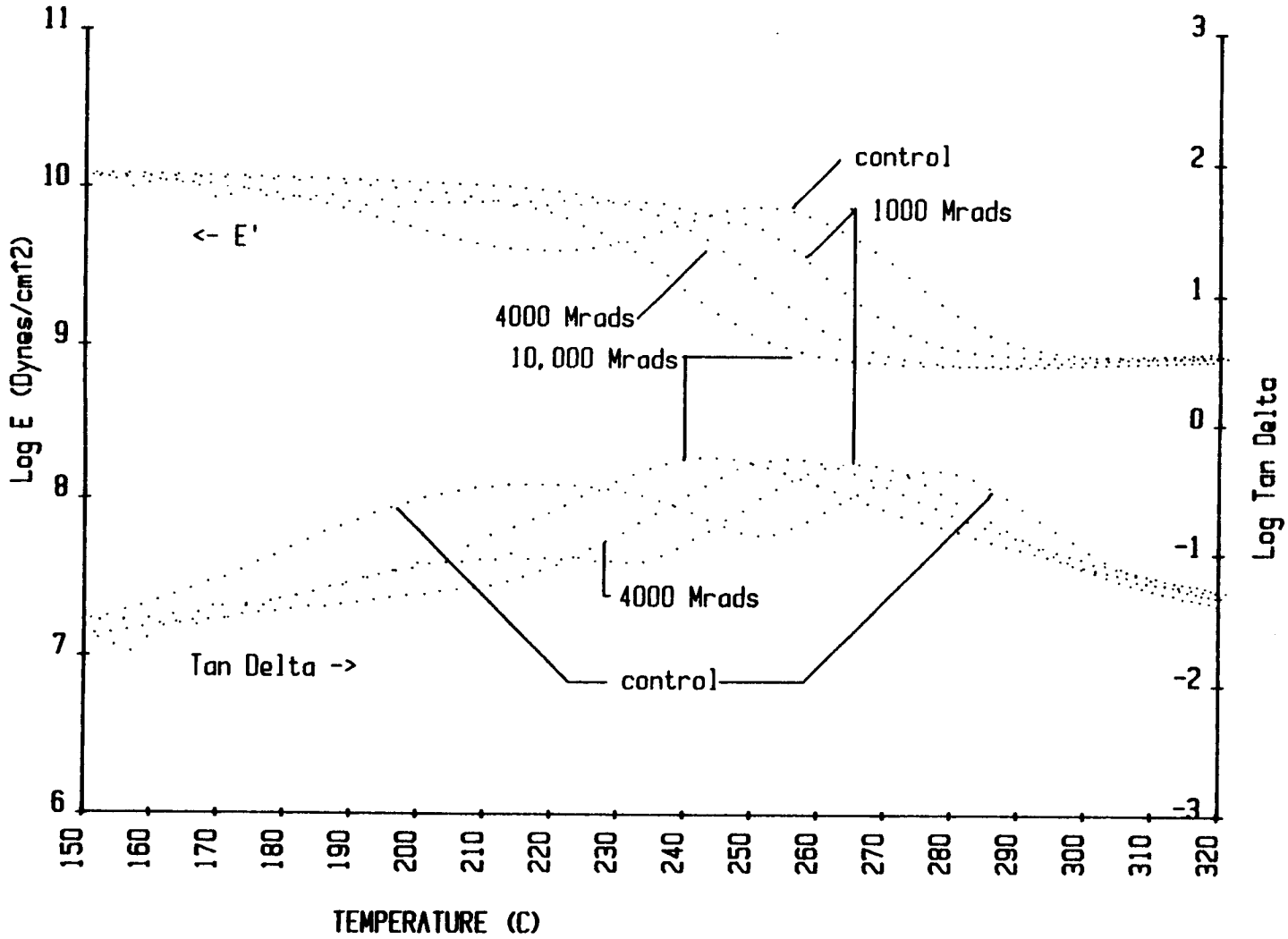

Figure 4.8 Elastic modulus and loss tangent of cured 80/20 TGDDM/DDS epoxy as a function of temperature (control, 1000 Mrads, 4000 Mrads and 10,000 Mrads)

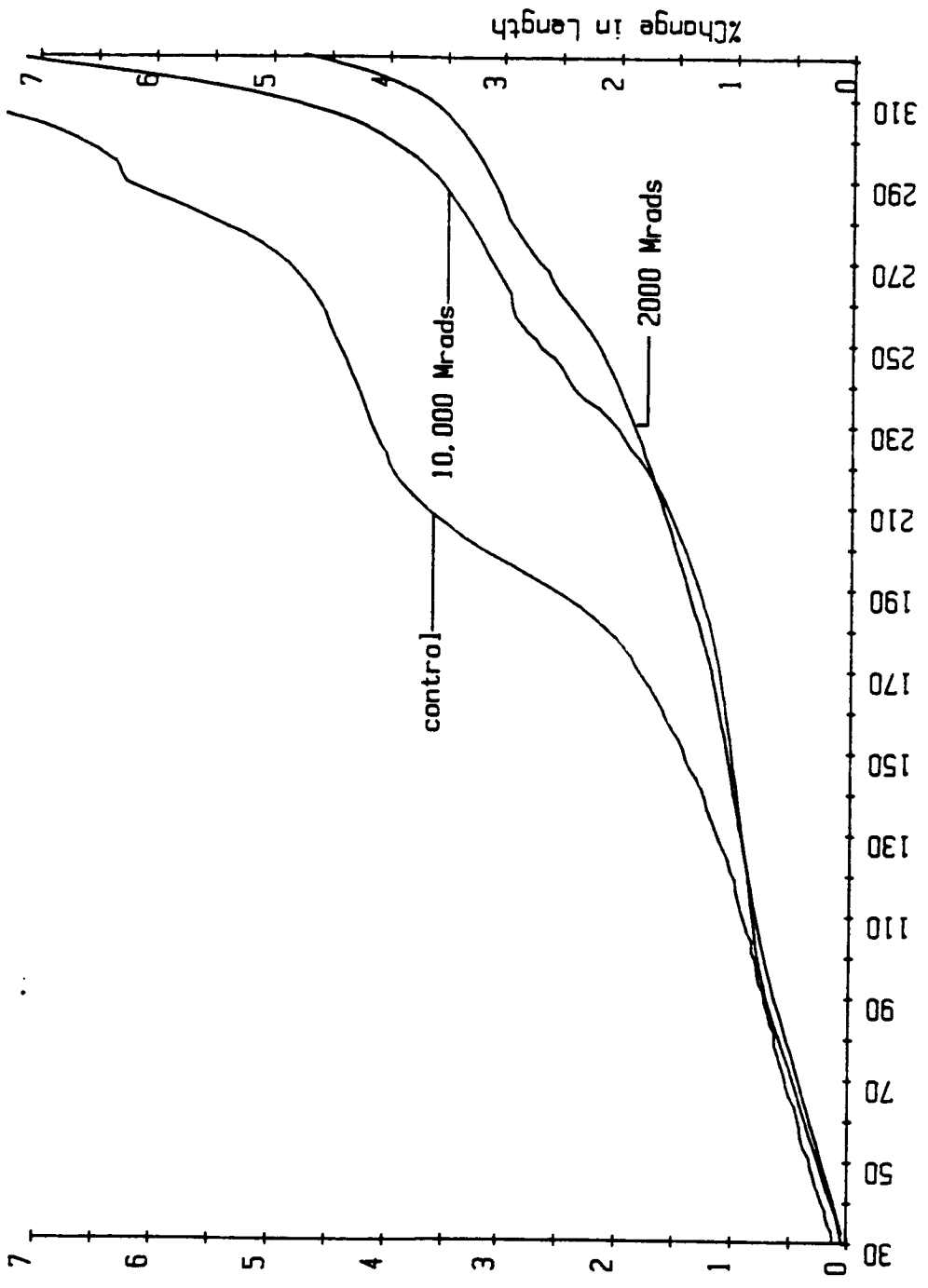

Figure 4.9 Percent change in length as a function of temperature for cured 73/27 TGDDM/DDS (control, 2000 Mrads and 10,000 Mrads)

temperature as a function of dose is presented in Table 4.1 for 73/27 and 80/20 TGDDM/DDS epoxy. The Tg of a control is 40°C higher than the Tg of specimens irradiated with 10,000 Mrads of 0.5 MeV electrons. Sykes et al. (4) found similar behavior in 90° composite specimens which were based predominantly on TGDDM/DDS. They observed a 50°C decrease in Tg (compared to a control) after an absorbed dose of 10,000 Mrads which compares with the 40°C decrease in the present investigation.

Some of the more subtle property changes are evident in E'_{Tg+40} and the intensity of the α-transition. The elastic modulus in the rubbery plateau region (E'_{Tg+40}) decreased 20% as a function of dose up to the 5000 Mrad level. At a dose of 10,000 Mrads, E'_{Tg+40} was only 6% below the control value (Table 4.2). The α-transition intensity increases as the absorbed dose increases (Table 4.3).

A preliminary examination of the property variations, suggests that some radiation induced degradation of the network has occurred. The 40°C decrease in Tg is the most obvious indication of degradation. The broadened transition region reveals that apparently a wider range of species (crosslink densities) are contributing to the α-transition than in the case of the control. Increases in α-transition intensity are indicative of a greater molecular weight between crosslinks (Mc) (5,6,48). The modulus in the rubbery plateau (E'_{Tg+40}) will decrease with increases in Mc (5,10).

Table 4.1 Glass transition temperature as a function of dose for 73/27 and 80/20 TGDDM/DDS epoxy

	Tg_∞(°C)	
Dose (Mrads)	73/27 TGDDM/DDS	80/20 TGDDM/DDS
control	283.3 ± 1.3[1]	275.4 ± 2.9
1000	271.8 ± 2.6	261.4 ± 3.9
2000	262.3 ± 4.5	257.6 ± 2.7
3000	260.7 ± 2.6	256.7 ± 3.7
4000	253.3 ± 3.9	251.7 ± 4.5
5000	252.6 ± 2.9	250.6 ± 1.8
10,000	237.7 ± 3.7	237.7 ± 3.4

[1] expressed as mean Tg ± the range for a 95% confidence interval.

Table 4.2 Percent change in elastic modulus above Tg_{∞} as a function of dose for 73/27 and 80/20 TGDDM/DDS epoxy

	$\%\Delta E'_{Tg+40}$ [1,2,3]	
Dose (Mrads)	73/27 TGDDM/DDS	80/20 TGDDM/DDS
control	0.0	0.0
1000	-9.7 ± 0.1	-7.8 ± 5.8
2000	-15.3 ± 5.5	-12.3 ± 9.6
3000	-4.6 ± 2.0	-19.6[4]
4000	-17.3 ± 4.3	-20.0 ± 5.1
5000	-18.8 ± 3.6	-19.3 ± 1.4
10,000	-5.8 ± 1.6	-5.6 ± 3.1

[1] percent changes in E' have been corrected by the error
[2] procedure in the Appendix.
[2] mean of two or three values ± the range of the values.
[3] $E'_{Tg+40} = 3 \times 10^9$ dynes/cm^2.
[4] single value.

Table 4.3 Loss tangent maximum (α-transition) as a function of dose for 73/27 and 80/20 TGDDM/DDS epoxy

	loss tangent maximum[1]	
Dose (Mrads)	73/27 TGDDM/DDS	80/20 TGDDM/DDS
control	0.403 ± 0.002	0.409 ± 0.040
1000	0.495 ± 0.021	0.482 ± 0.016
2000	0.490 ± 0.004	0.486 ± 0.014
3000	0.508 ± 0.008	0.542 ± 0.037
4000	0.538 ± 0.006	0.521 ± 0.008
5000	0.522 ± 0.010	0.546 ± 0.000
10,000	0.544 ± 0.007	0.526 ± 0.002

[1]mean of two or three values ± the range of the values.

There is also the possibility of plasticization of the polymer. Plasticization could occur due to degradation products or internal plasticization by an increase in the number of free chain ends. Each of the possibilities noted above could occur in specimens exposed to ionizing radiation. Plasticization of network polymers has been shown to cause decreases in Tg, increases in α-transition intensity and decreases in E'_{Tg+40} (5,10,14,15,51,53).

The percent changes in room temperature elastic modulus (E'rt) for 73/27 TGDDM/DDS and 80/20 TGDDM/DDS as a function of dose are listed in Table 4.4. The 73/27 TGDDM/DDS specimens display a decrease in E'rt up to a dose of 3000 Mrads. Above a dose of 3000 Mrads, E'rt increases and is 5% greater than a control specimen at the 10,000 Mrad level. The initial decrease in E'rt is presumed to occur due to a relaxation of internal stresses. As a sample returns to ambient temperature after fabrication, internal stresses can appear since some bonds are not free to relax. The relaxation arises from chain scission of the more highly strained bonds in the system. The increase in E'rt between 3000 and 10,000 Mrads is due to additional crosslinking. Analogous behavior has been shown for elastomers exposed to varying dose levels of ionizing radiation, ie. E' initially decreases due to chain scission and subsequently increases due to crosslinking (9,57,58).

Sykes et al. (4) observed that degradation products

Table 4.4 Percent change in elastic modulus at room temperature as a function of dose for 73/27 and 80/20 TGDDM/DDS epoxy

Dose (Mrads)	$\%\Delta E'_{rt}$[1,2] 73/27 TGDDM/DDS	80/20 TGDDM/DDS
control	0.0	0.0
1000	-4.2 ± 3.1	-1.1 ± 0.6
2000	-4.4 ± 2.1	+0.2 ± 2.0
3000	-13.2 ± 1.7	-11.2 ± 2.4
4000	-1.2 ± 4.8	-13.9 ± 0.9
5000	+0.6 ± 2.0	+4.7 ± 2.5
10,000	+5.2 ± 2.4	+8.8 ± 1.4

[1]percent changes in E' have been corrected by the error procedure outlined in the Appendix.
[2]mean of two or three values ± the range of the values.

which are present in the polymer network may increase E' at room temperature (sometimes referred to as antiplasticization). They measured E' and tanδ of 90° composite specimens (control and 10,000 Mrad dose) the elastic modulus at ambient temperature increased after an absorbed dose of 10,000 Mrads when compared to a control. However, above 100°C, E' of an irradiated specimen falls below E' of a control. Radiation created volatile degradation products as evidenced by vacuum weight loss studies. The changes in E' of the irradiated specimens were assumed to occur due to antiplasticization of the matrix at ambient temperature followed by plasticization of the matrix above 100°C. In Figure 4.10, analogous behavior is presented for 73/27 TGDDM/DDS specimens (control and 10,000 Mrad dose). The E' of the irradiated specimen falls below E' of a control at 140°C in agreement with the behavior described previously (4). However, contrary to the previous investigation, E' of a control is above E' of the irradiated specimen between -120°C and -40°C.

In the 80/20 TGDDM/DDS specimens, the changes in E'rt follow a slightly different pattern. Essentially there is little change in E'rt up to a dose of 2000 Mrads. Between 2000 and 4000 Mrads, E'rt decreases. As the dose is increased to 10,000 Mrads, E'rt is almost 9% greater than a control. During the first 2000 Mrads of absorbed dose, there is substantial additional cure (section 4.2). The

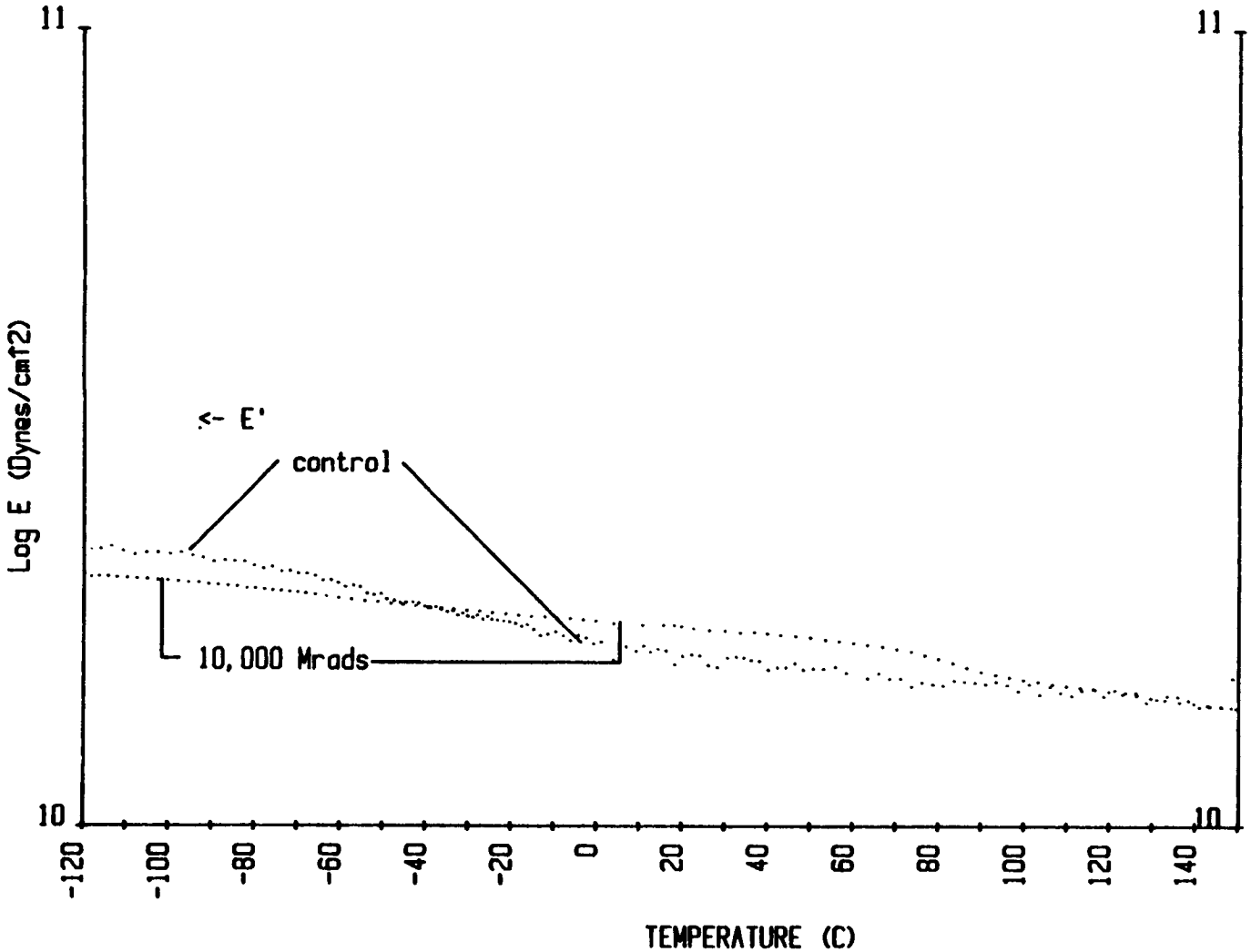

Figure 4.10 Elastic modulus of cured 73/27 TGDDM/DDS as a function of temperature between -120°C and 150°C (control and 10,000 Mrads)

competition between chain scission of highly strained bonds and further curing reactions which crosslink the network could "balance out" the changes in E'rt. Above 2000 Mrads there is sufficient chain scission to effect a significant decrease in E'rt. Additional crosslinking, as Sykes et al. (4) suggested, contributes to the 9% increase in E'rt at the 10,000 Mrad level.

The γ-transition is a region of the sample response that has not been addressed in previous work reported in the literature on radiation effects in epoxies. Listed in Table 4.5 are the γ-transition maxima as a function of dose. The temperature location of the γ-transition did not change (ca. $-60^{o}C$), but it displayed a general decrease in magnitude. Further reaction in epoxy systems previously has been shown to increase the γ-peak intensity (42). Investigations of γ-transitions, in general, reveal that plasticizers (degradation products in this case) can "freeze out" some of the small molecular motions which contribute to this transition. This would account for the discrepancy between increased extent of reaction with increasing dose and a lower γ-transition intensity. Apparently, plasticization by degradation products is altering the sample response and could be masking other radiation induced changes. A further discussion of plasticization effects can be found in section 4.3 and 8.2.

In summary, radiation induces further cure in a cured

Table 4.5 Loss tangent maximum (γ-transition) as a function of dose for 73/27 and 80/20 TGDDM/DDS epoxy

	loss tangent maximum[1]	
Dose (Mrads)	73/27 TGDDM/DDS	80/20 TGDDM/DDS
control	0.024 ± 0.003	0.025 ± 0.000
1000	0.020 ± 0.001	0.020 ± 0.001
2000	0.017 ± 0.000	0.019 ± 0.002
3000	0.018 ± 0.001	0.018 ± 0.004
4000	0.018 ± 0.001	0.020 ± 0.002
5000	0.019 ± 0.000	0.017 ± 0.000
10,000	0.011 ± 0.002	0.015 ± 0.003

[1]mean of two or three values ± the range of the values.

epoxy resin that has vitrified before all functional groups are reacted in the curing process. There is strong evidence for the formation of degradation products caused by ionizing radiation. The extent of network degradation (chain scission) is presently unclear. At very high doses (10,000 Mrads), additional crosslinking is implied by the increase in E'rt when compared to a control value. Furthermore, E'_{Tg+40} increased substantially between 5000 Mrads and 10,000 Mrads of absorbed dose suggesting additional crosslinking. Nevertheless, E'_{Tg+40} remains about 6% below the control value.

4.1.3 Composite Properties

4.1.3.1 T300/5208 Composites

The NARMCO 5208 resin, as mentioned previously, is a TGDDM/DDS based epoxy. Composite dynamic mechanical properties, especially in the matrix dominated orientations (90° and 45°), should exhibit analogous behavior to the 73/27 and 80/20 TGDDM/DDS epoxy resins. The fiber properties will dominate the response of the 0° composite where the applied stress is parallel to the fiber orientation.

The glass transition temperatures for the T300/5208 composite specimens before and after irradiation are listed in Table 4.6. The Tg's of the composites with 90° and 45° fiber orientations compare quite favorably with the Tg's for the epoxy resin systems (compare Table 4.6 with Table 4.1).

Table 4.6 Glass transition temperature as a function of dose for T300/5208 composites

Dose (Mrads)	Tg_∞(°C)			
	$90^\circ/1$[1]	$90^\circ/4$	$45^\circ/1$	$0^\circ/1$
control	282.1 ± 2.3[2]	274.6 ± 4.6	280.1 ± 2.4	306.9 ± 4.7
1000	273.4 ± 1.9	269.5 ± 2.1	270.2 ± 1.6	301.0 ± 0.4
2000	268.6 ± 1.8	265.0 ± 0.3	270.0 ± 2.1	297.0 ± 2.7
3000	263.5 ± 2.5	260.7 ± 1.5	260.7 ± 3.4	292.8 ± 2.6
4000	261.2 ± 3.4	258.0 ± 2.0	259.3 ± 3.8	290.4 ± 4.1
5000	257.9 ± 1.6	255.3 ± 2.7	255.9 ± 1.4	289.4 ± 3.1
10,000	248.2 ± 2.2	243.8 ± 2.2	243.1 ± 3.4	278.4 ± 2.1

[1] designation refers to: (fiber orientation to long dimension)/(number of ply layers).
[2] expressed as the mean Tg ± the range for a 95% confidence interval.

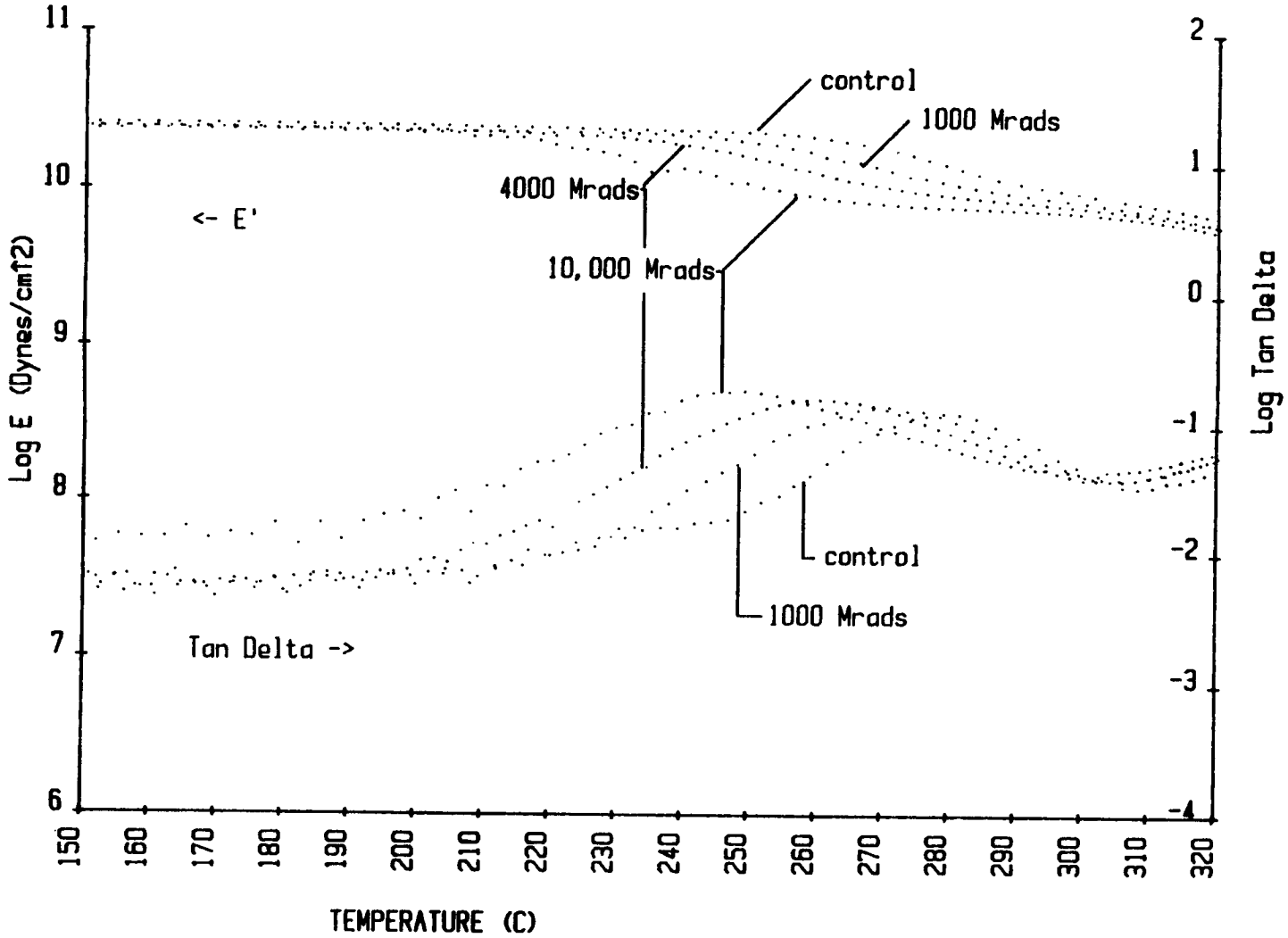

Figure 4.11 Elastic modulus and loss tangent of T300/5208 90 ^{o} 1-ply composite as a function of temperature (control, 1000 Mrads, 4000 Mrads and 10,000 Mrads)

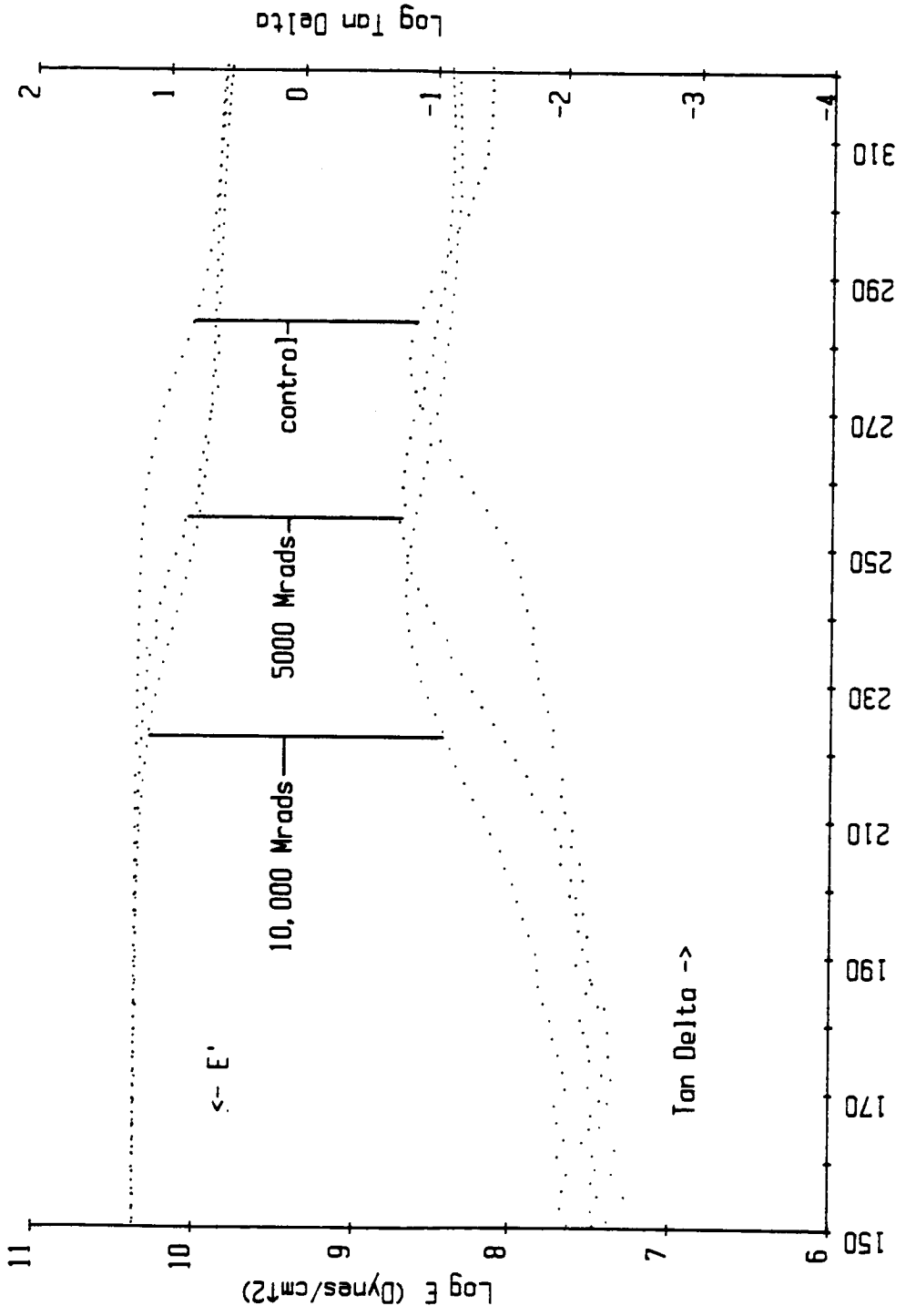

Figure 4.12 Elastic modulus and loss tangent of T300/5208 45^{o} 1-ply composite as a function of temperature (control, 5000 Mrads and 10,000 Mrads)

Table 4.7 Loss tangent maximum (α -transition) as a function of dose for T300/5208 composites

Dose (Mrads)	loss tangent maximum [1]			
	$90^{\circ}/1$	$90^{\circ}/4$	$45^{\circ}/1$	$0^{\circ}/1$
control	0.118 ± 0.008	0.115 ± 0.004	0.163 ± 0.003	0.039 ± 0.000
1000	0.141 ± 0.001	0.122 ± 0.007	0.168 ± 0.001	0.033 ± 0.002
2000	0.152 ± 0.003	0.128 ± 0.001	0.192 ± 0.001	0.031 ± 0.003
3000	0.146 ± 0.003	0.132 ± 0.002	0.190 ± 0.011	0.039 ± 0.018
4000	0.159 ± 0.002	0.140 ± 0.001	0.150 ± 0.009	0.038 ± 0.000
5000	0.169 ± 0.011	0.136 ± 0.000	0.183 ± 0.002	0.030 ± 0.011
10,000	0.180 ± 0.005	0.154 ± 0.001	0.168 ± 0.002	0.018 ± 0.002

[1] mean of two values ± the range of the values.

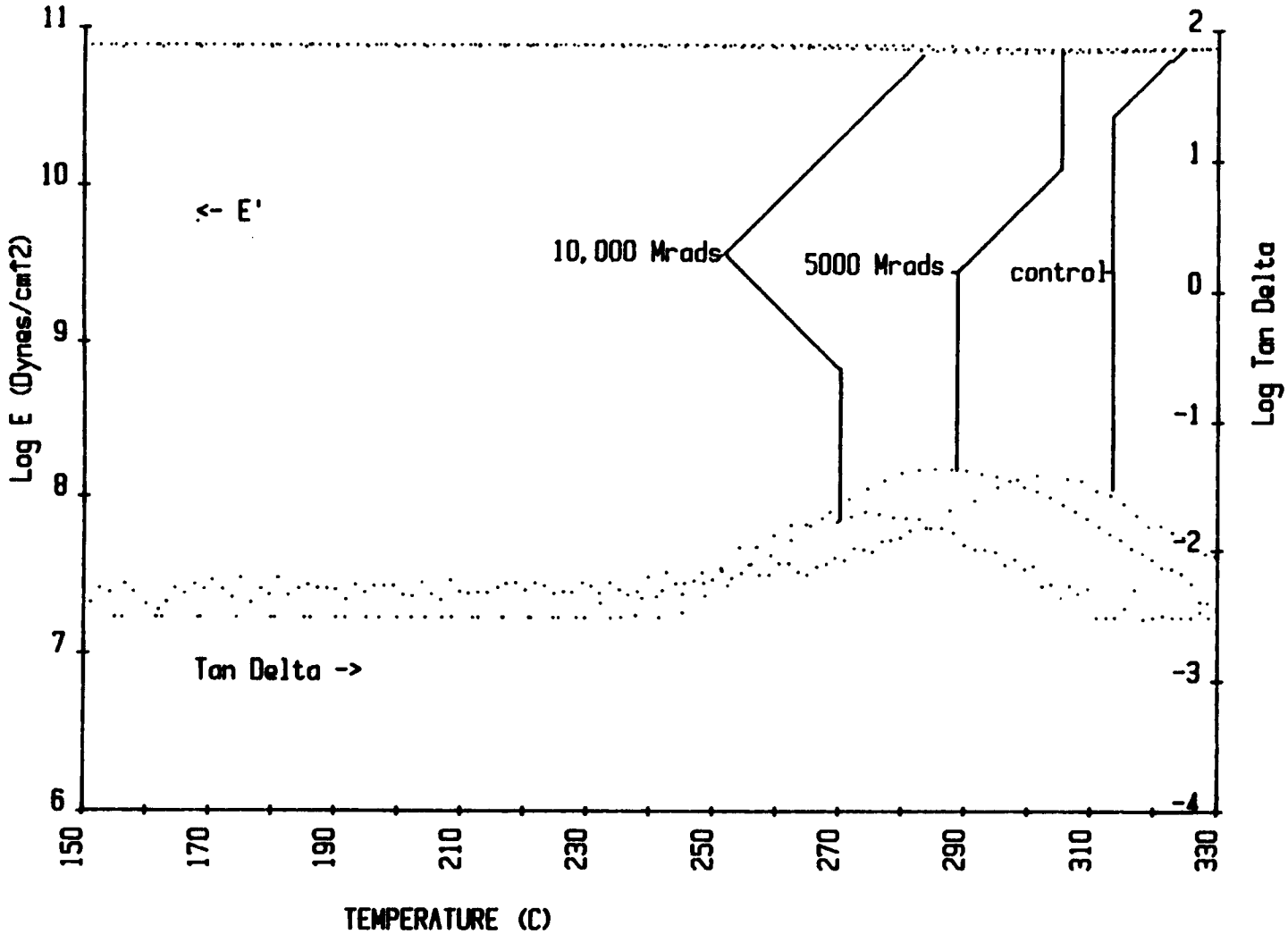

Figure 4.13 Elastic modulus and loss tangent of T300/5208 0^{o} 1-ply composite as a function of temperature (control, 5000 Mrads and 10,000 Mrads)

Obviously, the matrix influences the composite response in the 90^{o} and 45^{o} fiber orientations.

The 0^{o} composites display a glass transition temperature which is ca. $30^{o}C$ higher than the other orientations and the resin itself. The higher Tg for the 0^{o} composites is apparent in the T300/5209 composites as well (section 4.1.3.2).

The variations in both elastic moduli and loss tangent spectra of the T300/5208 90^{o} and 45^{o} composites are analogous to the variations in the epoxy resin systems (Figure 4.11 and 4.12). The decline in E' is shifted to lower temperature with increases in absorbed radiation dose. The α-dispersion increases in magnitude (Table 4.7), becomes more diffuse and shifts to lower temperature as the dosages are increased in all cases. The intensity of the loss tangent maxima shows no definite trend as a function of dose in the 45^{o} and 0^{o} composites. Furthermore, the magnitude of the loss tangent in 0^{o} composites is about 10 - 30% of the magnitude in the other orientations (90^{o} and 45^{o}).

The response of the 0^{o} composite is fiber dominated as evidenced by the higher E' (Figure 4.13). There is a small decrease in E' above Tg. The loss tangent intensity is very low. The Tg decreases about $30^{o}C$ between a control specimen and a specimen exposed to a dose of 10,000 Mrads. The measured E' (2×10^{11} dynes/cm^{2}) for the 0^{o} composite specimens is about 30% of the value reported by Keenan (8).

Furthermore, E' for graphite fibers is approximately an order of magnitude greater than E' for the 0° composite. The Autovibron is not capable of accurately determining E' for the 0° composites due to the fact that E' is above the range of the instrument and, therefore, caution should be noted regarding the measured DMA properties for the 0° composites.

Sample contraction (as measured by length changes in the test specimens) following a thermal cycle is an unusual phenomenon that only manifests itself in the composite specimens. The contraction is greatest for the 90° specimens and is essentially absent in the 0° specimens (Table 4.8). The percent shrinkage increases with dose with the exception that the 0° composites display no trend. Since the control specimens contract, the shrinkage must be an inherent property of the composite specimens as fabricated.

Sample expansion as a function of temperature exhibits anomalous behavior for the 90° composite specimens (Figure 4.14) compared to the behavior of the 0° composite specimens (Figure 4.15). For a control specimen, the expansion is essentially linear up to $290^{\circ}C$. In the temperature region above $290^{\circ}C$, the expansion curve reaches a maximum at $300^{\circ}C$, and the sample contracts between $300^{\circ}C$ and $320^{\circ}C$. This temperature region corresponds to the region at which the TGDDM/DDS epoxy specimens yielded. The same contraction phenomenon is exhibited in the expansion curve for a T300/5208 90° 1-ply composite after exposure to ionizing

Table 4.8 Percent shrinkage (following a thermal cycle) as a function of dose for T300/5208 composites

Dose (Mrads)	% Shrinkage[1]			
	$90^{o}/1$	$90^{o}/4$	$45^{o}/1$	$0^{o}/1$
control	1.22[2]	1.10[2]	0.48 ± 0.01	-0.01 ± 0.02
1000	1.28 ± 0.02	1.52 ± 0.01	0.55 ± 0.02	0.00 ± 0.00
2000	na[3]	1.69 ± 0.07	0.58 ± 0.02	0.07 ± 0.01
3000	1.51 ± 0.01	1.75 ± 0.07	0.56 ± 0.04	0.07 ± 0.01
4000	1.57 ± 0.08	1.79 ± 0.04	0.70 ± 0.09	0.03 ± 0.00
5000	1.56 ± 0.06	1.91 ± 0.04	0.70 ± 0.00	0.07 ± 0.01
10,000	1.63 ± 0.02	1.83 ± 0.01	0.75 ± 0.01	0.02 ± 0.01

[1] mean of two values ± the range of the values.
[2] single value (computer disk error).
[3] not available (computer disk error).

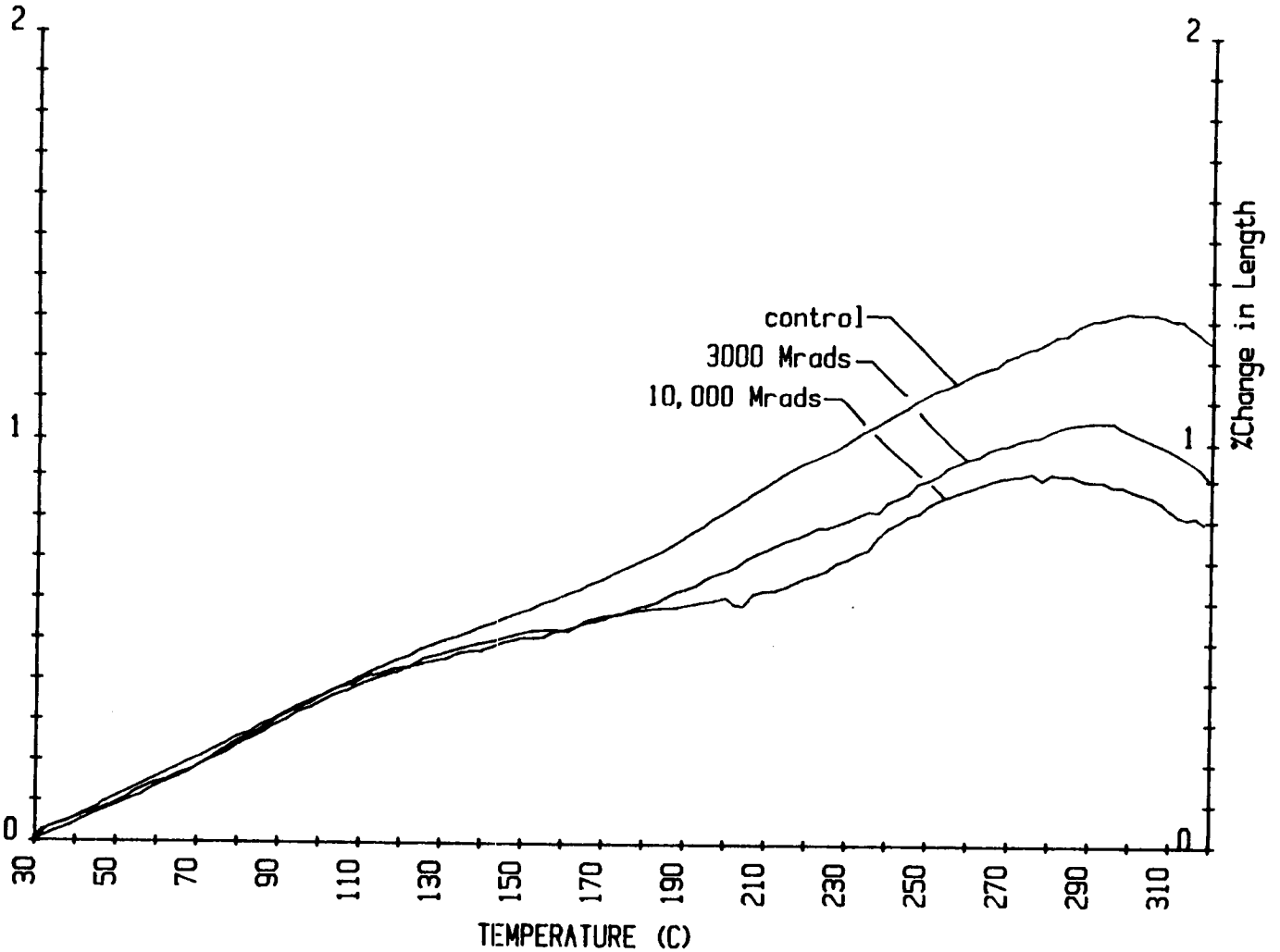

Figure 4.14 Percent change in length as a function of temperature for T300/5208 90° 1-ply composite (control, 3000 Mrads and 10,000 Mrads)

radiation. Following irradiation, total sample expansion is less than that of a control. Futhermore, after a dose of 10,000 Mrads, the onset of contraction is decreased by 20°C. The differences in total expansion are possibly due to a more crosslinked network structure after irradiation.

The expansion curve for the 0° composite (Figure 4.15) is essentially linear, and there are no apparent differences between control and irradiated specimens. In the 45° fiber orientation, the expansion behavior appears to be approaching a maximum at 320°C (Figure 4.16). The behavior of the 45° composite specimens is intermediate between the 90° and 0° orientations suggesting that the unusual expansion behavior (contraction) above Tg in the 90° composite is a matrix property. That is, as the fiber angle progresses from a matrix dominated response (90° composite) to a fiber dominated response (0° composite), the unusual behavior is eliminated.

The dynamic mechanical properties of the composites as a function of dose indicate some form of matrix degradation or physical change which does not approach catastrophic failure. The nature of the property changes is unclear. The property changes could arise from plasticization of the polymer by degradation products, without significant disruption of the network and/or chain scission of the network structure which effectively increases the molecular weight between crosslinks or creates an increase in the number of free chain ends.

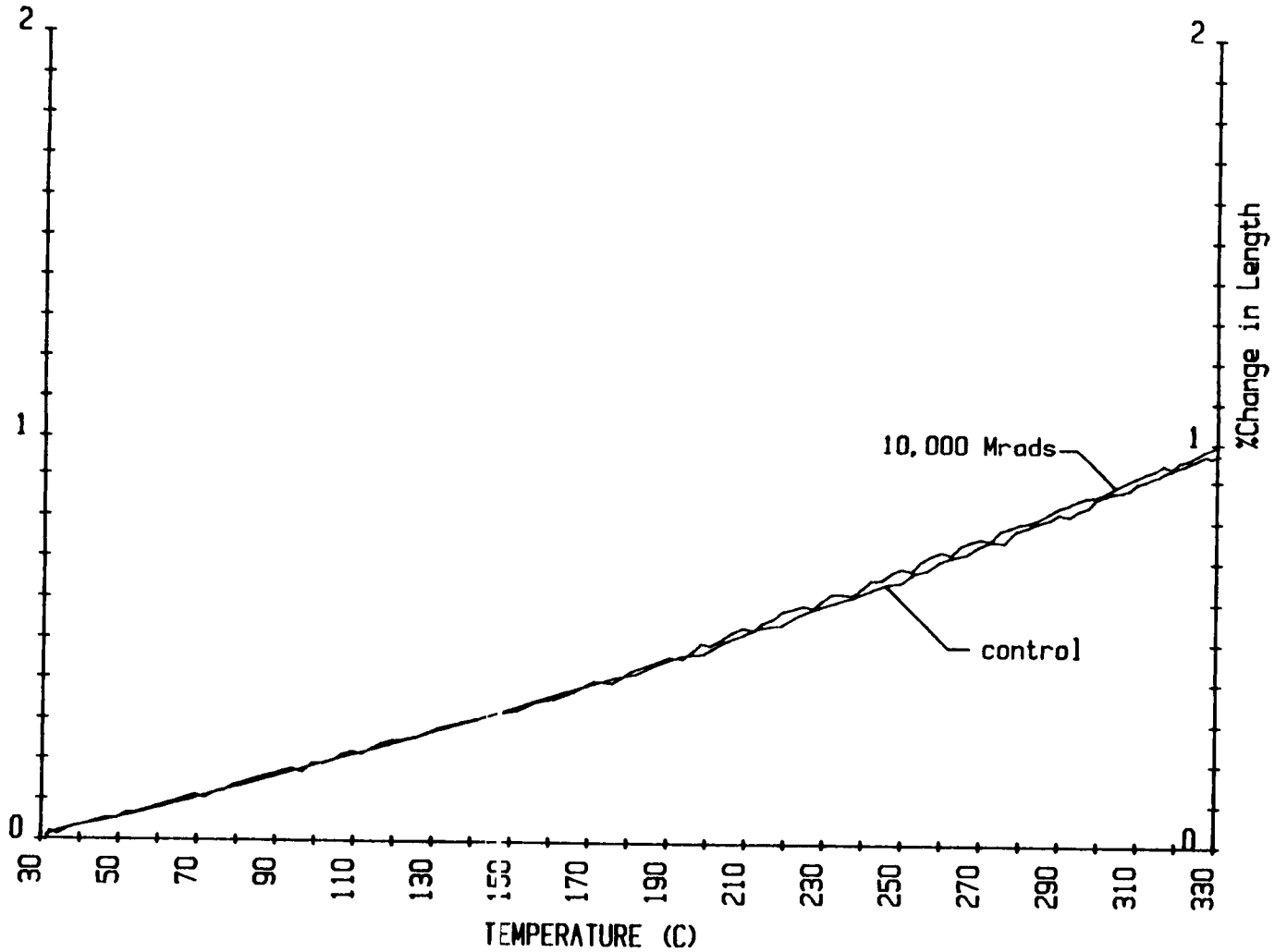

Figure 4.15 Percent change in length as a function of temperature for T300/5208 0° 1-ply composite (control and 10,000 Mrads)

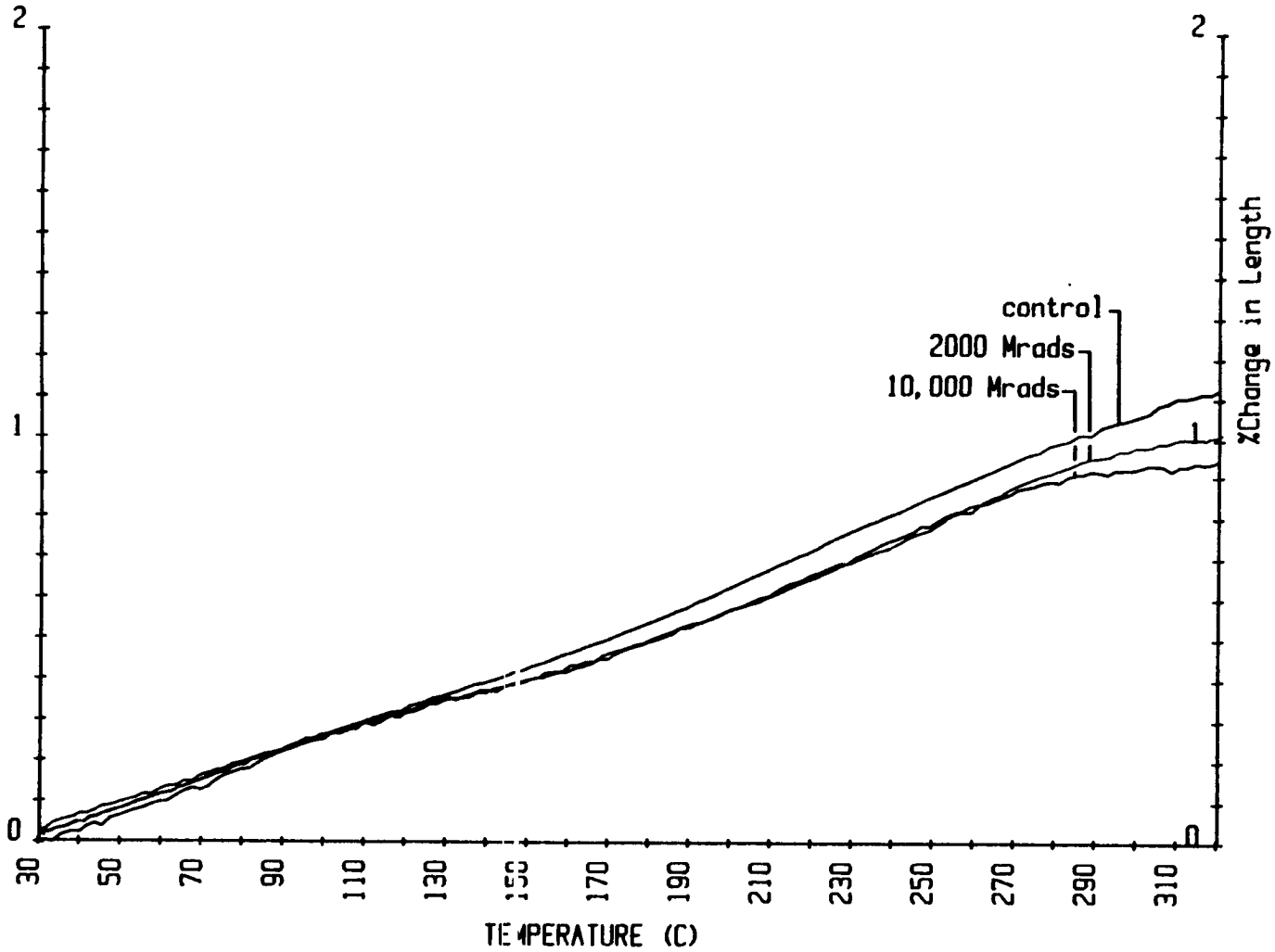

Figure 4.16 Percent change in length as a function of temperature for T300/5208 45° 1-ply composite (control, 2000 Mrads and 10,000 Mrads)

There is evidence of additional crosslinking in the epoxy resin alone, but these effects are not as evident in the composite specimens.

4.1.3.2 T300/5209 Composites

The T300/5209 composite specimens investigated in this study were based on a TGDDM/DDS/DGEBA system (section 3.1.2). Since DGEBA is difunctional, and TGDDM is tetrafunctional, the composites fabricated with NARMCO 5209 resin should and do exhibit substantially lower glass transition temperatures (Table 4.9) than the TGDDM/DDS based epoxies. The lower Tg would arise from an increased Mc (5,10). In fact, the Tg's of this system are about 100°C below either 73/27 or 80/20 TGDDM/DDS (compare Table 4.1 with Table 4.9).

The 90° 1-ply, 90° 4-ply and 45° 1-ply composite specimens exposed to 5000 Mrads of radiation show a decrease of 16°C to 21°C in glass transition temperature compared to the control specimens. The Tg is essentially unchanged at dose levels between 5000 Mrads and 10,000 Mrads. The 0° 1-ply specimens exhibit unusual behavior. First, the Tg is about 30°C to 40°C greater than the Tg of the 90° and 45° composite specimens as was the case with the T300/5208 composites. Next, the Tg for the 0° fiber orientation is only slightly affected upon irradiation. The maximum difference between any two dose levels is 8°C, and the 95% confidence intervals overlap in many cases.

Table 4.9 Glass transition temperature as a function of dose for T300/5209 composites

Dose (Mrads)	Tg_{∞}(°C)			
	$90^{\circ}/1$	$90^{\circ}/4$	$45^{\circ}/1$	$0^{\circ}/1$
control	163.2 ± 2.5[1]	150.4 ± 2.3	159.4 ± 1.4	193.7 ± 2.1
1000	160.4 ± 2.5	149.7 ± 2.1	154.5 ± 2.4	190.1 ± 3.7
2000	157.2 ± 2.5	144.3 ± 1.2	147.8 ± 1.4	188.7 ± 1.6
3000	152.6 ± 1.3	142.1 ± 2.4	145.0 ± 1.8	185.7 ± 3.7
4000	150.0 ± 2.2	139.0 ± 1.7	141.7 ± 1.9	187.1 ± 3.7
5000	147.0 ± 1.4	134.1 ± 2.7	138.1 ± 2.2	186.0 ± 2.6
10,000	146.9 ± 2.6	134.1 ± 1.2	138.5 ± 2.5	189.5 ± 1.5

[1]expressed as the mean Tg ± the range for a 95% confidence interval.

The presence of DGEBA in the T300/5209 system would imply certain property differences compared to the T300/5208 system. The matrix in the T300/5209 composites should possess a broad distribution of crosslink densities. The α-dispersions in Figure 4.17 and Figure 4.18 for T300/5209 composites is quite broad, as would occur with a wide distribution of crosslink densities (5,10). When the α-transition intensity is considered, it should be higher in the T300/5209 composites than in the T300/5208 composites with similar construction (compare Table 4.10 with 4.7). Indeed, the α-transition magnitude is greater in the T300/5209 composites, suggesting a wide distribution of crosslink densities and a higher average Mc than for T300/5208 composites and/or a higher percentage of free chain ends. The magnitude of the α-transition increases with dose similar to the TGDDM/DDS epoxy specimens in all cases except the 0^{o} 1-ply composite which does not exhibit any trend.

Ionizing radiation broadens the α-peak dispersion (Figure 4.17 and Figure 4.18). As evidenced by the E' spectra for the different dose levels, the onset of rubbery behavior is shifted to lower temperature. Although room temperature elastic modulus is essentially invariant with radiation dose, E'_{Tg+40} decreases monotonically with dose.

The T300/5208 composites (90^{o} and 45^{o}) displayed a greater contraction following a thermal cycle than do the T300/5209 composites of similar construction (compare Table

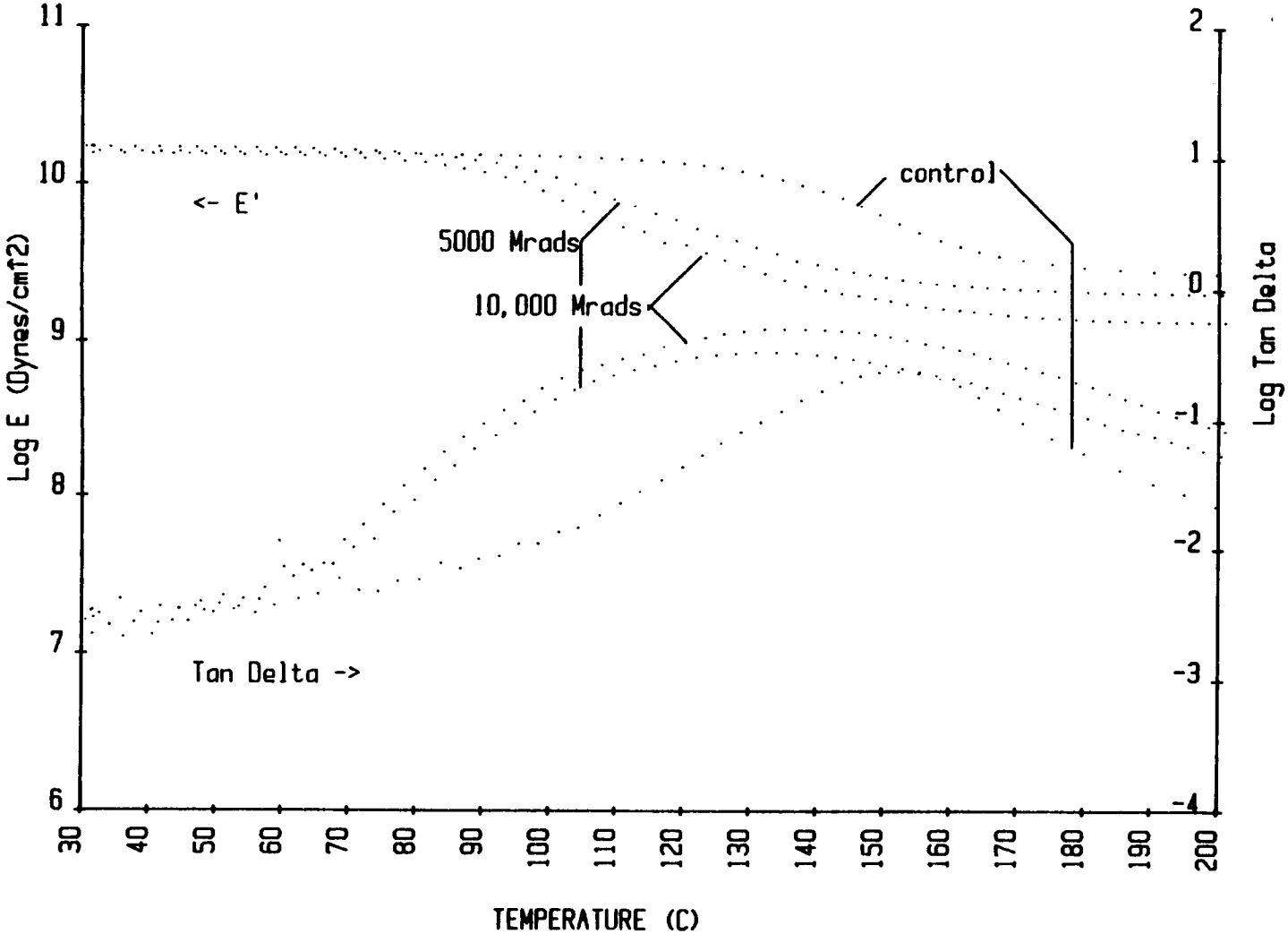

Figure 4.17 Elastic modulus and loss tangent of T300/5209 90° 4-ply composite as a function of temperature (control, 5000 Mrads and 10,000 Mrads)

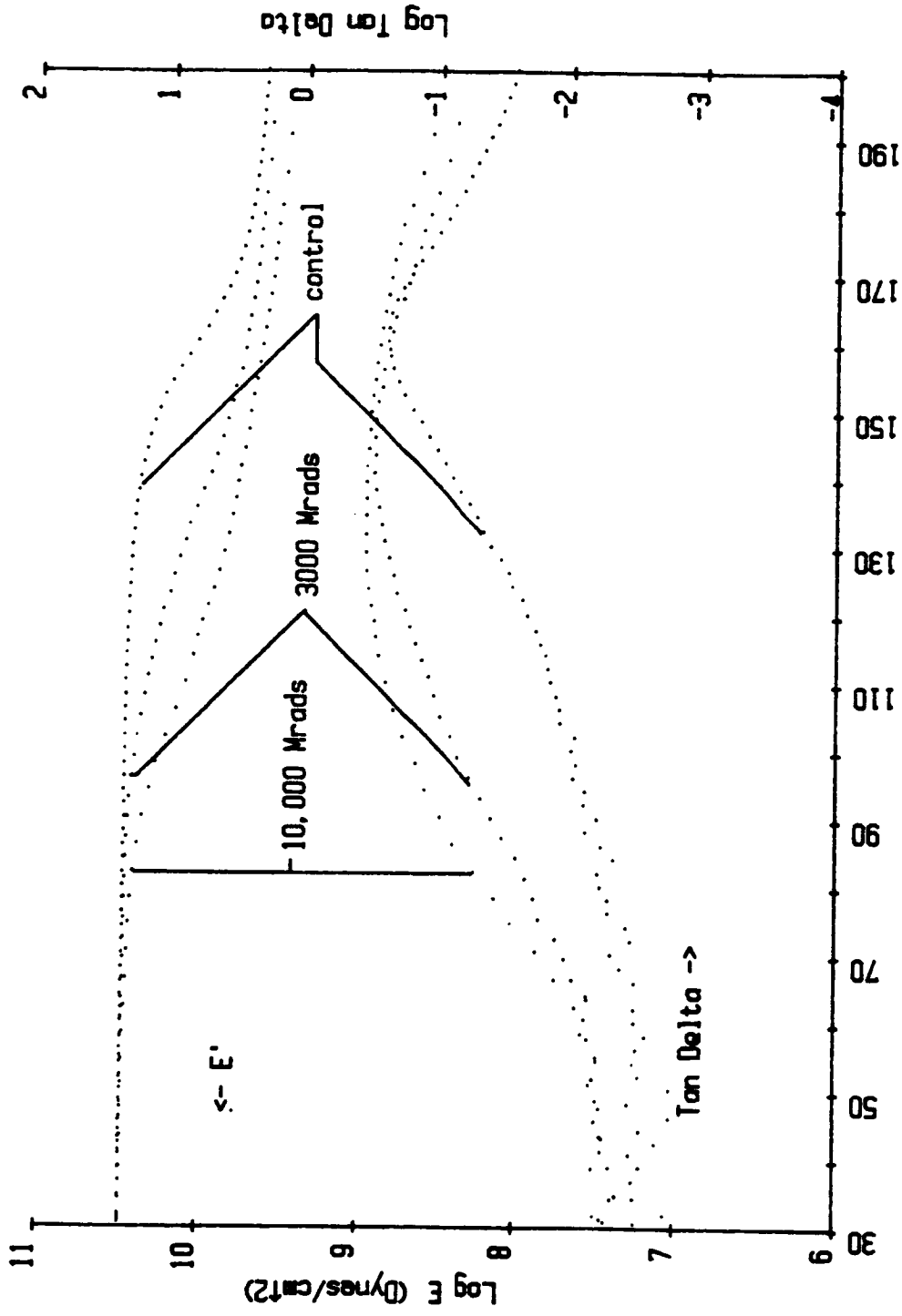

Figure 4.18 Elastic modulus and loss tangent of T300/5209 45° 1-ply composite as a function of temperature (control, 3000 Mrads and 10,000 Mrads)

Table 4.10 Loss tangent maximum (α -transition) as a function of dose for T300/5209 composites

Dose (Mrads)	loss tangent maximum [1]			
	$90^{o}/1$	$90^{o}/4$	$45^{o}/1$	$0^{o}/1$
control	0.216 $\pm$ 0.010	0.232 $\pm$ 0.004	0.243 $\pm$ 0.004	0.077 $\pm$ 0.026
1000	0.288 $\pm$ 0.003	0.263 $\pm$ 0.004	0.276 $\pm$ 0.005	0.135 $\pm$ 0.010
2000	0.308 $\pm$ 0.002	0.291 $\pm$ 0.005	0.280 $\pm$ 0.008	0.135 $\pm$ 0.002
3000	0.332 $\pm$ 0.007	0.328 $\pm$ 0.025	0.315 $\pm$ 0.003	0.151 $\pm$ 0.024
4000	0.407 $\pm$ 0.001	0.347 $\pm$ 0.000	0.333 $\pm$ 0.001	0.142 $\pm$ 0.014
5000	0.400 $\pm$ 0.001	0.347 $\pm$ 0.017	0.336 $\pm$ 0.001	0.135 $\pm$ 0.009
10,000	0.529 $\pm$ 0.005	0.497 $\pm$ 0.003	0.373 $\pm$ 0.012	0.130 $\pm$ 0.025

[1] mean of two values $\pm$ the range of the values.

4.11 with Table 4.8). Contraction generally increases in the 90^{o} and 45^{o} orientations with radiation dose up to 5000 Mrads. The contraction decreases between a dose of 5000 Mrads and 10,000 Mrads. The control specimens also contract following a thermal cycle; therefore, contraction is inherent to the systems.

The expansion behavior of the 90^{o} and 45^{o} T300/5209 composite specimens does not exhibit yielding in the rubbery plateau region for the temperature range investigated (Figures 4.19 and 4.20). The increase in slope of expansion versus temperature occurs ca. $155^{o}C$ for the control specimens, indicating a change in expansion behavior, ie. at Tg. Irradiation causes the change in length to exhibit unusual behavior compared to the control. A change in slope with temperature occurs at lower temperature but the slope returns to approximately its room temperature slope above $130^{o}C$. Plasticization by degradation products (from ionizing radiation) has been shown by Sykes et al. (4) to cause large expansions at Tg for a similar system (Fiberite 934).

As with the TGDDM/DDS epoxy resins, the T300/5209 composites show evidence of epoxy degradation upon irradiation; however, the Tg of the T300/5209 composites does not decrease sharply with dose as it did in the TGDDM/DDS epoxy resins. As the dose level is increased, the α-dispersion becomes more diffuse and increases in magnitude for the 90^{o} and 45^{o} fiber orientations (Table 4.10 and

Table 4.11 Percent shrinkage (following a thermal cycle) as a function of dose for T300/5209 composites

Dose (Mrads)	% Shrinkage[1]			
	$90^{\circ}/1$	$90^{\circ}/4$	$45^{\circ}/1$	$0^{\circ}/1$
control	0.15[2]	0.21[2]	0.05 ± 0.03	0.05 ± 0.03
1000	0.24 ± 0.05	0.49 ± 0.02	0.07[2]	0.03 ± 0.00
2000	0.34 ± 0.01	0.45 ± 0.02	0.14[2]	0.05 ± 0.01
3000	na[3]	0.54 ± 0.06	0.13 ± 0.01	0.02 ± 0.01
4000	0.35 ± 0.06	0.56 ± 0.03	0.13[2]	0.01 ± 0.01
5000	0.36 ± 0.00	0.70 ± 0.05	0.12 ± 0.03	0.02 ± 0.00
10,000	0.24 ± 0.02	0.58 ± 0.08	-0.03[2]	0.00[2]

[1] mean of two values ± the range of the values.
[2] single value (specimens were warped).
[3] not available (specimens were warped).

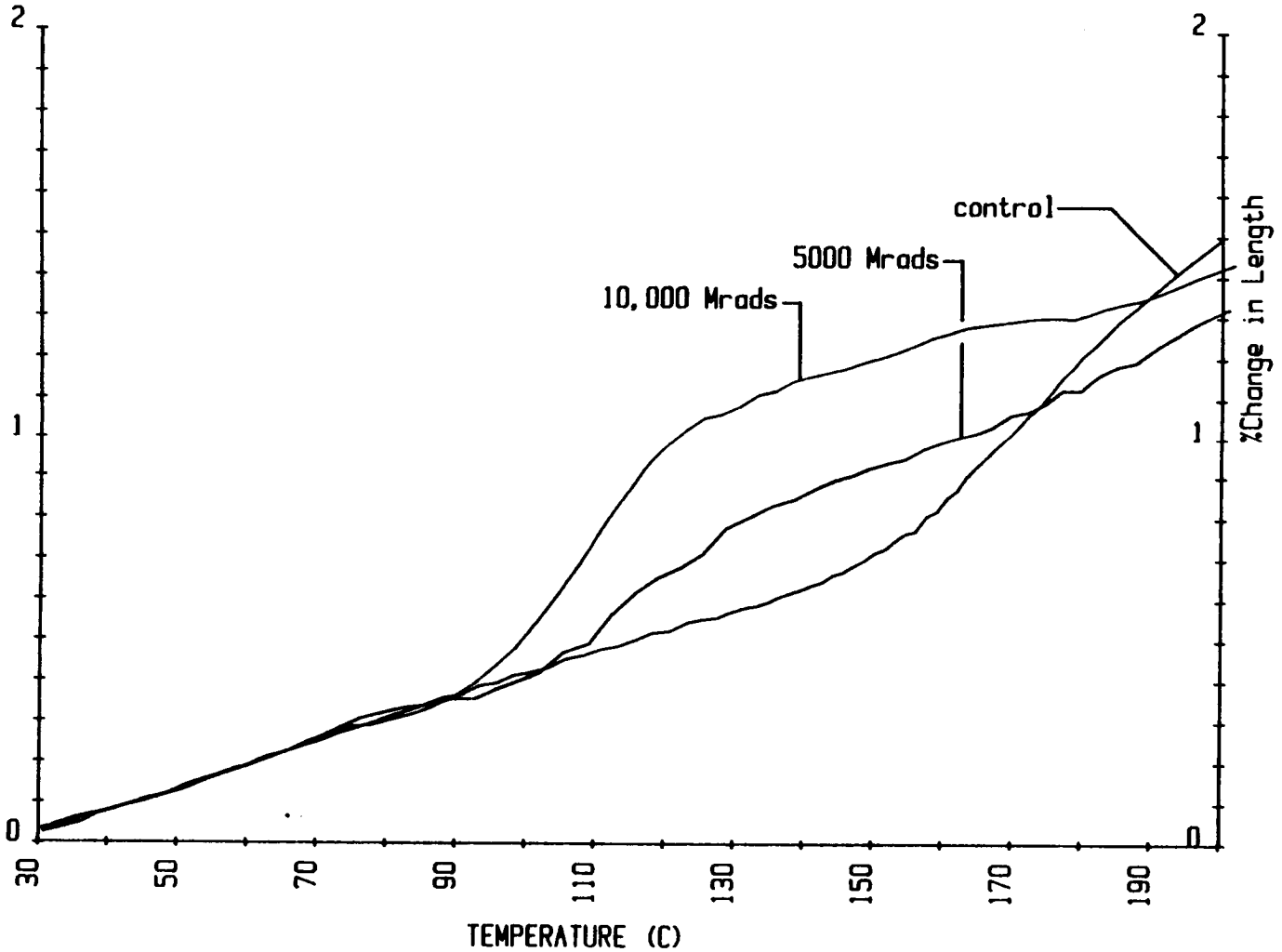

Figure 4.19 Percent change in length as a function of temperature for T300/5209 90° 1-ply composite (control, 5000 Mrads and 10,000 Mrads)

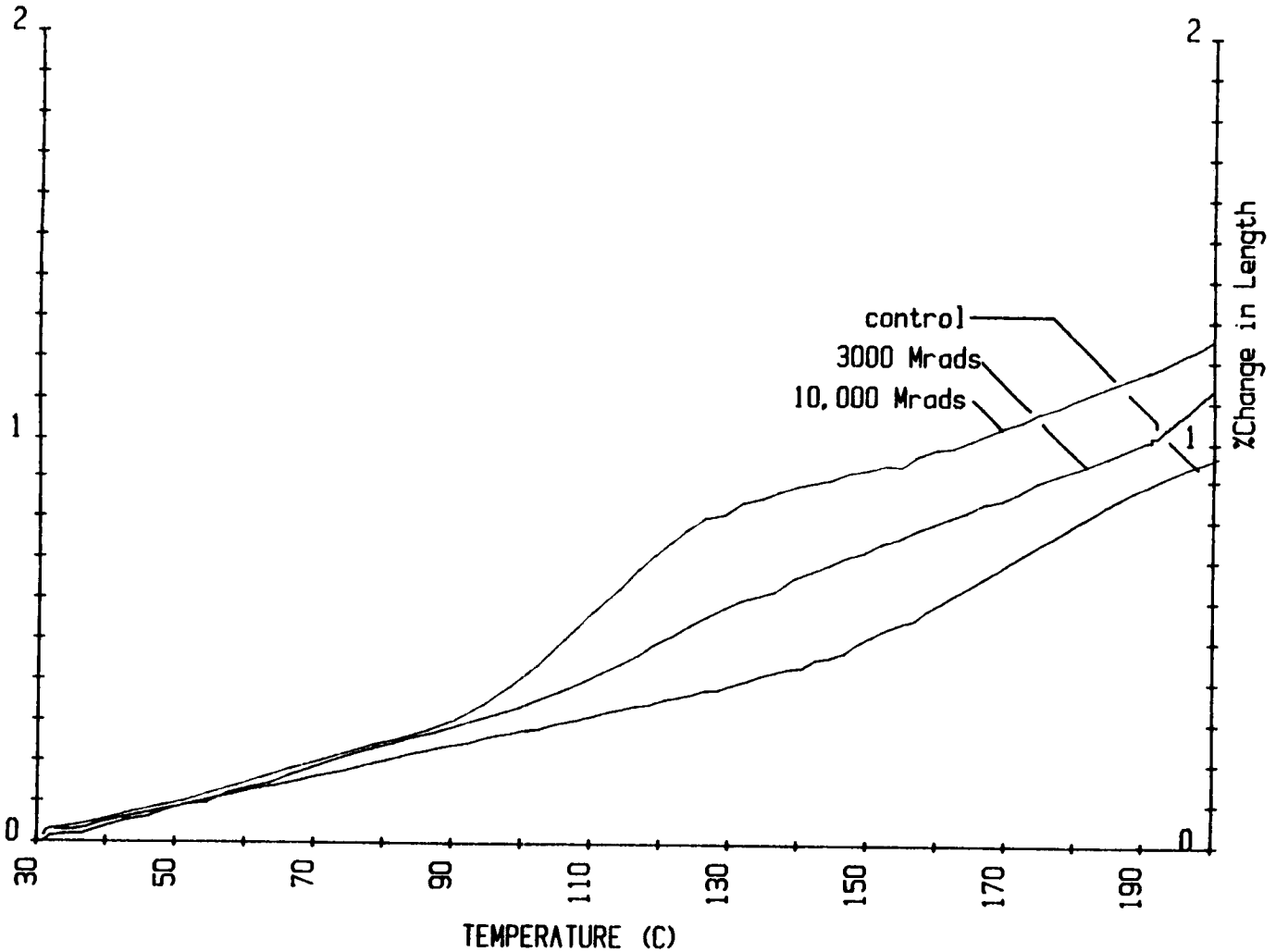

Figure 4.20 Percent change in length as a function of temperature for T300/5209 45° 1-ply composite (control, 3000 Mrads and 10,000 Mrads)

Figures 4.17 and 4.18). The dynamic mechanical properties of composites with 90° and 45° fiber orientations are matrix dominated; therefore, differences in matrix properties (network degradation, plasticization and/or additional crosslinking) would be more pronounced in these orientations than in the 0° orientation. The elastic modulus of the T300/5209 composites at ambient temperature is not affected by radiation. Since the matrix is a minor constituent (ca. 40 volume percent), evidence of property changes incurred in it will be suppressed compared to a pure resin system unless there is significant degradation of the interfacial bond between fiber and matrix.

The T300/5209 0° composite dynamic mechanical response is shown in Figure 4.21. Irradiation has minimal influences on E'. As noted in the 5208 composites, E' is significantly lower than would be expected considering the fiber modulus. The loss tangent spectra broadens and shifts to lower temperature with increasing doses. However, the intensity of the loss tangent is greater for the specimen at the 3000 Mrad dose level than the one at the 10,000 Mrad dose level. Changes in the α-transition indicate that additional crosslinking does occur between a dose of 3000 Mrads and 10,000 Mrads. The expansion behavior of the 0° composites is essentially invariant with dose similar to the 5208 based 0° composites (compare Figure 4.22 with Figure 4.15).

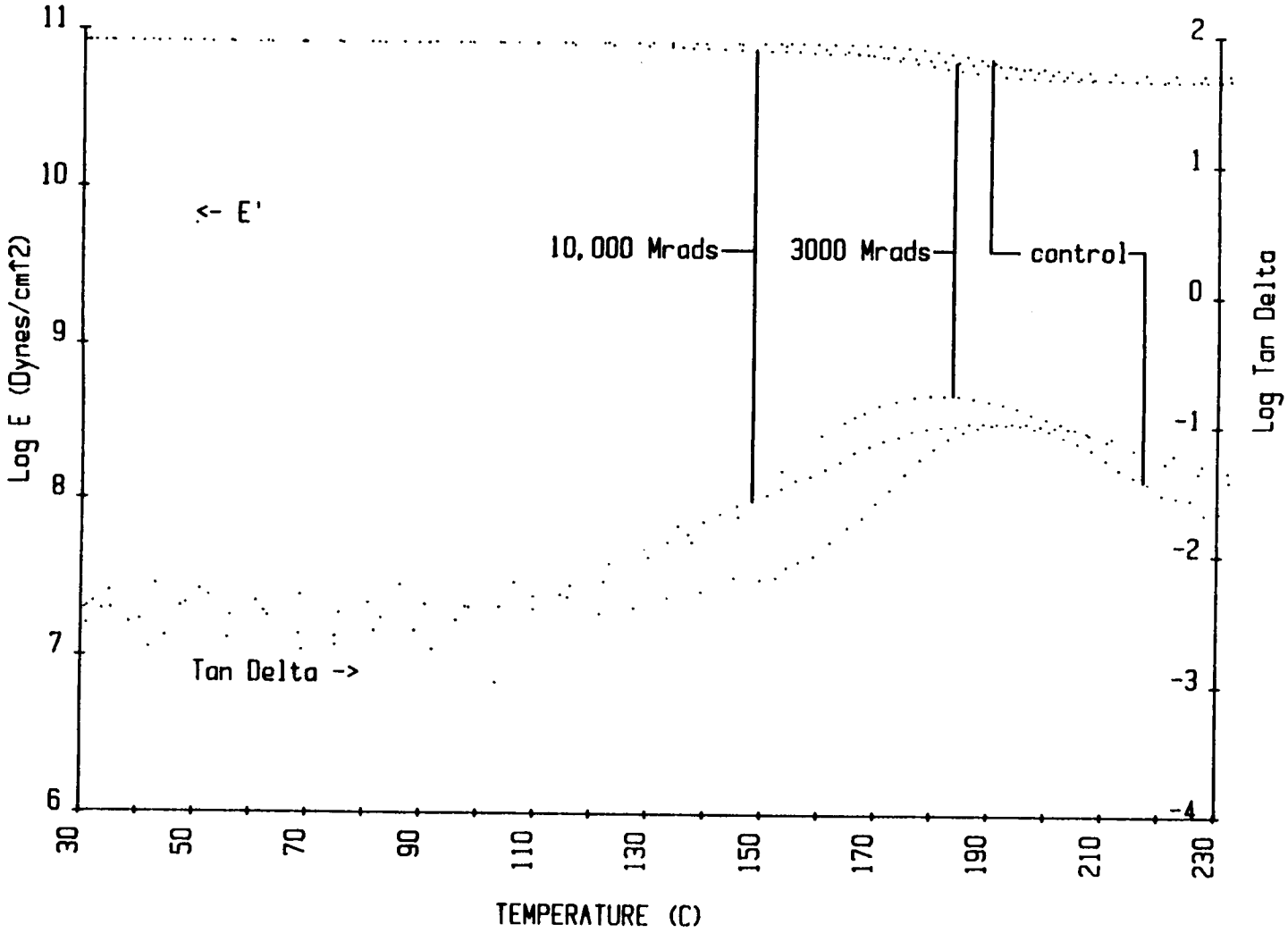

Figure 4.21 Elastic modulus and loss tangent of T300/5209 0^{o} 1-ply composite as a function of temperature (control, 3000 Mrads and 10,000 Mrads)

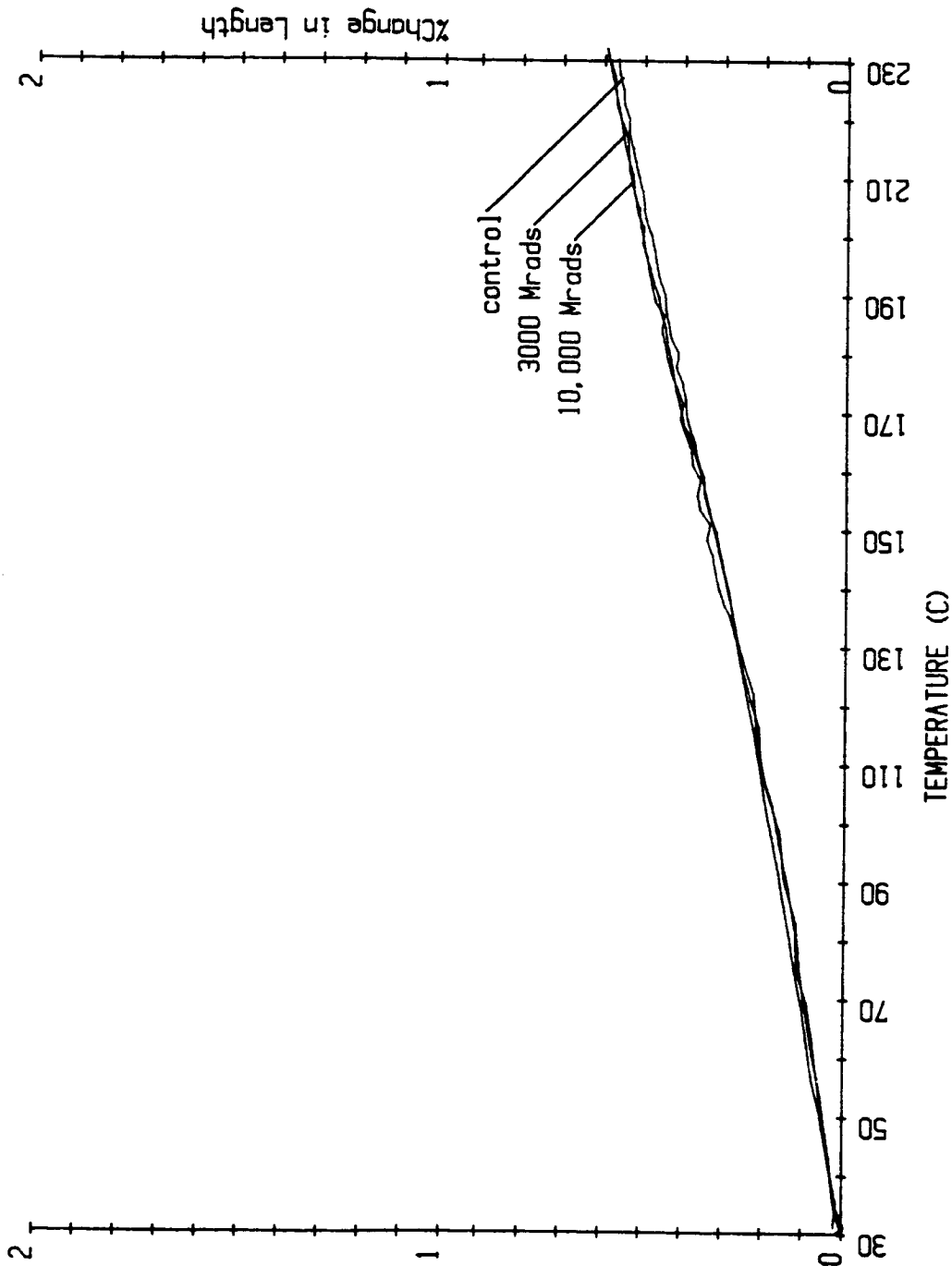

Figure 4.22 Percent change in length as a function of temperature for T300/5209 0° 1-ply composite (control, 3000 Mrads and 10,000 Mrads)

4.1.3.3 Interfacial Region in Composite Specimens

Three characteristics of the composite specimens are noteworthy and require explanation.

1. The Tg's of the 0^{o} oriented composites (T300/5208 and T300/5209) are substantially higher than the Tg's of 90^{o} and 45^{o} specimens (again, since E' of the 0^{o} composites is about an order of magnitude lower than expected based on E' of the fibers, caution should be used),
2. 90^{o} and 45^{o} composite orientations contract following a thermal cycle (control and irradiated specimens), and
3. 90^{o} T300/5208 composites exhibit a length contraction as the temperature above Tg is increased.

These somewhat unusual phenomena can be rationalized by assuming that an "interfacial" region exists which possesses physical and chemical properties that are different from that of the matrix phase. The interfacial region lies between the bulk of the matrix and the fiber surface, and it may or may not be a continuous phase.

An initial assumption will be that the interfacial region has a higher crosslink density than the matrix phase. Suitable models for 90^{o} and 0^{o} composites with an interfacial region layer are shown in Figures 4.23 and 4.24,

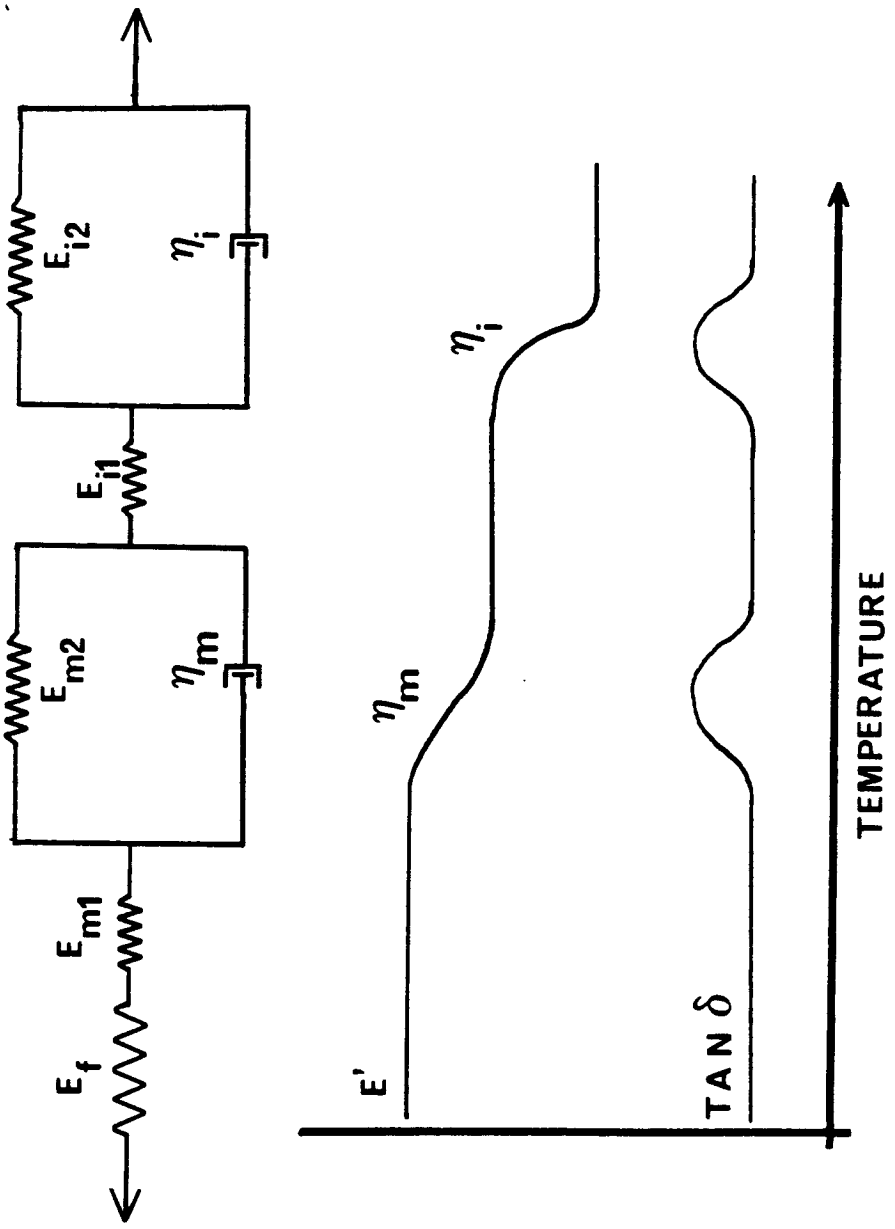

Figure 4.23 Model of 90° composite with an interfacial region

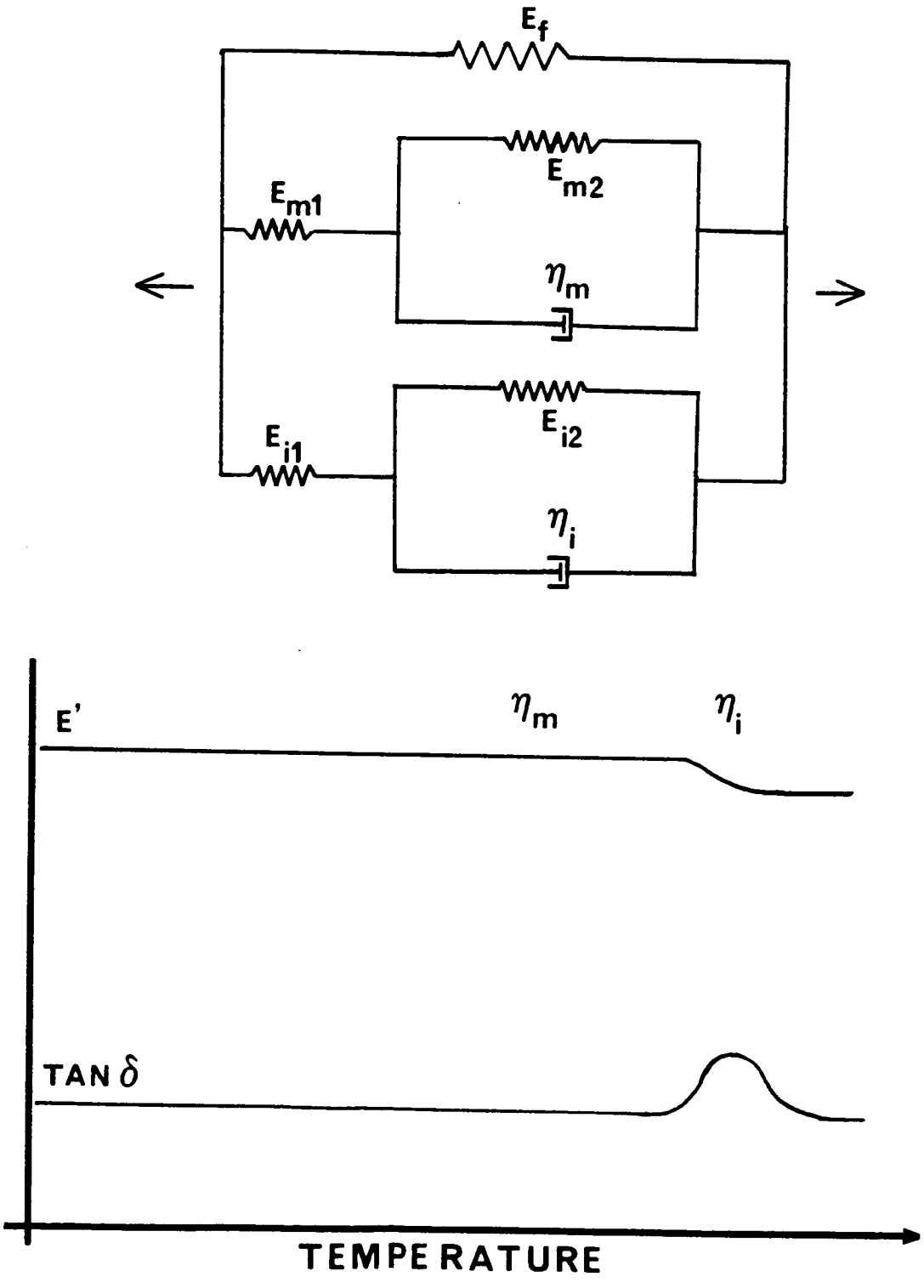

Figure 4.24 Model of 0° composite with an interfacial region

respectively. In the 90^{o} composite, a series model is used to describe the behavior. The response of the 0^{o} composite is best represented by a parallel model.

The response of the three components will be modelled in the following manner. The fiber response is assumed to be elastic throughout the temperature region in question; therefore, a spring (E_f) is used to represent the response of the fiber. A spring in series with a spring and dashpot in parallel are used to model the matrix (E_{m1},E_{m2},η_m) and the interfacial regions (E_{i1},E_{i2},η_i). Since the interfacial region is assumed to have a greater crosslink density than the matrix phase, the viscosity of the dashpots will be different, ie. $\eta_i > \eta_m$.

In Figure 4.23, the model behavior of the 90^{o} composite is illustrated. Below the transition region, the viscosities, η_i and η_m are very high, ie. the interfacial and matrix phases are below their respective Tg's. Consequently the springs E_{m1}, E_{i1} and E_f respond to an applied stress. As the temperature is increased, the viscosity, η_m, decreases, allowing E_{m2} to respond. The damping of η_m will cause E_{m2} to lag behind E_{m1}, E_{i1} and E_f. Since E_{m2} is out of phase with the other springs, a damping peak occurs in the loss tangent spectrum. In the first plateau region, η_m becomes very small and can not dissipate much energy. The spring, E_{m2}, is now responding to the applied stress, yielding a lower modulus. With a further increase in temperature, η_i decreases. The

decrease in η_i permits E_{i2} to react to the applied stress, but E_{i2} will be out of phase with the other springs. This phase difference creates another damping peak. Furthermore, as η_i decreases, E_{i2} and the other springs are responding to the applied stress. Thus the modulus decreases again (second plateau region).

The parallel model for a 0^o composite is illustrated in Figure 4.24. In the low temperature range the response is dominated by E_f. When the temperature is increased, η_m becomes less viscous. However, the elements are in parallel and E_{m2} can not respond to the applied stress, ie. it is constrained by η_i. After the temperature is raised to a point at which η_i decreases, E_{m2} and E_{i2} can respond. The response of E_{m2} and E_{i2} will be minimal because $E_f >> E_{m1}, E_{m2}, E_{i1}, E_{i2}$. Due to the fact that E_f is quite large, η_i will not create a significant degree of damping.

The models that have been presented permit a comparison to be made between specimen response and model response. In Tables 4.6 and 4.9, the glass transition temperatures for each composite (5208 and 5209) are listed. As is predicted by the models, the 0^o orientation in each composite has a significantly greater Tg than the 90^o orientation. In other words, the Tg measured in the 0^o composites is actually the Tg of the interfacial region (Tg_i). Additionally, as would be expected, the loss tangent intensity is suppressed in the 0^o composites when compared to the 90^o composite (Tables 4.7

and 4.10).

Contrary to the behavior predicted by the model, only one transition region is observed (experimentally) in the 90° composites. In Figure 4.11, there is evidence of the onset of another transition ca. 320°C. The loss tangent appears to be progressing toward another peak, and the elastic modulus is again declining. The onset of another transition appears possible. To measure this phenomenon, several samples were taken to higher temperature (360°C). Sample behavior is shown in Figure 4.25 and 4.26. Irradiated and unirradiated specimens exhibited two transition regions as evidenced by the two α-transitions and two plateau regions. The presence of an interfacial region seems plausible. (Note in Figure 4.26, that the scanning rate is higher by about 2°C/min and a curing peak appears at 230°C.)

The specimens in Figures 4.25 and 4.26 have been exposed to high temperatures which can cause thermal degradation. Netravali (53) showed that cured 73/27 TGDDM/DDS epoxy experienced a dynamic weight loss (measured by TGA) of 1.2% at 325°C. After the epoxy was exposed to ionizing radiation (700 Mrads), the dynamic weight loss increased to 1.7% at 325°C. Considering the present investigation with samples being exposed to a dose of 10,000 Mrads and temperatures of 360°C, the polymer network is altered. Thermal degradation at the interface could be an alternate explanation for the higher temperature α-transition. However, the fact that a

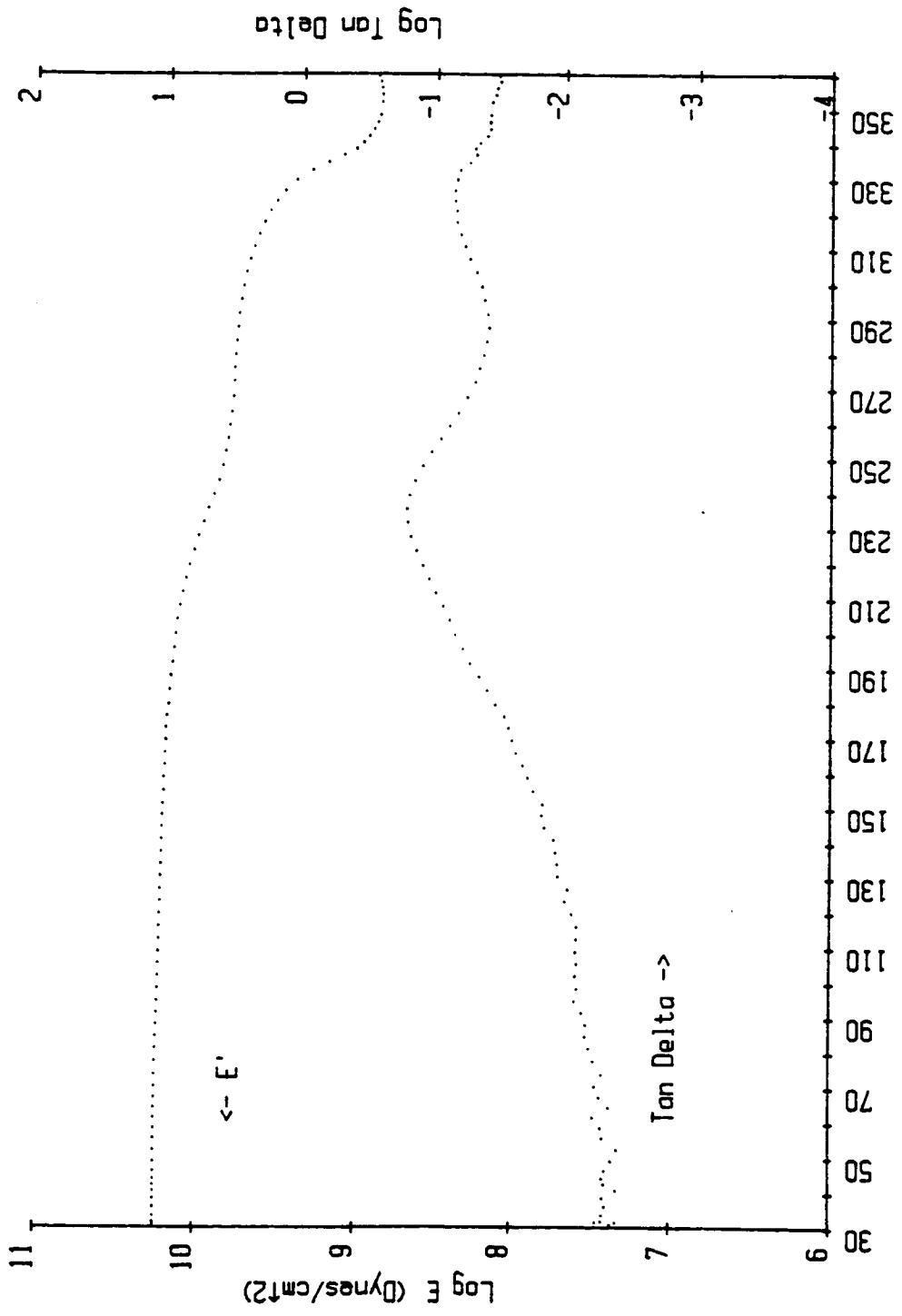

Figure 4.25 Elastic modulus and loss tangent of T300/5208 90^{o} 4-ply composite as a function of temperature (10,000 Mrads)

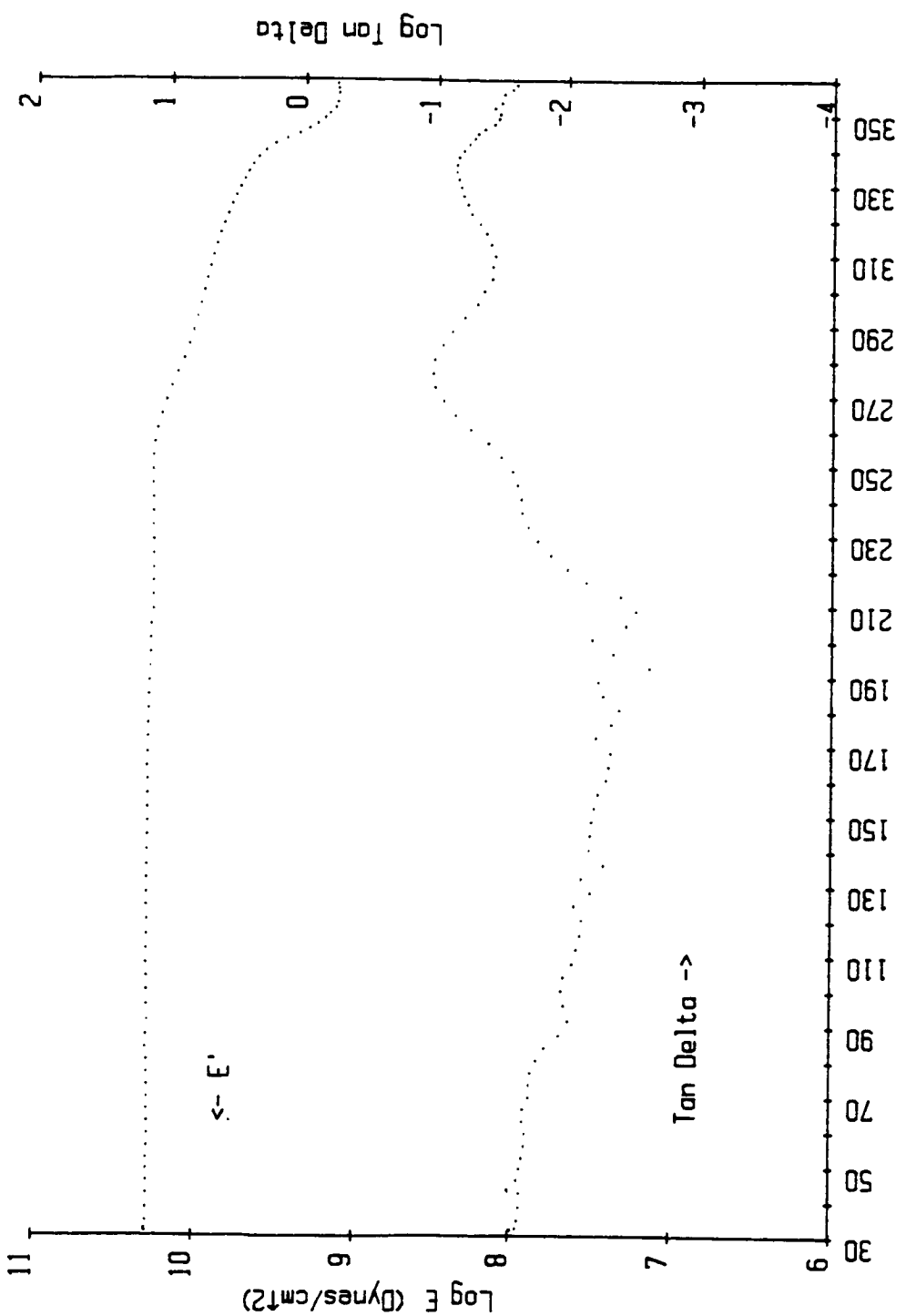

Figure 4.26 Elastic modulus and loss tangent of T300/5208 90^{o} 1-ply composite as a function of temperature (control)

plateau region (E') exists above the higher temperature transition implies that the sample did not experience catastrophic failure. Furthermore, when a specimen (T300/5208/90/4 - 1000 Mrads) is cooled (after being thermally cycled to 360°C) and tested again, E'rt is only 4.6% below the value of E'rt prior to the thermal cycle.

A further examination of T300/5208 90° composites may indicate whether or not an interfacial phase does exist. If the composite possesses only one phase in the matrix, then a calculation of E'rt and E'_{Tg+40} will indicate one phase. The following equation (section 8.3) provides a measure of E'rt and E'_{Tg+40} for a 90° composite specimen.

$$Ec = \frac{Ef\ Em}{Vf\ Em + Vm\ Ef} \qquad (4.1)$$

The terms Ec, Em and Ef are the moduli of the 90° composite, the matrix and the fiber in the transverse direction, respectively. The volume fractions of fiber and matrix are Vf and Vm, respectively. The transverse modulus of graphite fibers is not known, but it should be approximately the modulus of graphite (1×10^{11} dynes/cm^2 transverse to the basal planes). From Table 8.1, Em at ambient temperature is 2.5×10^{10} dynes/cm^2. The volume fractions are Vf = 0.6 and Vm = 0.4. Substituting the values into equation 4.1 yields Ec = 4.5×10^{10} dynes/cm^2. This value for Ec compares quite well with the value of Ec for the 90° composites found in Table 8.1, ie. 5.0×10^{10} dynes/cm^2. From the measured and

predicted Ec's at room temperature, it appears that the response can be adequately described by one phase in the matrix.

At E'_{Tg+40} in the first plateau region, Ec can also be estimated. The modulus of the matrix, Em, in this region is 5.0×10^8 dynes/cm^2 (10,000 Mrad dose level). The other parameters, Ef, Vf and Vm are listed above. For a system with only one matrix phase, the predicted Ec at Tg+40 is 1.2×10^9 dynes/cm^2. The measured Ec in the first plateau is 7.6×10^9 dynes/cm^2. In the second plateau region above 340°C, Ec = 0.9×10^9 (Figure 4.25). The measured Ec for the second plateau region closely approximates the predicted value for the continuous phase. The above finding suggests that a continuous interfacial region exists which has a substantially higher Tg than the resin phase, ie. two phases exist in the matrix. (The 10,000 Mrad dose level was presented due to the fact that the first plateau region is more apparent at this dose. The results are similar for the control).

The interfacial region is not resolved in the T300/5209 90° and 45° specimens. The T300/5209 0° composite specimens do have a higher Tg than their 90° and 45° counterparts, but the second peak is not evident in 90° and 45° orientations over the temperature range investigated. One possibility for the absence of an interfacial transition in 90° and 45°

orientations of T300/5209 is that the interfacial transition is masked by the transition of the bulk matrix. If the interfacial region is very small, then its transition may not be resolvable by the present technique.

The contraction of 90^{o} and 45^{o} specimens, after being exposed to a thermal cycle, can also be rationalized on the basis of the proposed model. First, assume that during fabrication the epoxy initially vitrifies on the surface of the graphite fibers (Figure 4.27). Next, this vitrified layer extends radially out from the fiber surface as the cure proceeds. At some point, the vitrified layers will impinge on each other. When the layers impinge, there are channels of "trapped" gel-like epoxy. As the gel-like regions of epoxy crosslink, the network tries to contract, but it is constrained by the vitrified regions which bound it. The previous curing condition would impose stresses in the epoxy that occupies the "channel" regions. As the specimens are heated, the epoxy in the "channels" becomes mobile and tries to contract, but it is still constrained. With further increases in temperature, the region between adjacent fibers becomes mobile. The matrix and interfacial region can relax, thus releasing the stresses which were imposed during fabrication. As the sample returns to ambient temperature, the stresses have been released, and the sample is free to contract. (Note: cooling may impose some stresses as well, ie. the sample may contract after another thermal cycle).

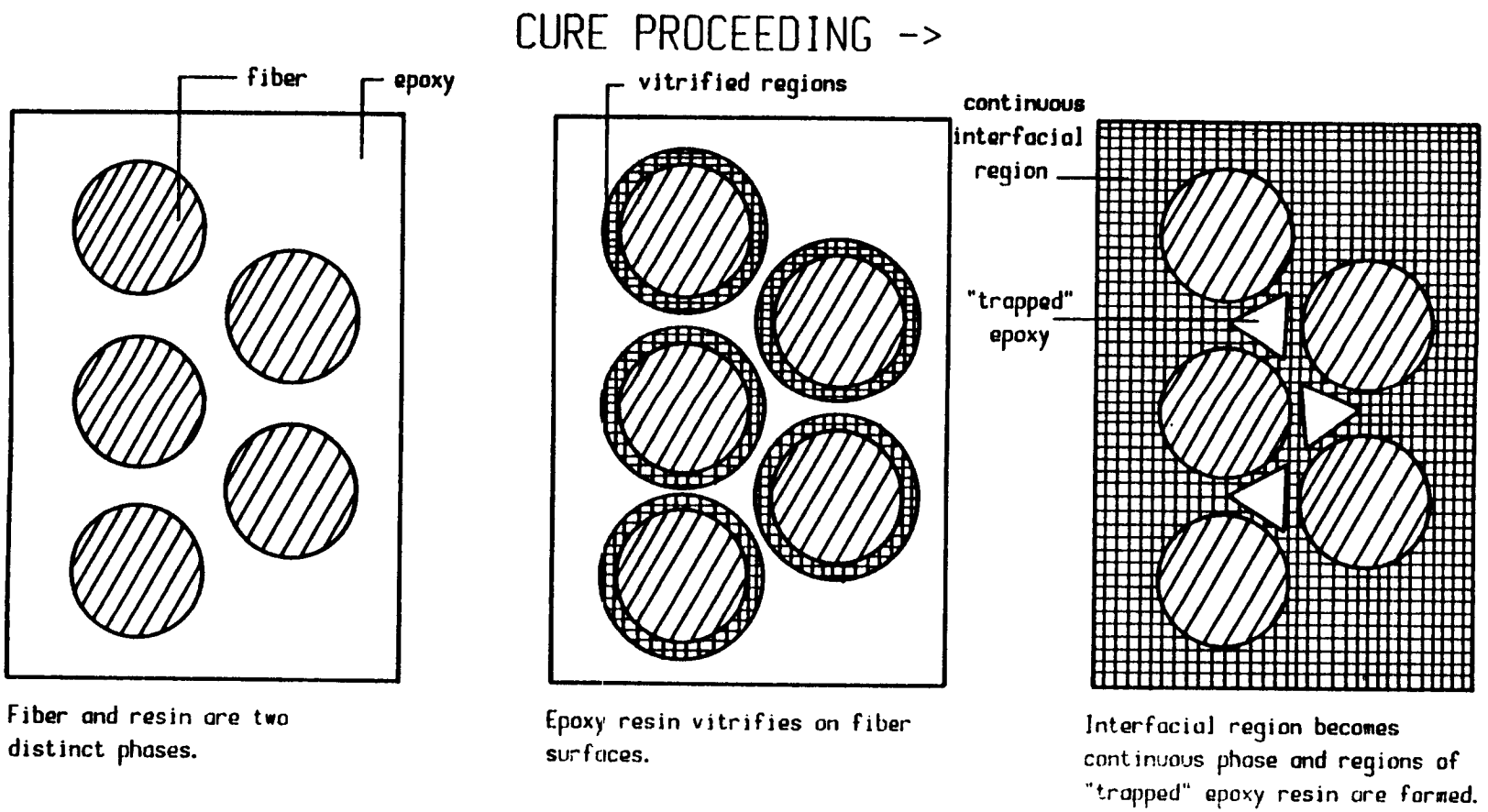

Figure 4.27 Diagram of composite cure

The explanation invoked for the sample contraction following a thermal cycle would also explain the contraction of the T300/5208 90^{o} specimens above Tg (ie. in the first plateau region). When the region between adjacent fibers becomes mobile, the sample (if it possesses sufficient internal stress) could contract. The contraction above the first Tg indicates the onset of the Tg of the interfacial region (Tg_i) between the fibers, ie. the onset of Tg_i=290^{o}C - 300^{o}C.

An interfacial region with different properties is certainly possible and its presence explains some of the conflicting data. Another desirable piece of information would be the extent of the interfacial region. Babich and Lipatov (66) have suggested that when the fiber volume fraction is 0.6 - 0.7, the interfacial region may be continuous. If the interfacial region is the continuous phase, then sample yielding would not occur until at or above the α-transition maximum of the interfacial region. The expansion behavior of the specimen shown in Figure 4.26 is illustrated in Figure 4.28. Sample yielding occurs at 340^{o}C, which is slightly above the α-transition maximum associated with the Tg of the interfacial region. The temperature at which the composite specimen yields implies that the interfacial region and not the epoxy resin is the continuous phase in the specimen. If the resin were the continuous phase, then the yielding would have occurred $\leq$290^{o}C.

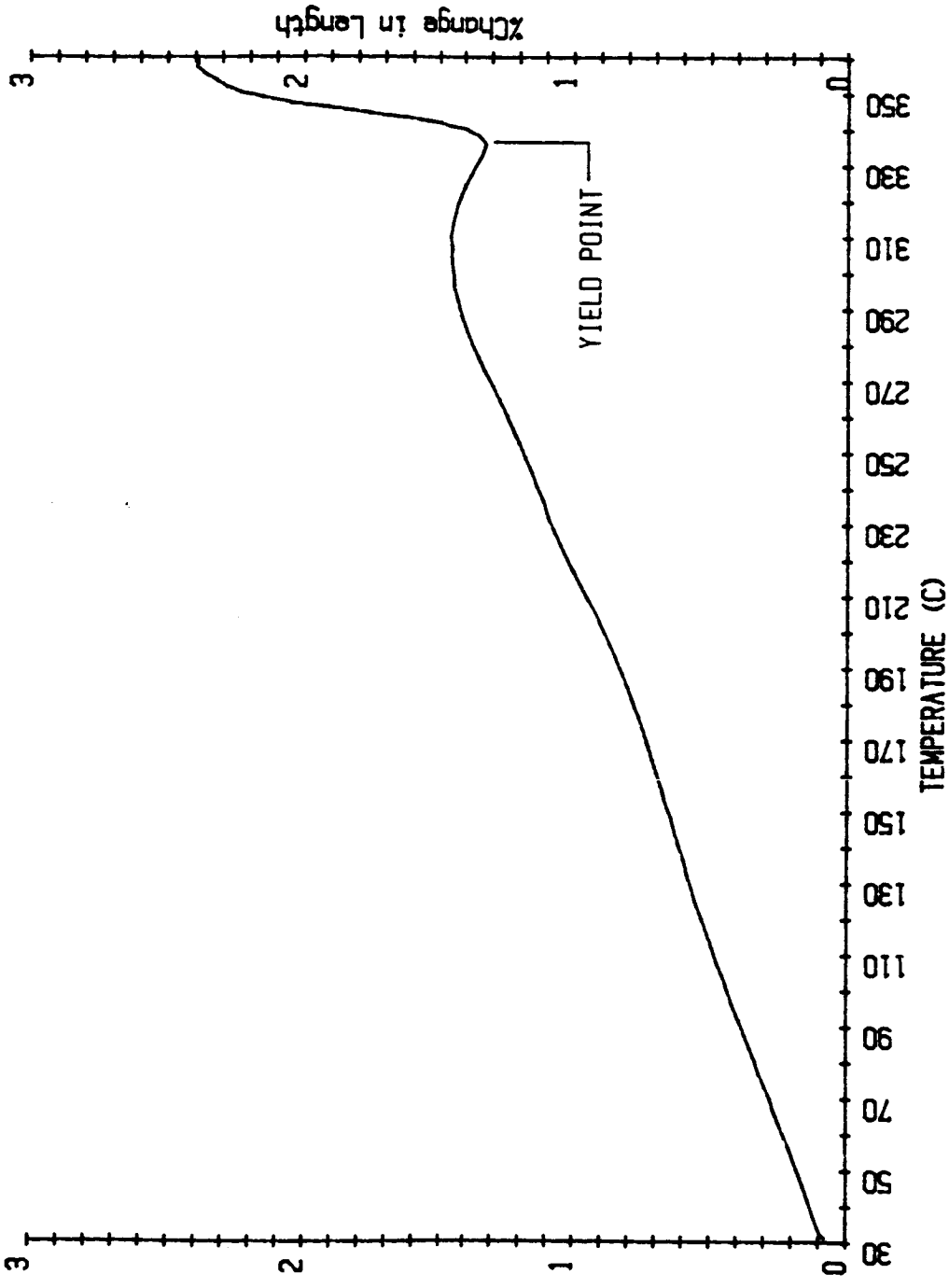

Figure 4.28 Percent change in length as a function of temperature for T300/5208 90° 1-ply composite (control)

Composite specimens which are heated past their yield point do not contract when returned to ambient temperature. Similar behavior is exhibited by the epoxy resins.

In the present investigation, it appears that composites based on TGDDM/DDS may possess an interfacial region which is (probably) continuous. Considering the models, Tg_{∞} for 90^{o} and 45^{o} composites and Tg_{∞} for the 0^{o} composites, composites based on TGDDM/DDS/DGEBA appear to have a less extensive interfacial region than that in the TGDDM/DDS based composites. The extent of the interfacial region in the two resin systems can be illustrated by the results previously presented. The contraction following a thermal cycle for the 5209 based composites is less than that of the 5208 based composites of similar construction. The differences in contraction are probably due to the interfacial region being less extensive in the 5209 based composites. The 5209 based composites do not contract above Tg, implying that the "channel" regions are not under a large stress. The fact that the α-transition for the interfacial region in the 5209 90^{o} composites has not been resolved suggests that the interfacial region may not be as extensive when compared to 5208 composites.

At this point, no hypothesis has been made concerning the composition of the interfacial region. Since the ratio of reactants in the 5209 resin formulation is not available, speculation concerning the composition of the interfacial

region would be difficult. However, in 5208 based composites, there are two (hypothetical) possibilites: a region that has a concentration of DDS greater than the original formulation, and a region that has a concentration of TGDDM greater than the original formulation.

Examination of the first situation suggests that a DDS "rich" phase would not be probable. The DDS, being predominantly difunctional due to steric hindrance, would effectively increase Mc and decrease Tg (5,6,13-15).

The second possibility seems most probable. The lowest Mc and highest Tg for the present systems would occur in a phase consisting exclusively of TGDDM with all the available epoxide groups reacted. A situation such as this is not probable, but a TGDDM "rich" phase with a high degree of conversion would provide similar responses to the measured properties. (Note: the above explanation of the composition of the interface is only speculative).

In summary, the composites considered in this investigation are highly resistant to radiation induced degradation. There appears to be a heterogeneous matrix which consists of an "interfacial" region and the resin. The interfacial region exhibits a glass transition temperature which is about $30^{\circ}C$ - $40^{\circ}C$ higher than that of the resin phase.

4.2 DSC Studies

The thermal properties of the epoxy resin samples were characterized by differential scanning calorimetry. The exothermic curing energy decreases monotonically with increasing doses of absorbed radiation (Table 4.12). The value of 24.2 cal/gm for the 73/27 TGDDM/DDS control specimen compares with 18.7 cal/gm found by Netravali (53). Netravali found a greater percentage decrease in curing energy as a function of dose than was measured in the present work. The exothermic curing energy for a 73/27 TGDDM/DDS epoxy decreased 20% after a dose of 700 Mrads (53). A similar decrease does not occur in the present study until the dose is >2000 Mrads.

The curing energy for a 63/37 TGDDM/DDS specimen (unirradiated) is 18.9 cal/gm. In the dynamic mechanical spectrum, a small damping peak associated with additional curing reactions is displayed by the 63/37 ratio (Figure 4.1). The 73/27 and 80/20 ratios also exhibit this curing behavior (damping peak) up to a dose of 1000 Mrads. From the exothermic curing energy of the epoxy resins and specimen response in the Autovibron, it appears that as the ionizing radiation dose increases the sample is cured further, and the additional curing reactions are not resolved. Therefore, the Autovibron provides only a limited measure of the additional cure in these systems. However, the DSC results confirm the

Table 4.12 Exothermic curing energy as a function of dose for 73/27 and 80/20 TGDDM/DDS epoxy measured by DSC at 20°C/min

	curing energy[1] (cal/gm)	
Dose (Mrads)	73/27 TGDDM/DDS	80/20 TGDDM/DDS
control	24.2 ± 2.6	35.3 ± 3.2
1000	23.3 ± 2.8	25.1 ± 1.6
2000	21.0 ± 1.4	21.0 ± 1.6
3000	13.7 ± 1.1	18.4 ± 0.9
4000	10.7 ± 0.4	14.0 ± 1.2
5000	4.5 ± 0.7	6.1 ± 0.3
10,000	2.2 ± 0.4	2.7 ± 0.0

[1]mean of three values ± the range of the values.

dynamic mechanical analysis in that the epoxy resin is not "fully" reacted, and radiation promotes additional curing reactions in the epoxy.

4.3 Sorption/Desorption Studies on Epoxy Resin Specimens

The purpose of the sorption/desorption studies was to eliminate the effects of degradation products on the dynamic mechanical response. Selected specimens of 73/27 TGDDM/DDS and a 80/20 TGDDM/DDS were allowed to absorb acetonitrile to equilibrium. The acetonitrile was desorbed, and the dynamic mechanical response of the samples was determined.

After a sorption/desorption cycle, the control specimen (73/27 TGDDM/DDS) does not exhibit a curing peak (Figure 4.29). The acetonitrile plasticizes the network, and the system Tg is sufficiently lowered to permit further curing probably during desorption. The Tg_∞ after a sorption/desorption cycle is 2.0°C below the mean Tg_∞ of the untreated control specimens. Also, the loss tangent intensity is essentially unchanged between the two treatments. Evidently, the sorption/desorption cycle permits additional cure to occur but does not drastically alter the final network structure.

The glass transition temperature (Tg_∞) at the 10,000 Mrad dose level increases for the 80/20 and 73/27 TGDDM/DDS samples after a sorption/desorption cycle. The glass transition temperatures for the 73/27 (Figure 4.30) and 80/20

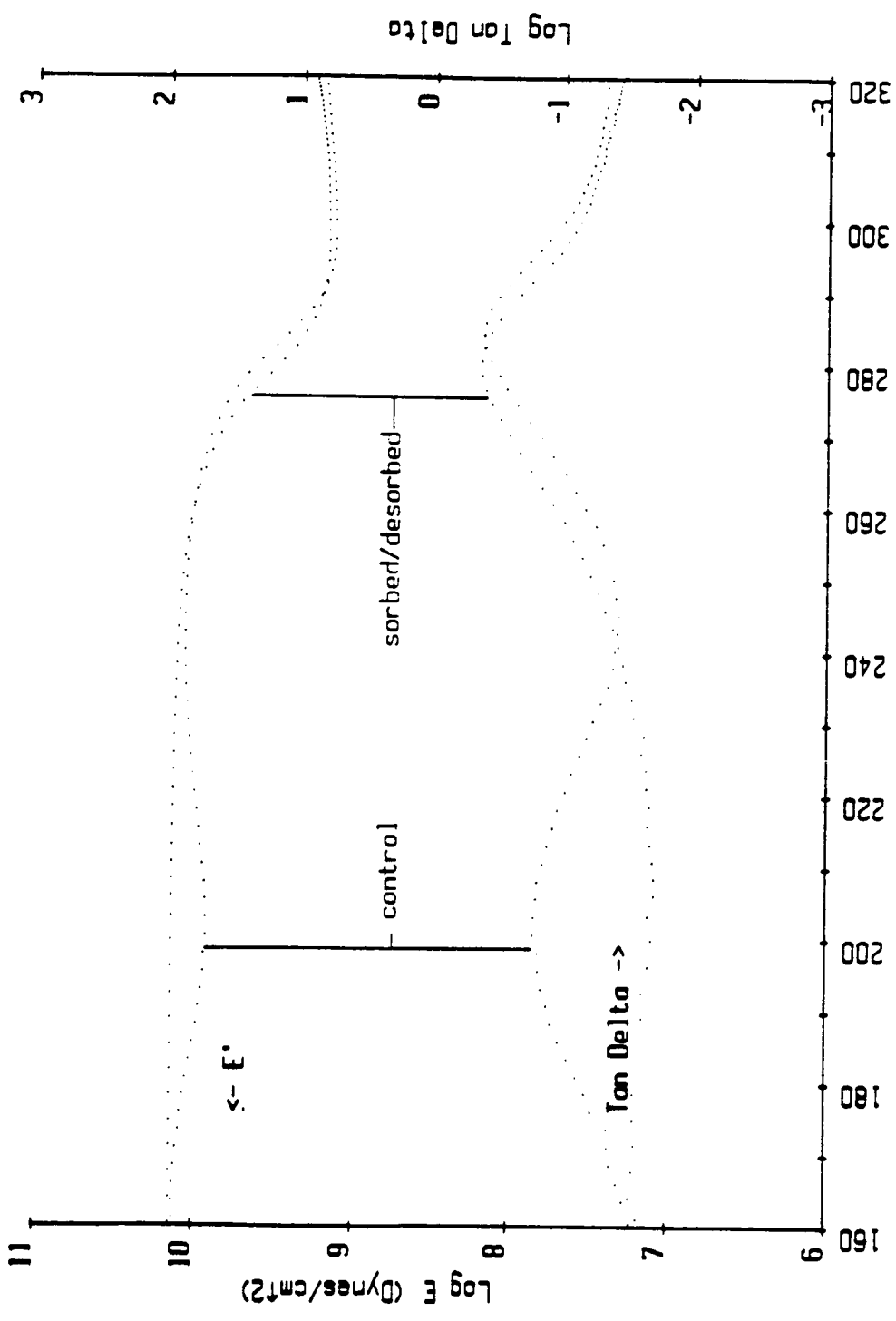

Figure 4.29 Elastic modulus and loss tangent of cured 73/27 TGDDM/DDS epoxy as a function of temperature (control and control sorbed/desorbed CH_3CN)

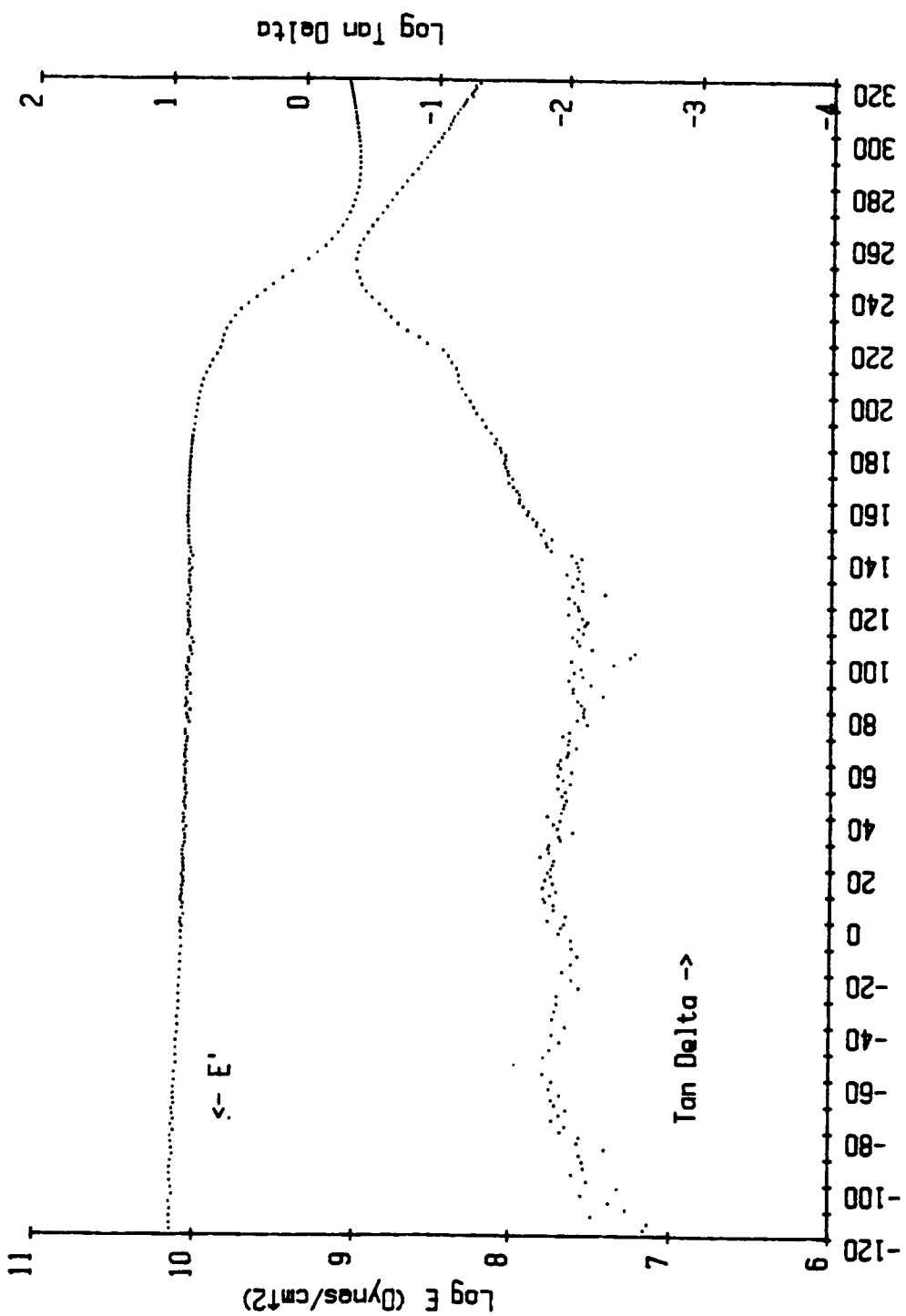

Figure 4.30 Elastic modulus and loss tangent of 73/27 TGDDM/DDS (10,000 Mrads - sorbed/desorbed CH_3CN)

(Figure 4.31) ratios are 248°C and 250°C, respectively. In samples that had not been sorbed/desorbed, both ratios exhibit a Tg of 238°C. The loss tangent peak is decreased in magnitude about 20% after the sorption/desorption cycle, indicating that degradation products plasticized the network.

The weight loss after the sorption/desorption cycle is 1.3% for the specimens irradiated to 10,000 Mrads. The low weight loss indicates that only a small amount of degradation products are formed. Yang (50) found a similar weight loss in a cured resin that had not been irradiated, showing that a weight loss of 1.3% is a reasonable value and limited degradation occurs. The glass transition temperature should have returned to approximately the value of the unirradiated epoxy (280°C) if the degradation products are the only species plasticizing the network.

It is possible that either Mc has been effectively increased by degradation of the network structure or the resin is internally plasticized by free chain ends resulting from chain scission. If Mc has increased, then the modulus in the rubbery plateau region for irradiated specimens should be less than that of a control. Referring to Table 4.2, E'_{Tg+40} decreases up to a dose of 5000 Mrads. Between a dose of 5000 Mrads and 10,000 Mrads, E'_{Tg+40} is increased but remains about 6% below the control value. For the 73/27 TGDDM/DDS and 80/20 TGDDM/DDS samples (10,000 Mrads) which have been sorbed/desorbed, E'_{Tg+40} is 18.5% greater than the

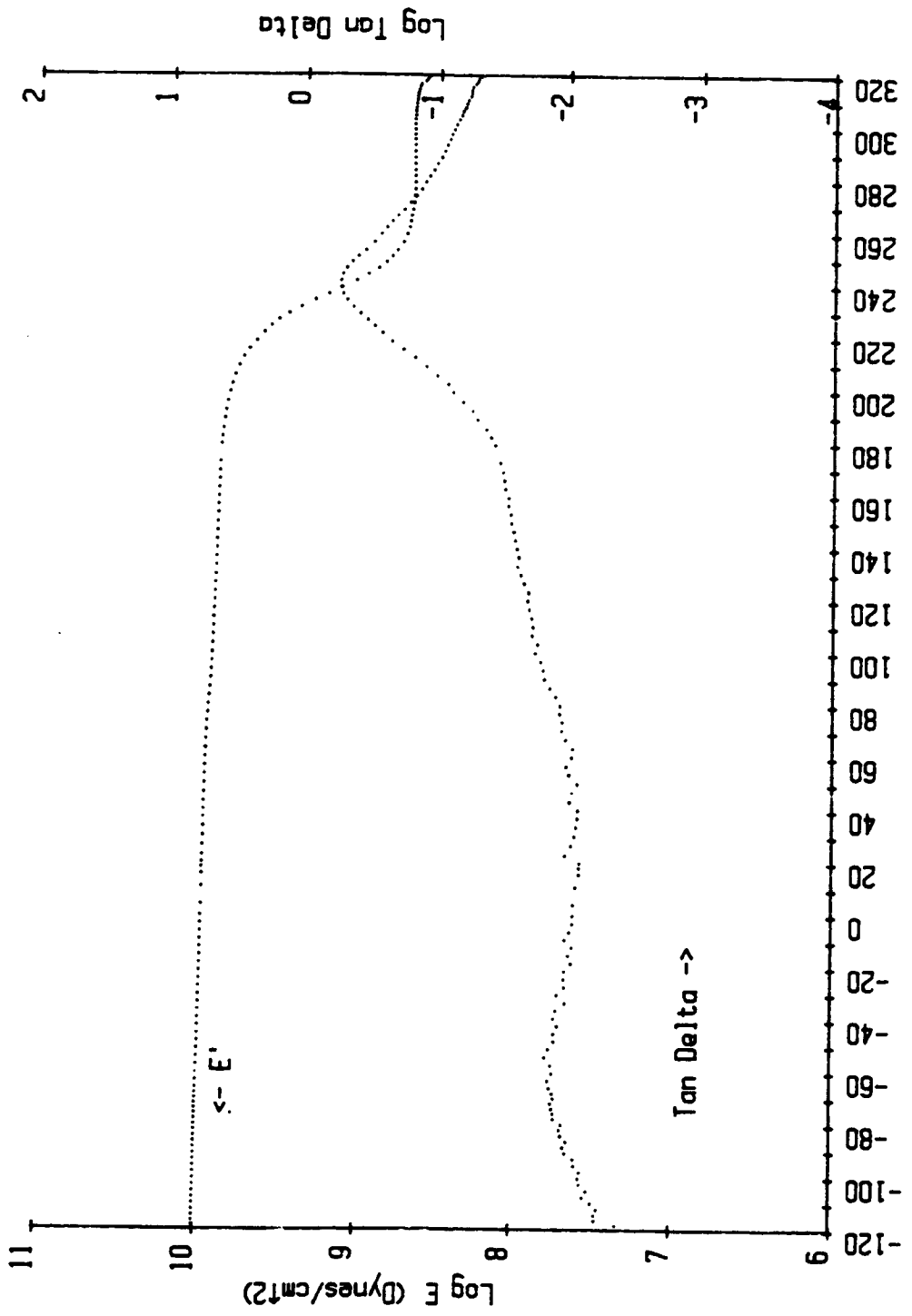

Figure 4.31 Elastic modulus and loss tangent of 80/20 TGDDM/DDS (10,000 Mrads - sorbed/desorbed CH_3CN)

control value. It may be concluded that irradiated specimens (10,000 Mrad dose) are more crosslinked than the control specimens, and there is limited degradation. That is irradiation causes both chain scission and additional crosslinking.

The Tg's of the irradiated specimens are not as high as anticipated if only crosslinking occurs. In that case the Tg of irradiated specimens should be $\geq 280^{\circ}C$. To account for the experimental observations, the following explanation is suggested. As a sample is irradiated, chain scission and crosslinking occur. The chain scission, though not castrophically degrading the network, will create a number of free chain ends. An increase in the number of free chain ends will have several effects. The polymer density will decrease due to the greater free volume swept out by the chain ends (65). The α-transition will be shifted to lower temperature, and it will increase in magnitude due to internal plasticization (10). The rubbery plateau region is not affected by an increase in the number of chain ends if Mn (number average molecular weight) is very large (5,65). However, crosslinking would increase Tg, but this is offset by the chain scission.

The changes in the dynamic mechanical spectrum as a function of irradiation arise from an increase in the number of free chain ends and additional crosslinking.

5. CONCLUSIONS

The present research program was designed to investigate the effects of ionizing radiation on the structure of TGDDM/DDS epoxies and two graphite fiber/epoxy composites (T300/5208 and T300/5209) using dynamic mechanical analysis. The major conclusions of this investigation are listed below:

1. The most noticeable property change is a decrease in the glass transition temperature of the epoxy resin and composite systems as a function of absorbed dose.

2. Degradation products are generated in the epoxy resin by ionizing radiation. The degradation products and free chain ends created by scission plasticize the matrix, resulting in a lower Tg.

3. The epoxy resins, as fabricated, have a number of unreacted functional groups. Ionizing radiation causes some of these groups to react.

4. The main network structure is not degraded, but an increase in the number of free chain ends is thought to contribute to the lower glass transition temperatures.

5. Chain scission is the predominant process at lower dose levels (<5000 Mrads), resulting in a decrease in elastic modulus at ambient temperature for the epoxy resin.

6. Additional crosslinking in the epoxy resins at high doses (>5000 Mrads), results in an increase in elastic modulus at ambient temperature and in the rubbery region

above Tg.

7. Elastic moduli of the composite specimens are not adversely affected by radiation, suggesting that the fiber matrix interface is not significantly degraded.

8. Certain anomalies are present in the glass transition temperature and the expansion/contraction behavior of selected composite orientations. Specifically, the anomalies are:

a) glass transition temperatures of 0° composite specimens are $30^{\circ}C$ to $40^{\circ}C$ greater than the glass transition temperatures of the 90° and 45° specimens,

b) 90° and 45° composite specimens contract up to 2.0% following a thermal cycle to $320^{\circ}C$, and

c) T300/5208 90° composite specimens exhibit a length contraction as a function of temperature above Tg. The anomalous behavior in the composite specimens is rationalized by assuming the presence of an "interfacial" region between the fiber and the matrix. Suitable models, which incorporate the "interfacial" region, are presented for the 90° and 0° orientations. The "interfacial" region is predicted to cause differences in the dynamic mechanical response of composites, depending upon the fiber orientation in the specimen. The experimental results on 90° and 0° (fiber orientation) composites are comparable to the model predictions. Due to the thermal cycle to which the specimens are exposed, the interfacial effects noted in the composite specimens could

occur due to thermal degradation at the interface.

6. RECOMMENDATIONS

The present investigation has provided a means to probe the "interfacial" region in graphite fiber/epoxy composites. Future areas of study could include the effects of cure temperature, fiber/epoxy volume fraction and epoxy stoichiometry on the extent of the "interfacial" region, ie. whether or not it is a continuous phase. A study which utilizes sorption/desorption cycles to release internal stresses would prove useful in characterizing the "interfacial" region. A practical investigation could focus on the amount of an "interfacial" region which would optimize the properties of structural composites.

7. LIST OF REFERENCES

1. Parkinson, W. W. and O. Sisman. 1971. The use of plastics and elastomers in nuclear radiation. Nuc. Eng. Des. 17:247-280.

2. Wolf, K. W. 1982. Effect of Ionizing Radiation on the Mechanical and Structural Properties of Graphite Fiber Reinforced Composites. PhD Dissertation. North Carolina State University.

3. Seehra, S., D. Benton, J. Rosen and R. Gounder. 1985. Effects of space environmental conditions on graphite epoxy composites. SAMPE J. 21(2):18-23.

4. Sykes, G. F., S. M. Milkovich and C. T. Herakovich. 1985. Simulated space radiation effects on a graphite epoxy composite. Proceedings of Am. Chem. Soc., Polym. Mats.: Sci. and Eng. 52:598-603.

5. Murayama, T. 1978. Dynamic Mechanical Analysis of Polymeric Materials. Elsevier Scientific Publishing Corporation, New York.

6. Murayama, T. and J. P. Bell. 1970. Relation between the network structure and dynamic mechanical properties of a typical amine-cured epoxy polymer. J. Polym. Sci.: Part A-2 8:437-445.

7. Takahama, T. and P. H. Geil. 1982. The β relaxation behavior of bisphenol-type resins. J. Polym. Sci.: Polym. Phys. Ed. 20:1979-1986.

8. Keenan, J. D. 1979. Structure and Dynamic-Mechanical Properties of TGDDM-DDS Epoxy, Graphite Fibers, and Their Composite. Masters Thesis. University of Washington.

9. Jenkins, R. K. 1964. Dynamic modulus properties of some polymers during gamma radiation. J. Polym. Sci. Part B Polym. Letters. 2:999-1003.

10. Nielsen, L. E. 1974. Mechanical Properties of Polymers and Composites, Vol. 1. Marcel Dekker Inc., New York.

11. Mones, E. T. and R. J. Morgan. 1981. FTIR studies of the chemical structure of high performance composite matrices. Am. Chem. Soc., Div. Polym. Chem. Polym. Prepr. 22(2):249-250.

12. Skeist, I. 1958. Epoxy Resins. Reinhold Publishing Corporation, New York.

13. Gupta, A., M. Cizmecioglu, D. Coulter, R. H. Liang, A. Yavrouian, F. D. Tsay and J. Moacanin. 1983. The mechanisms of cure of tetraglycidyl diaminodiphenyl methane with diaminodiphenyl sulfone. J. Appl. Polym. Sci. 28:1011-1024.

14. Morgan, R. J. and J. E. O'Neal. 1978. The durability of epoxies. Polym.-Plast. Technol. Eng. 10(1):49-116.

15. Morgan, R. J., J. E. O'Neal and D. B. Miller. 1979. The structure, modes of deformation and failure, and mechanical properties of diaminodiphenyl sulfone-cured tetraglycidyl 4,4' diaminodiphenyl methane epoxy. J. Mat. Sci. 14:109-124.

16. Morgan, R. J. and E. T. Mones. 1980. Further studies on the chemical and physical structure and deformation and failure-mode relationships of amine-cured epoxies. Am. Chem. Soc., Div. Polym. Chem. Polym. Prepr. 21(2):231-232.

17. Morgan, R. J. and E. T. Mones. 1980. Structure-property relations of composite matrices. Am. Chem. Soc. Symp. Ser. 132, Resins for Aerospace, Chap. 18:233-245.

18. Danieley, N. D. and E. R. Long. 1981. Effects of curing on the glass transition temperature and moisture absorption of a neat epoxy resin. J. Polym. Sci.: Polym. Chem. Ed. 19:2443-2449.

19. Babayevsky, P. G. and J. K. Gillham. 1973. Epoxy thermosetting systems: dynamic mechanical analysis of the reactions of aromatic diamines with the diglycidyl ether of bisphenol-A. J. Appl. Polym. Sci. 17:2067-2088.

20. Gillham, J. K. 1974. Review: torsional braid analysis of polymers. J. Macromol. Sci.-Phys. B9(2):209-237.

21. Gillham, J. K., J. A. Benci and A. Noshay. 1974. Isothermal transitions of a thermosetting system. J. Appl. Polym. Sci. 18:951-961.

22. Lewis, A. F., M. J. Doyle and J. K. Gillham. 1979. Effect of cure history on dynamic mechanical properties of an epoxy resin. Polym. Eng. Sci. 19(10):683-686.

23. Gillham, J. K. 1979. Formation and properties of network polymeric materials. Polym. Eng. Sci. 19(10):676-682.

24. Gillham, J. K. 1976. Characterization of thermosetting materials by torsional braid analysis. Polym. Eng. Sci. 16(5):353-356.

25. Gillham, J. K. 1974. A semimicro thermomechanical technique for characterizing polymeric materials: torsional braid analysis. AIChE. J. 20(6):1066-1078.

26. Enns, J. B., J. K. Gillham and R. Small. 1981. TTT state diagrams of epoxy/amine thermosets. Am. Chem. Soc., Div. Polym. Chem. Polym. Prepr. 22(2):123-124.

27. Gillham, J. K. and A. F. Lewis. 1963. Dynamic mechanical properties of supported polymers. II. Application of the torsional braid technique to the study of the curing and stability of resins. J. Appl. Polym. Sci. 7:2293-2306.

28. Schneider, N. S., J. F. Sprouse, G. L. Hagnauer and J. K. Gillham. 1979. DSC and TBA studies of the curing behavior of two dicy-containing epoxy resins. Polym. Eng. Sci. 19(4):304-312.

29. Doyle, M. J., A. F. Lewis and H.-M. Li. 1979. Time-temperature cure behavior of epoxy based structural adhesives. Polym. Eng. Sci. 19(10):687-691.

30. Prime, R. B. and E. Sacher. 1972. Kinetics of epoxy cure: 2. The system bisphenol-A diglycidyl ether/polyamide. Polymer 13:455-458.

31. Patterson-Jones, J. C. and D. A. Smith. 1968. The thermal degradation of an amine-cured epoxide resin at temperatures between 200_C and 310_C. J. Appl. Polym. Sci. 12:1601-1620.

32. Traeger, R. K. 1966. Dynamic mechanical testing to evaluate radiation induced changes in polymers. Rubber Chem. Tech. Part 2 39(4):1268-1273.

33. Takayanagi, M. 1963. Viscoelastic properties of crystalline polymers. Mem. of the Fac. of Eng., Kyushu Univ. 23(1).

34. Murayama, T. 1980. Measurement of dynamic mechanical properties. Rheology, Vol. 3: Applications. Edited by G. Astarita, G. Marrucci and L. Nicolais. Plenum Publishing Corporation, New York. 397-408.

35. Wedgewood, A. R. and J. C. Seferis. 1981. Error analysis and modelling of non-linear stress-strain behaviour in measuring dynamic mechanical properties of polymers with the Rheovibron. Polymer 22:966-991.

36. Massa, D. J. 1973. Measuring the dynamic moduli of glassy polymers: analysis of the Rheovibron. J. Appl. Phys. 44(6):2595-2600.

37. Ramos, A. R., F. S. Bates and R. E. Cohen. 1978. Importance of the Massa correction for loss tangent measurements on the Rheovibron. J. Polym. Sci.: Polym. Phys. Ed. 16:753-758.

38. Murayama, T. 1982. Measurement of dynamic viscoelastic properties of polymer melts and liquids by the modified Rheovibron. J. Appl. Polym. Sci. 27:89-96.

39. Kenyon, A. S., W. A. Grote, D. A. Wallace and McC. Rayford. 1977. Automation of the Rheovibron. J. Macromol. Sci.-Phys. B13(4):553-570.

40. Murayama, T. 1982. Determination of the glass transition of polymer by the Autovibron. Polym. Eng. Sci. 22(12):788-792.

41. Gillham, J. K. 1981. Torsion pendulum and torsional braid analysis of polymers: A review. Am. Chem. Soc., Div. Polym. Chem. Polym. Prepr. 22(1):252.

42. Keenan, J. D., J. C. Seferis and J. T. Quinlivan. 1979. Effects of moisture and stoichiometry on the dynamic mechanical properties of a high-performance structural epoxy. J. Appl. Polym. Sci. 24:2375-2387.

43. Bucknall, C. B. and I. K. Partridge. 1983. Addition of polyethersulphone to epoxy resins. Brit. Polym. J. 15:71-75.

44. Bucknall, C. B. and I. K. Partridge. 1983. Phase separation in epoxy resins containing polyethersulphone. Polymer 24:639-644.

45. Private communication with J. K. Gillham.

46. Von Kuzenko, M., C. E. Browning and C. F. Fowler. 1980. Dynamic mechanical characterization of advanced composite epoxy matrix resins of altered composition. Am. Chem. Soc. Symp. Ser. 132, Resins for Aerospace, Chap. 18:233-245.

47. Rheovibron Product Bulletin. IMASS Inc. Hingham, MA.

48. Bell, J. P. 1970. Structure of a typical amine cured epoxy resin. J. Polym. Sci.:Part A-2 8:417-436.

49. May, C. A. and F. E. Weir. 1962. Dynamic mechanical properties of epoxy resins. SPE Trans. 2:207-212.

50. Yang, F., R. D. Gilbert, R. E. Fornes and J. D. Memory. To be published. Factors affecting H_2O absorption of the epoxy tetraglycidyl-4,4'-diaminodiphenyl methane cured with diaminodiphenyl sulfone. J. Polym. Sci., Chem. Ed.

51. McKague, Jr., E. L., J. D. Reynolds and J. E. Halkias. 1978. Swelling and glass transition relations for epoxy matrix material in humid environments. J. Appl. Polym. Sci. 22:1643-1654.

52. Browning, C. E. 1978. The mechanisms of elevated temperature property losses in high performance structural epoxy resin matrix materials after exposure to high humidity environments. Polym. Eng. Sci. 18(1):16-24.

53. Netravali, A. N. 1984. The Influence of Water and High Energy Radiation on the Thermal and Spectroscopical Characteristics of an Epoxy. PhD Dissertation. North Carolina State University.

54. Naranong, N. 1980. Effect of High Energy Radiation on Mechanical Properties of Graphite Fiber Reinforced Composites. Masters Thesis. North Carolina State University.

55. Park, J. S., R. D. Gilbert, J. D. Memory and R. E. Fornes. 1985. Effect of ionizing radiation on the interlaminar shear strength (ILSS) of graphite fiber/epoxy composites. Bull. Am. Phys. Soc. 30(3):490.

56. Seo, K. S. 1985. Electron Spin Resonance Investigations and Surface Characterization of TGDDM-DDS Epoxy and T-300 Graphite Fiber Exposed to Ionizing Radiation. PhD Dissertation. North Carolina State University.

57. Traeger, R. K. and T. T. Castonguay. 1966. Effect of γ-radiation on the dynamic mechanical properties of silicone rubbers. J. Appl. Polym. Sci. 10:535-550.

58. Traeger, R. K. and T. T. Castonguay. 1966. Effect of γ-radiation on the dynamic mechanical properties of styrene-butadiene rubbers. J. Appl. Polym. Sci. 10:491-509.

59. Araldite MY-720 Product Data. Ciba-Geigy.

60. Hardener HT-976 Product Data. Ciba-Geigy.

61. Cizmecioglu, M., S. D. Hong, J. Moacanin and A. Gupta. 1981. Spectroscopic characterization of NARMCO 5208 epoxy neat-resin formulations. Am. Chem. Soc., Div. Polym. Chem. Polym. Prepr. 22(2):224-225.

62. Autovibron. Automation system for the Rheovibron viscoelastometer AV-0082. Instruction Manual. Imass, Hingham, MA.

63. Pangrle, S., A. Chen, C. C. Wu and P. H. Geil. 1985. Epoxy resins - low temperature relaxation behavior. Bull. Am. Phys. Soc. 30(3):437.

64. Netravali, A. N., R. E. Fornes, R. D. Gilbert and J. D. Memory. 1984. Investigations of water and high energy radiation interactions in an epoxy. J. Appl. Polym. Sci. 29:311-318.

65. Bueche, F. 1962. Physical Properties of Polymers. Interscience, New York.

66. Babich, V. F. and Yu. S. Lipatov. 1982. On shift and resolubility of relaxation maxima with change in properties of the boundary polymer layer in composite materials. J. Appl. Polym. Sci. 27:53-62.

67. Private communication with D. J. Massa.

8. APPENDIX

8.1 Error Analysis and Correction Procedure

The error correction procedure, which Massa (36) developed for the Rheovibron, is not directly applicable to the Autovibron. A different approach has been suggested (67). The error correction for the Autovibron is outlined below.

Elastic moduli obtained from the Autovibron are dependent upon the (length)/(cross sectional area) of the specimens, ie. L/A. The dependence is not linear, but instead as $L/A \to \infty$, the measured sample modulus approaches the true sample modulus.

The following equations 8.1 and 8.2 represent the apparent sample modulus, Ea (E measured on the Autovibron), and the true sample modulus, Et (E corrected for machine and sample compliance):

$$Ea = \frac{C}{D}\frac{L}{A} \qquad (8.1)$$

$$Et = \frac{C}{D-Do}\frac{L}{A} \qquad (8.2)$$

Equation 8.1 is equivalent to equation 2.4 in the text, and equation 8.2 is equivalent to equation 2.10 in the text with AF=1 (AF=1 for the Autovibron). The constant term, C, equals 2×10^9. The term D is the "dynamic force," and D is analogous to a compliance. The term Do is the combined

compliance of the drive train and the compliance of the specimen in the grips. Solving equation 8.2 for D and substituting into equation 8.1 yields:

$$Ea = \frac{Et}{((Do*Et)/(C*L/A))+1} \qquad (8.3)$$

Since the parameters obtainable from Autovibron measurements are L/A and Ea, the following rearrangement provides a more manageable form:

$$Ea = \frac{L/A}{(Do/C)+((L/A)/Et)} \qquad (8.4)$$

A regression line was developed for the following equation:

$$Y = \frac{X}{B+(M*X)} \qquad (8.5)$$

with:

Y = Ea
X = L/A
B = Do/C
M = 1/Et.

The 73/27 and 80/20 TGDDM/DDS epoxies had been characterized previously on a Rheovibron. After error correction, the true moduli for the 80/20 and 73/27 TGDDM/DDS were 2.65 X 10^{10} dynes/cm^2 and 2.55 X 10^{10} dynes/cm^2, respectively. The true moduli, which were determined by using the above error correction for the Autovibron, were 2.65 X 10^{10} dynes/cm^2 and 2.53 X 10^{10} dynes/cm^2 for 80/20 and 73/27 TGDDM/DDS, respectively. There

is excellent agreement between the two error correction methods.

Listed in Table 8.1 are the Et and Do values for the epoxy and composite specimens. In the text, when the moduli have been corrected for percent changes in E', the following equation was used:

$$\%\Delta E' = \frac{Ex-Ea}{Ea} * 100 \qquad (8.6)$$

In the above equation, Ex is the modulus measured by the Autovibron, and Ea is the modulus that would be expected from equation 8.3 using the appropriate values for Do and Et found in Table 8.1.

8.2 Sorption/Desorption Study on a Composite Specimen

Only one composite specimen was exposed to a sorption/desorption cycle. Since the NARMCO 5209 formulation is proprietary, and the pure resin has not been evaluated, comparisons are at best qualitative. Shown in Figure 8.1 is the dynamic mechanical response of the T300/5209 90^{o} 4-ply specimen (10,000 Mrads dose level) which has been sorbed/desorbed with acetonitrile (compare with Figure 4.17). As evidenced by the two plateau regions and two α-transitions, an interfacial region may be present in the 5209 composites. The second α-transition (Tg_i) is ca. $196^{o}C$. This value compares quite favorably with the Tg for the 0^{o} composites ($186^{o}C$ to $194^{o}C$) in agreement with the models

Table 8.1 True moduli (Et), error constants (Do) and correlation coefficients (r) for epoxy and composite specimens on the Autovibron

Specimen	Et (dynes/cm^2)	Do	r
73/27 TGDDM/DDS	2.53×10^{10}	23.5	0.97
80/20 TGDDM/DDS	2.65×10^{10}	25.0	0.95
T300/5208/90°/1	4.90×10^{10}	21.3	1.00
T300/5208/90°/4	4.82×10^{10}	20.2	1.00
T300/5208/45°/1	7.27×10^{10}	20.2	0.98
T300/5208/0°/1	1.98×10^{11}	20.7	1.00
T300/5209/90°/1	3.98×10^{10}	21.3	1.00
T300/5209/90°/4	4.84×10^{10}	22.1	1.00
T300/5209/45°/1	7.79×10^{10}	21.1	1.00
T300/5209/0°/1	1.99×10^{11}	20.5	1.00
epoxy resin (E'_{Tg+40})	3.36×10^{9}	618	0.97

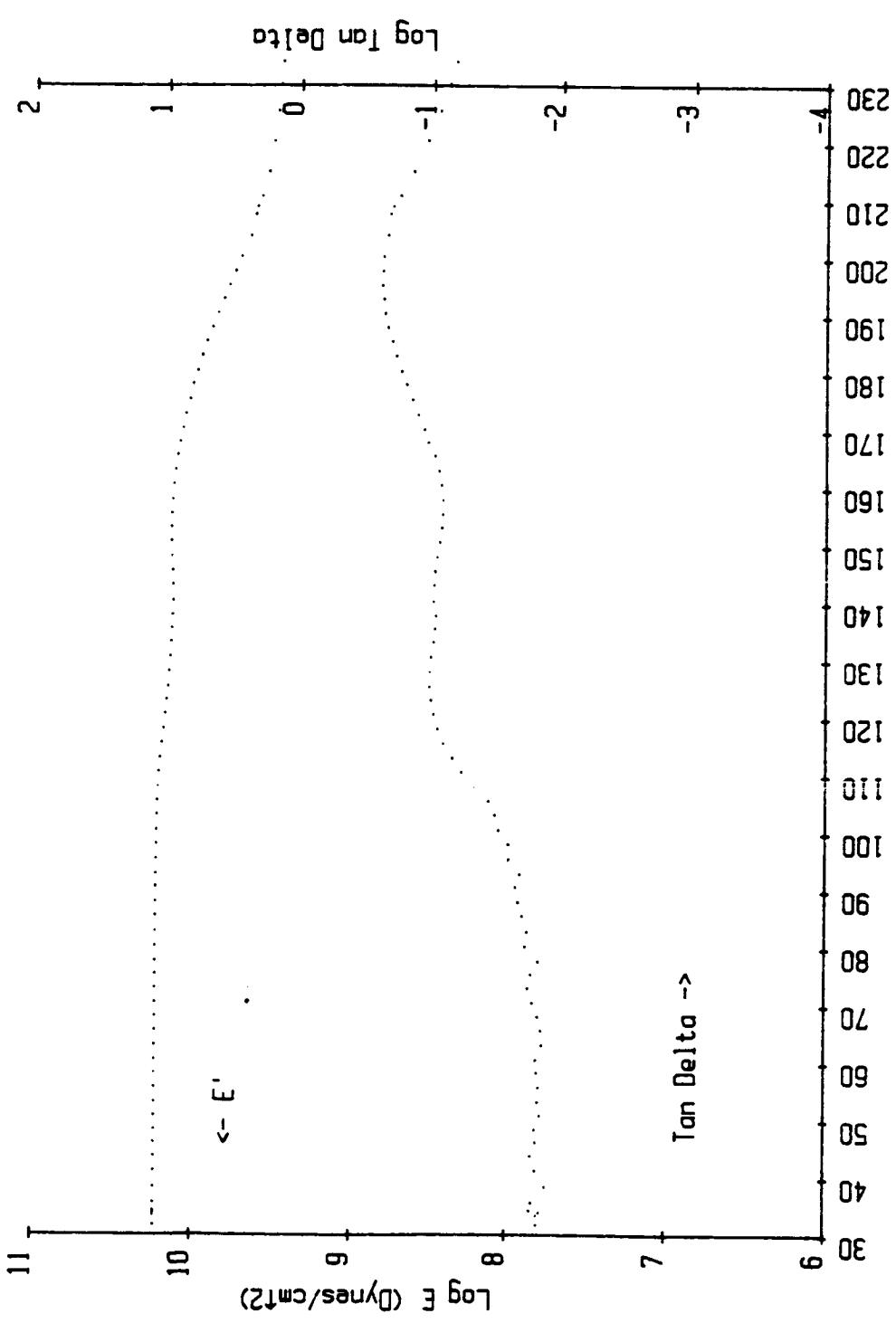

Figure 8.1 Elastic modulus and loss tangent of T300/5209 90° 4-ply composite as a function of temperature (10,000 Mrads - sorbed/desorbed CH_3CN)

(Figures 4.23 and 4.24).

The T300/5209 composites are plasticized by degradation products. A weight loss of 9% (on weight of resin) occurred for the composite after desorption. The degradation products plasticize the matrix to such an extent that the response of the interfacial region is not resolvable. When the small changes in Tg for the 0° composite are considered (0° composite Tg is essentially Tg of the interfacial region), the interfacial region is not greatly affected by plasticization in the T300/5209 composites.

When comparing differences in expansion behavior of the present sample with a sample that has not been desorbed, plasticization by degradation products is apparent (Figure 8.2). The plasticization effects, evidenced by the slope changes, are obvious in the sample that has not been sorbed/desorbed.

The model for the curing behavior (Figure 4.27) agrees with the sample contraction following a thermal cycle. The composite sample, in its swollen state, is quite leathery. The solvent could conceivably release the internal stresses (created during cure) by plasticizing the matrix and/or the interfacial regions. If the specimen is subjected to a thermal cycle after desorption, the contraction should be less. The contraction of a typical specimen exposed to a dose of 10,000 Mrads is 0.58%. The contraction of the sample with equivalent dose that had been sorbed/desorbed is 0.04%.

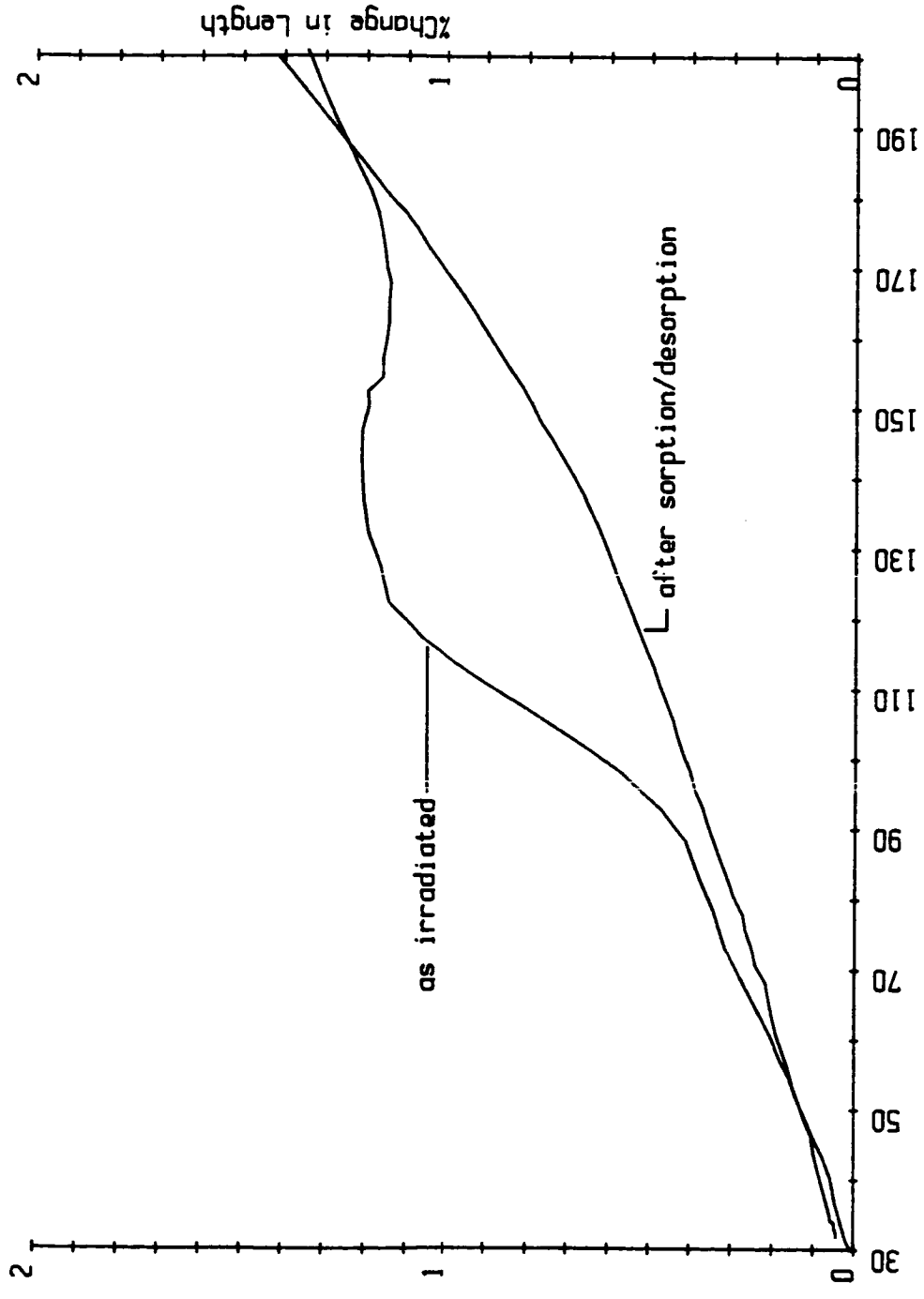

Figure 8.2 Percent change in length as a function of temperature for T300/5209 90°
4-ply composite (10,000 Mrads - sorbed/desorbed CH_3CN and 10,000 Mrads)

8.3 Equation for Ec of a 90° Composite

The two phase system, fiber and matrix, in a 90° composite can be represented by a spring for the transverse modulus of the fiber (Ef) and a spring and dashpot in parallel (Voigt element) for the matrix (Em,ηm). The total strain, ε, with a sinusoidal driving force is:

$$\varepsilon = Vf\ \varepsilon f + Vm\ \varepsilon m = \varepsilon_o \sin\omega t \qquad (8.7)$$

with Vf and Vm being the volume fractions of fiber and matrix, respectively. The stress on the fiber and matrix are given below:

$$\sigma_f = Ef\ \varepsilon f \qquad (8.8)$$

$$\sigma_m = Em\ \varepsilon m + \eta(d\varepsilon m/dt) \qquad (8.9)$$

and $\sigma_f = \sigma_m$, therefore;

$$Ef\ \varepsilon f = Em\ \varepsilon m + \eta(d\varepsilon m/dt) \qquad (8.10)$$

Substituting for εf from equation 8.7 into 8.10 yields:

$$Ef\ \varepsilon f = (Ef/Vf)(\varepsilon_o \sin\omega t - Vm\ \varepsilon m) \qquad (8.11)$$

Dividing by Ef yields:

$$\varepsilon f = \frac{\varepsilon_o \sin\omega t - Vm\ \varepsilon m}{Vf} \qquad (8.12)$$

Substituting for εf from equation 8.12 into equation 8.10 and rearranging yields:

$$(d\varepsilon m/dt)+(Vf\ Em + Vm\ Ef)(\varepsilon m/\eta) = (Ef\ \varepsilon_o/\eta)\sin\omega t \quad (8.13)$$

Let

$$\varepsilon m = A\sin(\omega t - \delta') \quad (8.14)$$

$$\varepsilon m = A\sin\omega t\cos\delta' - A\cos\omega t\sin\delta' \quad (8.15)$$

$$d\varepsilon m/dt = \omega A\cos\omega t\cos\delta' + \omega A\sin\omega t\sin\delta' \quad (8.16)$$

therefore,

$$\sin\omega t(\omega A\sin\delta' + (Vf\ Em + Vm\ Ef)A\cos\delta'/\eta) = (Ef\ \varepsilon_o/\eta)\sin\omega t \quad (8.17)$$

$$\cos\omega t(\omega A\cos\delta' - (Vf\ Em + Vm\ Ef)(A\sin\delta'/\eta)) = 0 \quad (8.18)$$

$$A = (Ef\ \varepsilon_o)/(\eta\omega\sin\delta' + (Vf\ Em + Vm\ Ef)\cos\delta') \quad (8.19)$$

Combining equations 8.11 and 8.14 yields:

$$Ef\ \varepsilon f = (Ef/Vf)(\varepsilon_o\sin\omega t - Vm\ A\sin(\omega t - \delta')) \quad (8.20)$$

$$Ef\ \varepsilon f = (Ef/Vf)(\varepsilon_o\sin\omega t - Vm\ A\cos\delta'\sin\omega t + Vm\ A\sin\delta'\cos\omega t) \quad (8.21)$$

The stress, $\sigma\ (= Ef\ \varepsilon_o)$, can also be represented as:

$$\sigma = \varepsilon_o(E'\sin\omega t + E''\cos\omega t) \quad (8.22)$$

Thus an equation for E' of the composite can be determined:

$$E' = (Ef/Vf)(1-(Vm\ A\cos\delta'/\varepsilon_o)) \quad (8.23)$$

Substituting for A from equation 8.19 gives:

$$E' = \frac{Ef}{Vf}\left[1 - \frac{Vm\ \cos\delta'\ Ef}{\eta\omega\sin\delta' + (Vf\ Em + Vm\ Ef)\cos\delta'}\right] \qquad (8.24)$$

At room temperature $\sin\delta' \cong 0$ and $\cos\delta' \cong 0$. Furthermore, in the rubbery plateau region, the same identies are valid. Thus, the equation which approximates E' of a 90° composite in these two regions is:

$$Ec = \frac{Ef\ Em}{Vf\ Em + Vm\ Ef} \qquad (8.25)$$

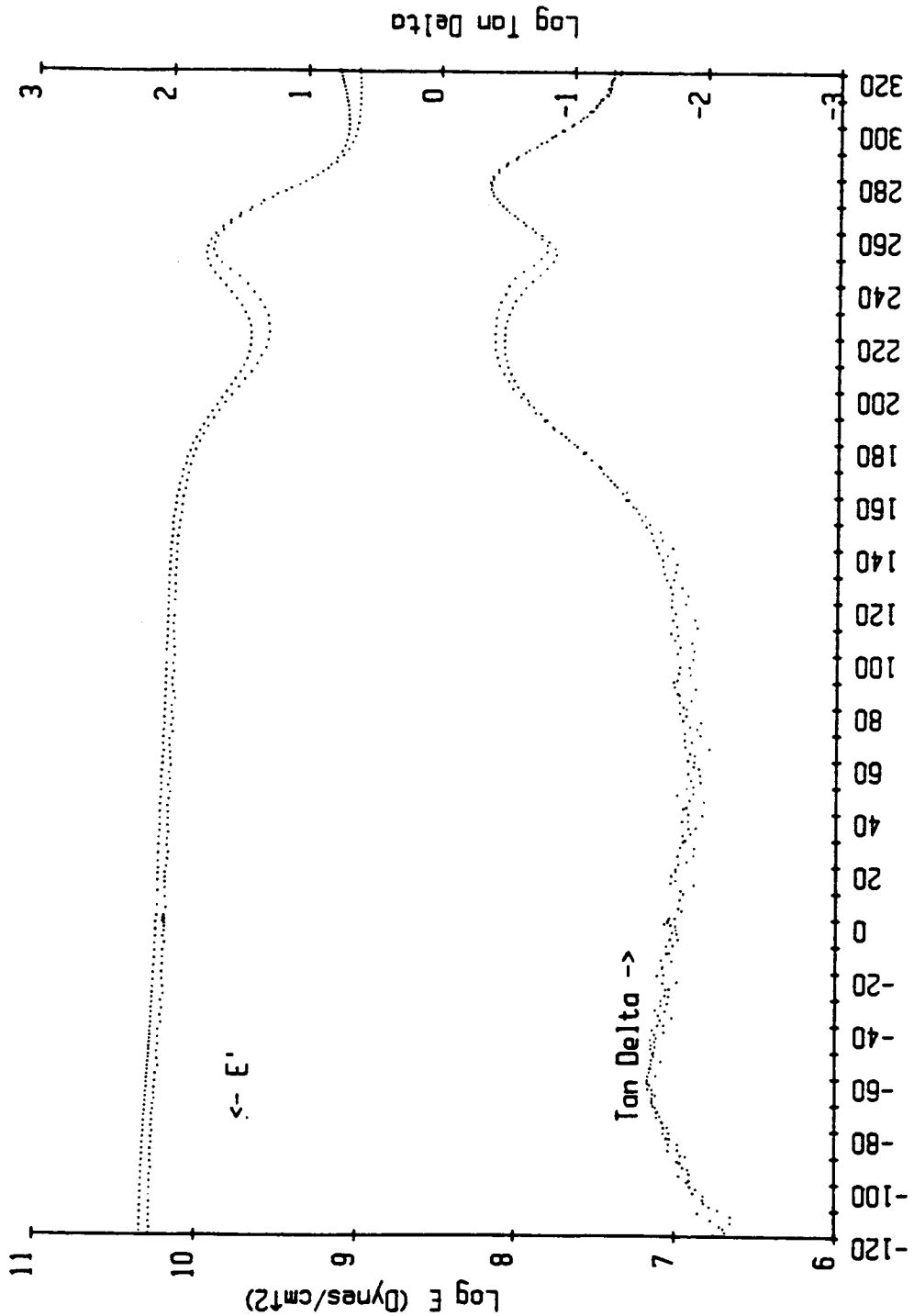

Figure 8.3 Dynamic mechanical spectrum of two cured 80/20 TGDDM/DDS epoxy specimens (control)

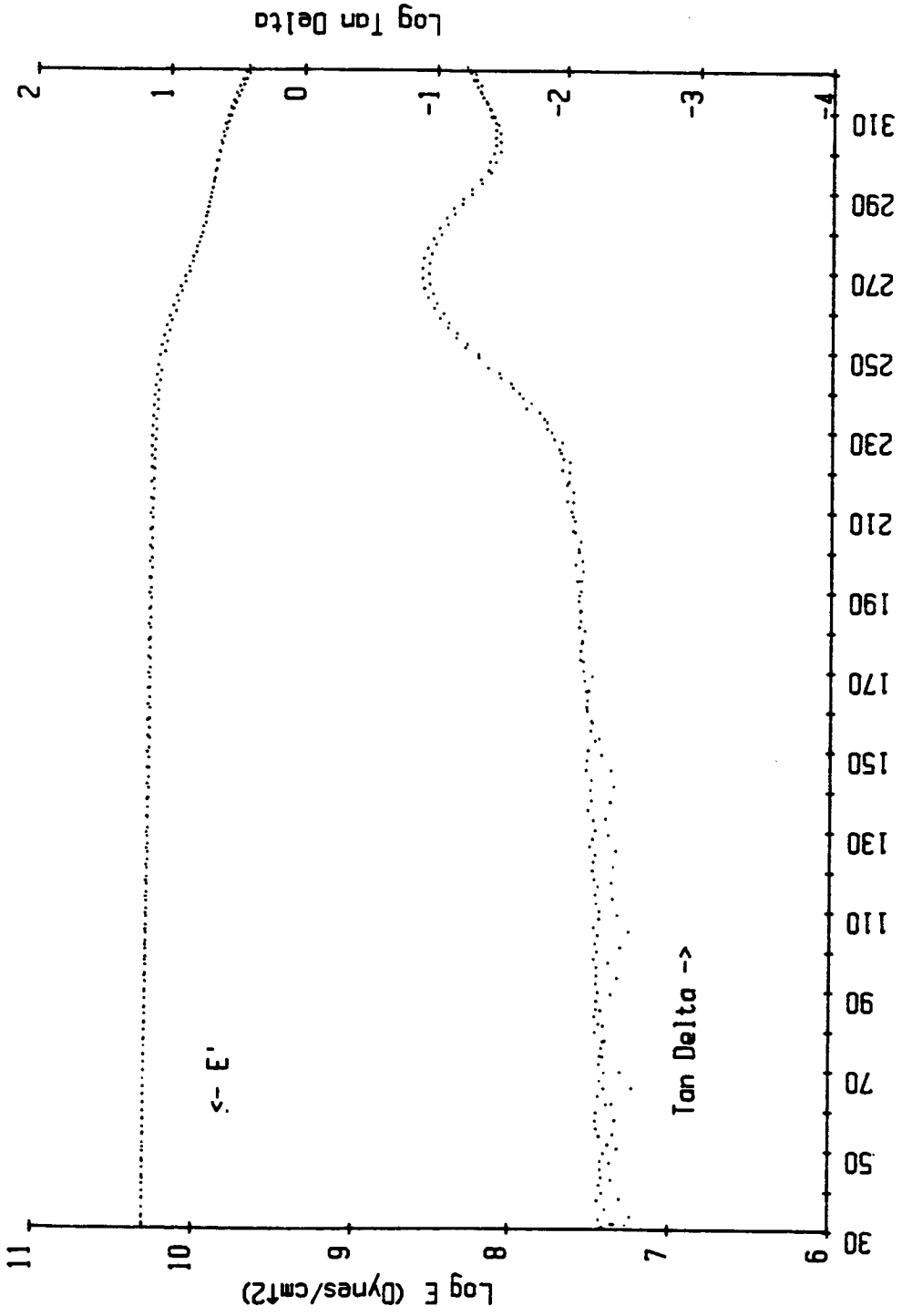

Figure 8.4 Dynamic mechanical spectrum of two T300/5208 90° composite specimens (irradiated)